Slides can be found here:
https://wt.imphys.tudelft.nl/

Physics of Waves

Modelling and imaging with ultrasound

2024 IEEE South Asian Ultrasonics Symposium (SAUS)

Koen W.A. van Dongen
Department of Imaging Physics, Delft University of Technology, the Netherlands
K.W.A.vanDongen@tudelft.nl

Tuesday, March 26, 2024, Gandhinagar, India

TU Delft
Delft University of Technology

Introduction

- Please don't hesitate to ask questions during my presentation!

- Topics
  - Introduction
  - Field equations
  - Wave equation
  - Non-linear ultrasound
  - Rayleigh
  - Heterogeneous media
    - Forward problem
    - Inverse problem

Introduction

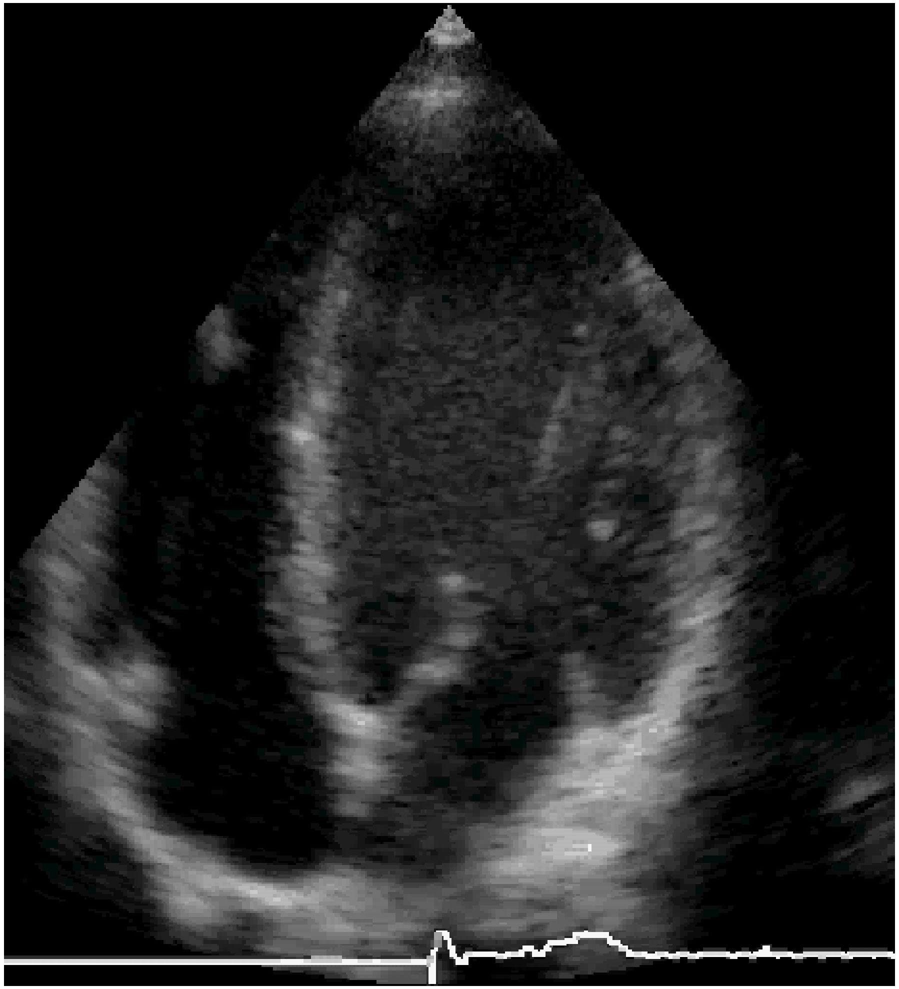

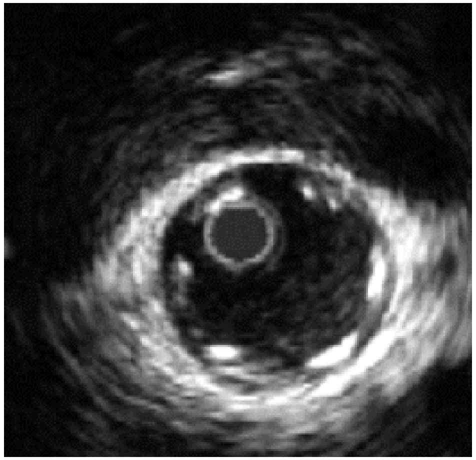

[1] www.philips.com
[2] Erasmus MC, Rotterdam, the Netherlands

Introduction

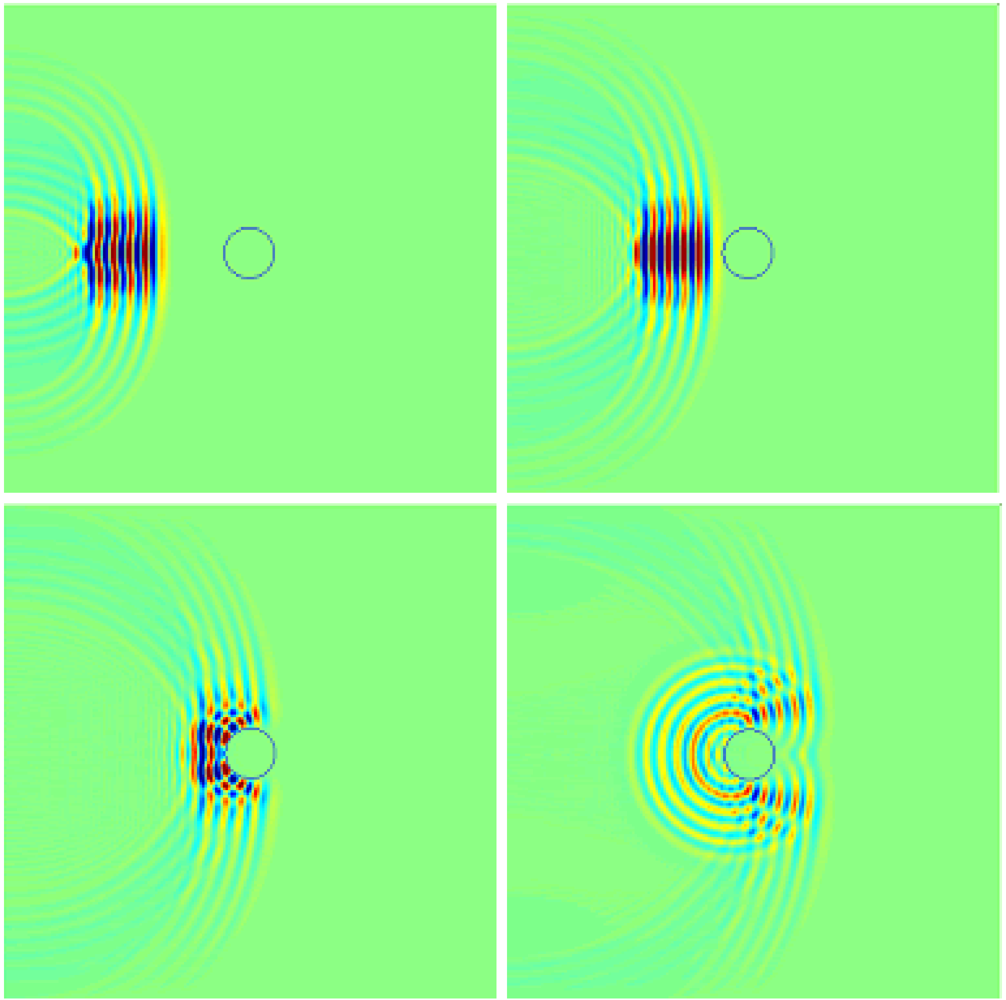

[1] http://www.mathworks.com/

Introduction

- Field radiated by a point source / acoustic monopole [1]

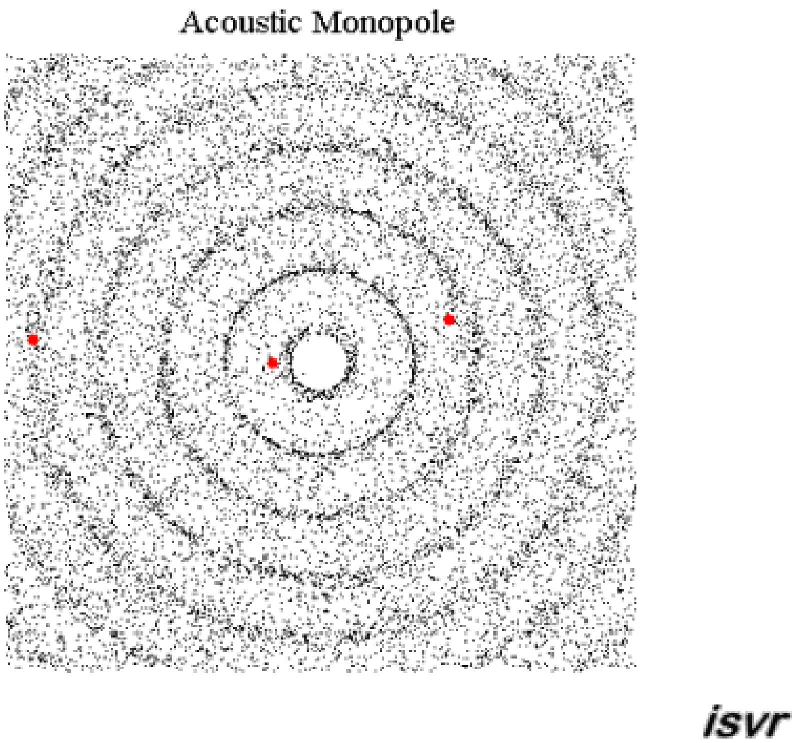

[1] http://resource.isvr.soton.ac.uk/spcg/tutorial/tutorial/Tutorial_files/Web-basics-pointsources.htm

Introduction

- Two plane waves with different velocities [1]

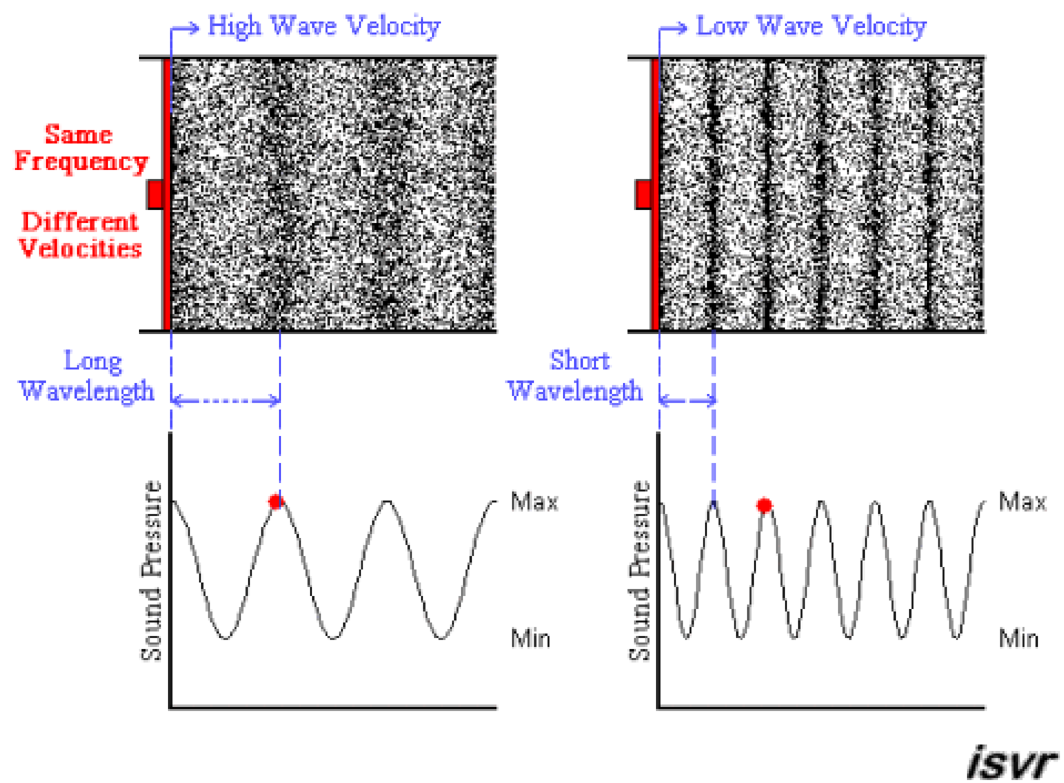

[1] http://resource.isvr.soton.ac.uk/spcg/tutorial/tutorial/Tutorial_files/Web-basics-frequency.htm

Acoustic Field Equations

Volume: $\Delta V = \Delta x \Delta y \Delta z$

Location: $\underline{r} = (x, y, z)$

Displacement field: $\underline{d}(\underline{r},t) = \left[\xi(\underline{r},t), \eta(\underline{r},t), \zeta(\underline{r},t)\right]$

Velocity field: $\underline{v}(\underline{r},t) = \dfrac{d}{dt}\underline{d}(\underline{r},t)$

Pressure field: $p(\underline{r},t) = p_{tot}(\underline{r},t) - p_0$

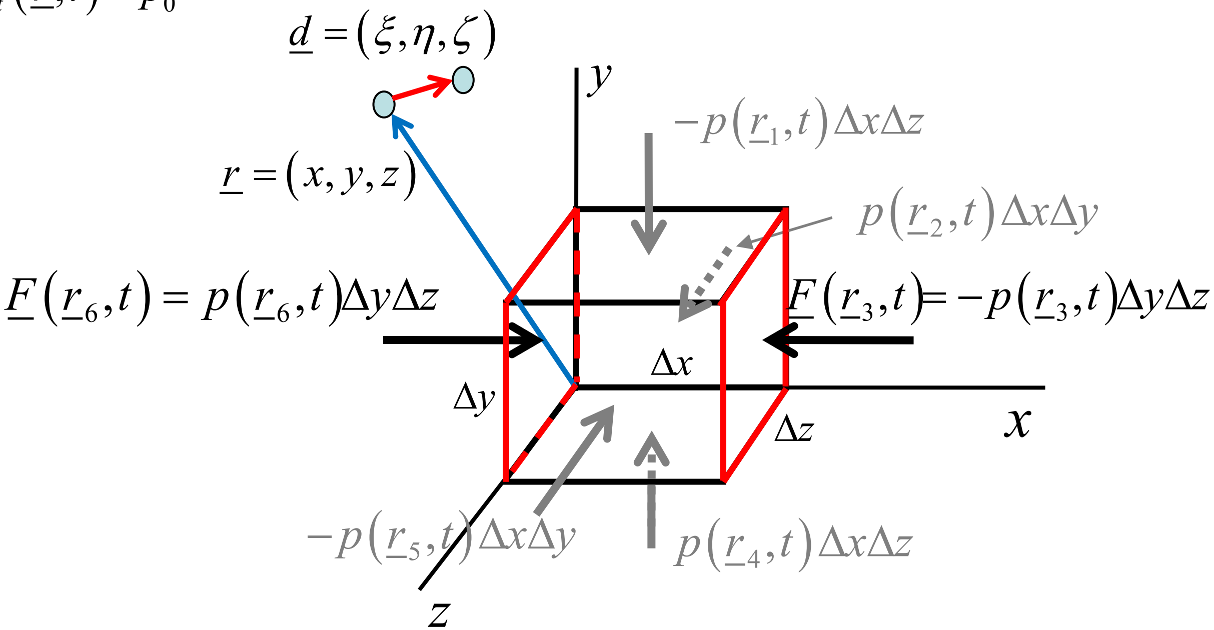

1-D Acoustic Field Equation – Hooke's Law

A fluid volume element ΔV is distorted by an excess pressure field $p(x,t)$ and volume injection $Q(x,t)$:

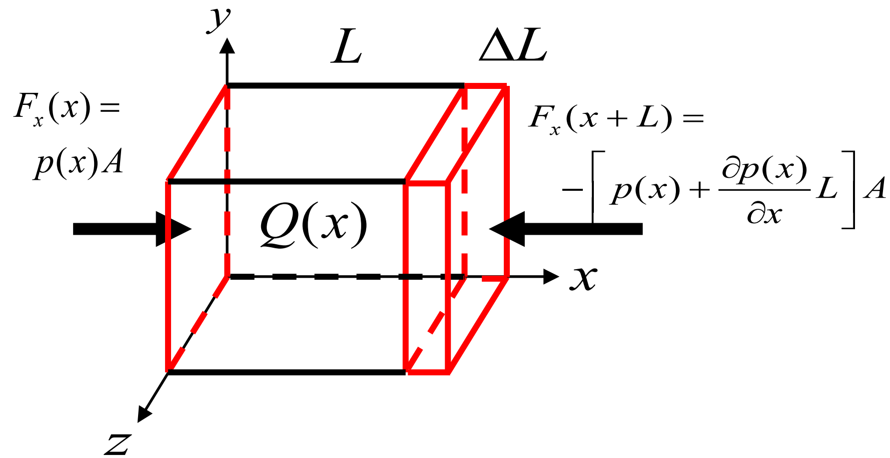

$$\Rightarrow \quad p_{tot}(x,t) = p_0 + p(x,t)$$

$$\Rightarrow \quad \Delta V \rightarrow \Delta V + A\Delta L$$

$$\Rightarrow \quad F = -k\frac{\Delta L}{L} \text{ (Hooke's law: extension of a spring)}$$

Amount of deformation depends on compressibility κ: $\frac{\Delta L}{L} = -\kappa p(x,t) + Q(x,t)$

Deformation can also be described by a displacement of the particle location $d_x(x,t)$: $\frac{\Delta L}{L} = \frac{\partial d_x(x,t)}{\partial x}$

$$\Rightarrow \quad -\kappa p(x,t) + Q(x,t) = \frac{\partial d_x(x,t)}{\partial x} \quad \xrightarrow{\frac{1}{\kappa}\frac{d}{dt} = \cancel{\frac{1}{\kappa}v\cdot\nabla} + \frac{1}{\kappa}\frac{\partial}{\partial t}} \quad \boxed{\frac{\partial p(x,t)}{\partial t} = -\frac{1}{\kappa}\frac{\partial v_x(x,t)}{\partial x} + \frac{1}{\kappa}q(x,t)}$$

with volume density of injection rate source $q(x,t)$.

Note that two linearizations are made: $\frac{d}{dt} = \cancel{v\cdot\nabla} + \frac{\partial}{\partial t}$ and $\kappa(p) = \kappa(p_0) + \cancel{(p-p_0)\left.\frac{\partial\kappa(p)}{\partial p}\right|_{p=p_0}}$

3-D Acoustic Field Equation – Hooke's Law

Changing from one to three dimensions means that the volume will change in three dimensions and that the particles may move in the ξ, η and ζ –direction, hence

$$\frac{\delta \Delta V}{\Delta V}=\frac{\{\Delta x+\delta\xi\}\{\Delta y+\delta\eta\}\{\Delta z+\delta\zeta\}-\Delta x\Delta y\Delta z}{\Delta x\Delta y\Delta z}=\frac{\delta\xi\Delta y\Delta z+\delta\eta\Delta x\Delta z+\delta\zeta\Delta x\Delta y}{\Delta x\Delta y\Delta z}+O(\ldots)\approx\frac{\partial\xi}{\partial x}+\frac{\partial\eta}{\partial y}+\frac{\partial\zeta}{\partial z}$$

$$\Rightarrow \quad \boxed{\frac{\delta\Delta V}{\Delta V}=\nabla\cdot\underline{d}}$$

Consequently, Hooke's law will change into

$$\boxed{\frac{\partial p(\underline{r},t)}{\partial t}=-\frac{1}{\kappa}\nabla\cdot\underline{v}(\underline{r},t)+\frac{1}{\kappa}q(\underline{r},t)}$$

1-D Acoustic Field Equation – Newton's Law

With $p(x+L) = p(x) + \dfrac{\partial p}{\partial x} L$

we find for the net excess force ΔF on ΔV:

$$\Delta F = -A\left(\frac{\partial p(x,t)}{\partial x} L\right) + f_x(x,t)\Delta V$$

with $f_x(x,t)$ the volume source density of volume force.

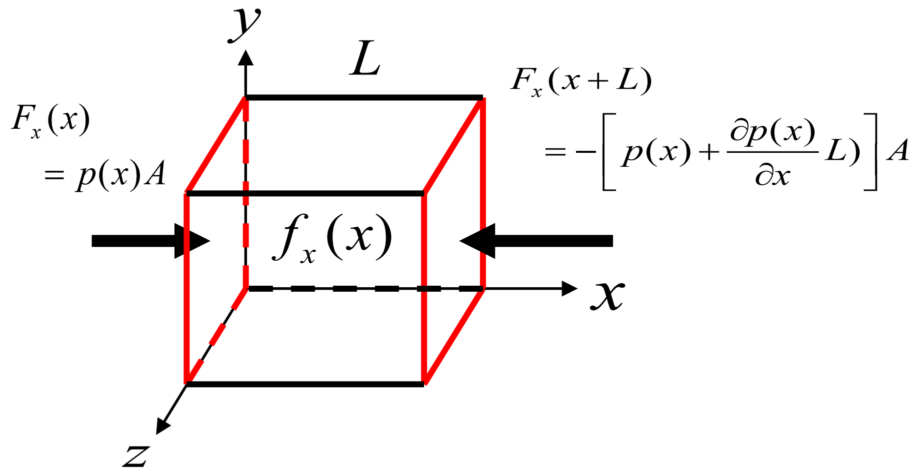

Newton's Law, $F = ma$, for a fixed mass element $m = \Delta V \rho$ and $a = \dfrac{d\,v_x}{dt} = \cancel{v_x \dfrac{\partial v_x}{\partial x}} + \dfrac{\partial v_x}{\partial t} = \dfrac{\partial v_x}{\partial t}$ now reads:

$$\underbrace{-\Delta V \frac{\partial p(x,t)}{\partial x} + f_x(x,t)\Delta V}_{F} = \underbrace{\Delta V \rho}_{m} \underbrace{\frac{\partial v_x(x,t)}{\partial t}}_{a}$$

or:

$$\boxed{-\frac{\partial p(x,t)}{\partial x} = \rho \frac{\partial v_x(x,t)}{\partial t} - f_x(x,t)}$$

in 3-D the Newton's law reads:

$$\boxed{-\nabla p(\underline{r},t) = \rho \frac{\partial \underline{v}(\underline{r},t)}{\partial t} - \underline{f}(\underline{r},t)}$$

Note that two linearizations are made: $\dfrac{d}{dt} = \cancel{\underline{v}\cdot\nabla} + \dfrac{\partial}{\partial t}$ and $\rho(p) = \rho(p_0) + \cancel{(p-p_0)\left.\dfrac{\partial \rho(p)}{\partial p}\right|_{p=p_0}}$

Acoustic Field Equations

The obtained acoustic field equations read

Hooke's law: $$\frac{\partial p(\underline{r},t)}{\partial t} = -\frac{1}{\kappa}\nabla\cdot\underline{v}(\underline{r},t) + \frac{1}{\kappa}q(\underline{r},t)$$ (equation of deformation)

Newton's law: $$-\nabla p(\underline{r},t) = \rho\frac{\partial\underline{v}(\underline{r},t)}{\partial t} - \underline{f}(\underline{r},t)$$ (equation of motion)

This set of equations shows large similarities with Maxwel Equations

$$\nabla\cdot\underline{E} = \frac{1}{\varepsilon_0}\rho_f \qquad \nabla\cdot\underline{B} = 0$$

$$\nabla\times\underline{E} = -\frac{\partial\underline{B}}{\partial t} \qquad \nabla\times\underline{B} = \mu\sigma\underline{E} + \mu\varepsilon\frac{\partial\underline{E}}{\partial t}$$

Wave Equation

The acoustic field equations may be combined to obtain (in the absense of sources):

a) a scalar wave equation for the pressure field:

$$\left.\begin{array}{l} \rho\kappa \dfrac{\partial}{\partial t}\left[\dfrac{\partial\, p(\underline{r},t)}{\partial t}\right] = \rho\kappa \dfrac{\partial}{\partial t}\left[-\dfrac{1}{\kappa}\nabla\cdot\underline{v}(\underline{r},t)\right] \\ \nabla\cdot\left[-\nabla p\left(\underline{r},t\right)\right] = \nabla\cdot\left[\rho\dfrac{\partial\underline{v}\left(\underline{r},t\right)}{\partial t}\right] \end{array}\right\} \Rightarrow \boxed{\nabla^2 p\left(\underline{r},t\right) - \rho\kappa\dfrac{\partial^2\, p(\underline{r},t)}{\partial t^2} = 0}$$

$$= \frac{1}{c^2}$$

b) a vectorial wave equation for the velocity wave field:

$$\left.\begin{array}{l} \kappa\nabla\left[\dfrac{\partial\, p(\underline{r},t)}{\partial t}\right] = \kappa\nabla\left[-\dfrac{1}{\kappa}\nabla\cdot\underline{v}(\underline{r},t)\right] \\ \kappa\dfrac{\partial}{\partial t}\left[-\nabla p\left(\underline{r},t\right)\right] = \kappa\dfrac{\partial}{\partial t}\left[\rho\dfrac{\partial\underline{v}\left(\underline{r},t\right)}{\partial t}\right] \end{array}\right\} \Rightarrow \boxed{\nabla\left[\nabla\cdot\underline{v}\left(\underline{r},t\right)\right] - \rho\kappa\dfrac{\partial^2\,\underline{v}(\underline{r},t)}{\partial t^2} = 0}$$

remember: $\nabla^2\underline{E}\left(\underline{r},t\right) - \dfrac{1}{c^2}\dfrac{\partial^2\,\underline{E}(\underline{r},t)}{\partial t^2} = 0$

$\nabla^2\underline{B}\left(\underline{r},t\right) - \dfrac{1}{c^2}\dfrac{\partial^2\,\underline{B}(\underline{r},t)}{\partial t^2} = 0$

Wave Equation

There are two types of sources, which can generate an acoustic field

1) A volume source density of injection rate: $q(\underline{r},t)$ [s^{-1}]

2) A volume source density of volume source: $\underline{f}(\underline{r},t)$ [N/m^3]

Hooke's law: $$\frac{\partial p(\underline{r},t)}{\partial t} = -\frac{1}{\kappa}\nabla\cdot\underline{v}(\underline{r},t) + \frac{1}{\kappa}q(\underline{r},t),$$ (equation of deformation)

Newton's law: $$-\nabla p(\underline{r},t) = \rho\frac{\partial \underline{v}(\underline{r},t)}{\partial t} - \underline{f}(\underline{r},t).$$ (equation of motion)

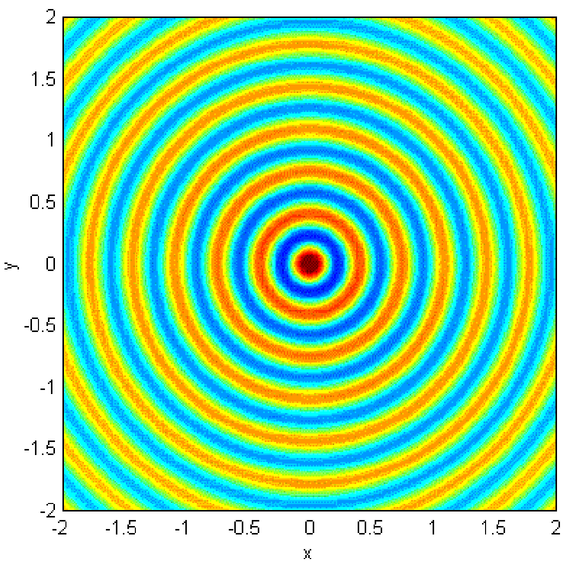

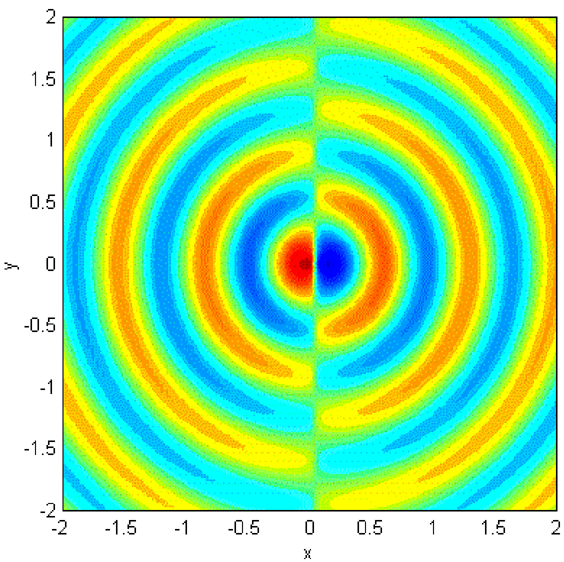

[1] http://en.wikibooks.org/wiki/Aeroacoustics/Acoustic_Sources

Finite Difference Time Domain (FDTD)

Finite-difference time-domain (FDTD) or Yee's method was originally developed for electrodynamics but is also used to model other wave phenomena. With FDTD, the time-dependent acoustic wave equation

$$\nabla^2 p(\underline{r},t) - \frac{1}{c_0^2}\partial_t^2 p(\underline{r},t) = -S_{pr}(\underline{r},t) \quad \text{or} \quad \partial_t^2 p(\underline{r},t) = c_0^2 \nabla^2 p(\underline{r},t) + c_0^2 S_{pr}(\underline{r},t)$$

is discretized using central-difference approximations for the spatial and temporal partial derivatives. E.g, the temporal derivative is approximated as

$$\partial_t^2 p(\underline{r},t) = \frac{p(\underline{r},t+\Delta) - 2p(\underline{r},t) + p(\underline{r},t-\Delta)}{\Delta t^2}.$$

To predict the wave at $t+\Delta$, the discretised wave equation is rewritten as

$$\boxed{p(\underline{r},t+\Delta) = 2p(\underline{r},t) - p(\underline{r},t-\Delta) + \Delta t^2 c_0^2 \nabla^2 p(\underline{r},t) + \Delta t^2 c_0^2 S_{Pr}(\underline{r},t)}$$

Finite Difference Time Domain (FDTD)

There are three important challenges with FDTD.

1. Absorbing Boundary Conditions (ABC) or Perfectly Matching Layers (PML) are needed to account for the finite size of the spatial domain.

2. A dense temporal and spatial grid is needed to accurately employ the central difference approximation.

3. The discretisation needs to satisfy the convergence or Courant–Friedrichs–Lewy condition:

$$C_{CFL} = c_0 \Delta t / \Delta t \ < \ 1$$

Note that for a heterogeneous speed of sound c_0 is replaced by $c(\underline{r})$.

Helmholtz Equation

Definition of the temporal Fourier transform of a function $g(\underline{r},t):\hat{g}(\underline{r},\omega)=\int\limits_{-\infty}^{\infty} g(\underline{r},t)\, e^{-i\omega t} dt$

Fourier transformation of the wave equation $\nabla^2 p(\underline{r},t)-\frac{1}{c^2}\frac{\partial^2 p(\underline{r},t)}{\partial t^2}=0$

using: $\int\limits_{-\infty}^{\infty}\left(\frac{\partial g(\underline{r},t)}{\partial t}\right) e^{-i\omega t} dt = i\omega\, \hat{g}(\underline{r},\omega)$ yields the Helmholtz equation

$$\boxed{\nabla^2 \hat{p}(\underline{r},\omega)+\frac{\omega^2}{c^2}\hat{p}(\underline{r},\omega)=0}$$

Frequency domain Acoustic Field Equations

In the frequency domain, the obtained acoustic field equations equal

Hooke's law: $$i\omega\hat{p}(\underline{r},\omega) = -\frac{1}{\kappa}\nabla\cdot\hat{\underline{v}}\left(\underline{r},\omega\right),$$

Newton's law: $$-\nabla\hat{p}\left(\underline{r},\omega\right) = i\omega\rho\hat{\underline{v}}\left(\underline{r},\omega\right).$$

Spherical Waves

Transforming the Helmholtz equation to polar coordinates
for spherical symmetric solutions yields

$$\nabla^2 \hat{p}(\underline{r},\omega) + \frac{\omega^2}{c^2}\hat{p}(\underline{r},\omega) = -\hat{S}(\underline{r},\omega) \quad \Rightarrow \quad \frac{1}{r^2}\frac{\partial}{\partial r}\left(r^2 \frac{\partial}{\partial r}\hat{p}(r,\omega)\right) + \frac{\omega^2}{c^2}\hat{p}(r,\omega) = -\delta(\underline{r})\hat{S}(\omega).$$

The most general solution of this equation equals:

$$\hat{p}(r,\omega) = \hat{A}(\omega)\frac{e^{-i\omega r/c_0}}{r} + \hat{B}(\omega)\frac{e^{i\omega r/c_0}}{r}, \quad \text{for } r \neq 0.$$

Why *exp[…]* ?

Why $1/r$?

In practise, with acoustics only the outgoing spherical wave is encountered. In literature, the spherical wave created by a Dirac delta source is referred to as

Green's function $\hat{G}(\underline{r},\omega)$, or the impulse response of the medium: $\boxed{\hat{G}(\underline{r},\omega) = \frac{e^{-i\omega|\underline{r}|/c_0}}{4\pi|\underline{r}|}}$

TUDelft

Exercise

Model the acoustic wavefield generated by a point source.

```
%---------------------------------------------------------------%
constants
f0     = 1e6;          % center frequency of the gaussian pulse [Hz]
c0     = 1500;         % speed of sound of the background [m/s]
L      = 50e-3;        % width and height of spatial domain [m]
src    = [L/2,L/2];    % (x,y)-location of source [m]

% definition of the excitation pulse s0
tw     = (1/f0);       % length of the pulse [s]
t0     = 3*tw;         % temporal offset of the pulse
s0     = exp(-((time-t0)/tw).^2).*cos(2*pi*f0*(time-t0));
S0     = fft(s0);
```


TU Delft

Plane Waves

Any pulse can be described by a combination of sine and cosine functions:

$$\hat{F}(\omega) = \int_{-\infty}^{\infty} f(t)\, e^{-i\omega t}\, dt$$

$$f(t) = \frac{1}{2\pi} \int_{-\infty}^{\infty} \hat{F}(\omega)\, e^{+i\omega t}\, d\omega$$

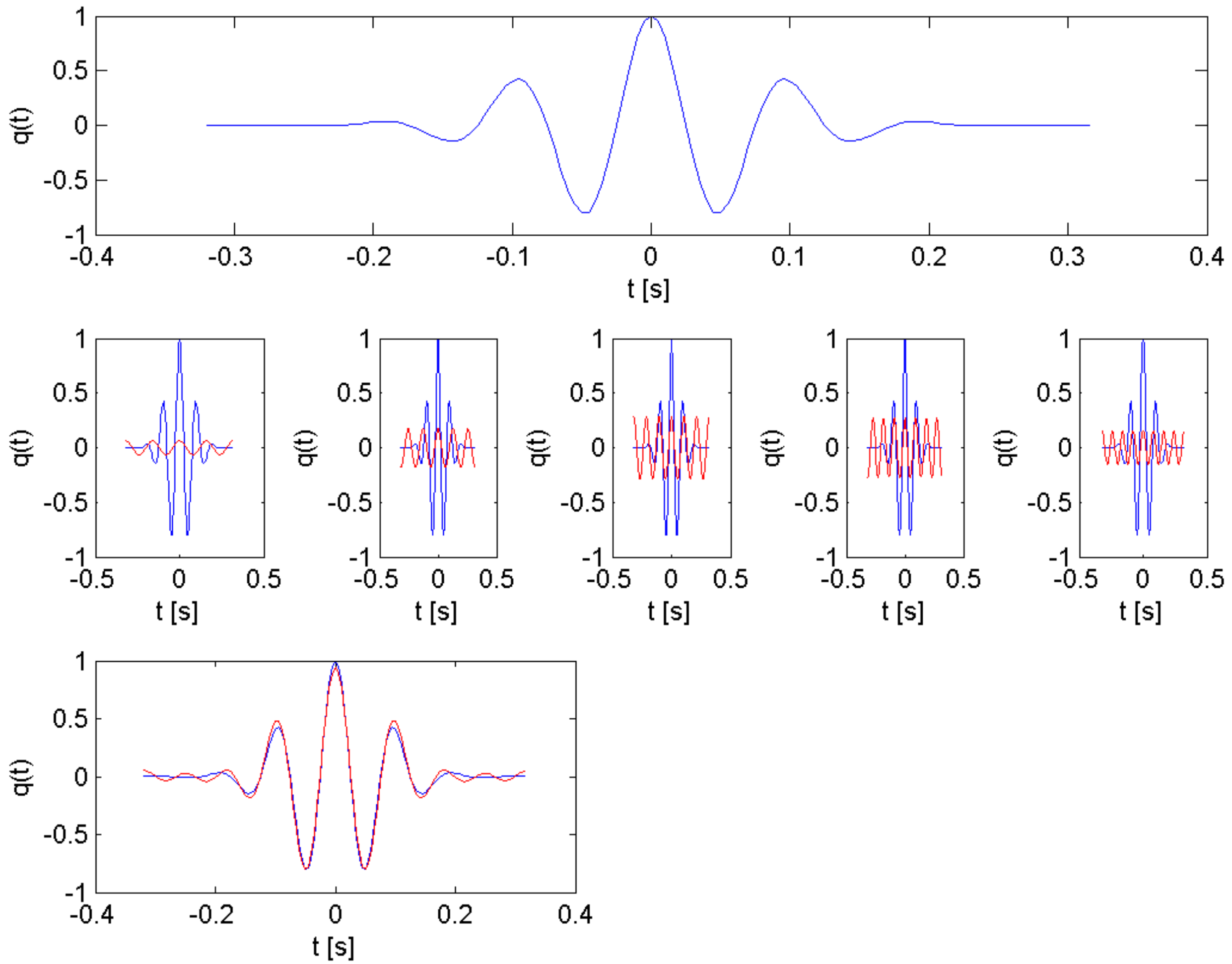

TU Delft

Plane Waves – Acoustic Impedance

The concept of describing a pulse using Fourier series can be extended to 1-D, 2-D and 3-D wave fields, leading to the introduction of plane waves.

General solutions of the Helmholtz equation, $\nabla^2 \hat{p}(\underline{r},\omega) + \frac{\omega^2}{c^2}\hat{p}(\underline{r},\omega) = 0$,

in terms of plane waves equal $\boxed{\hat{p}(\underline{r},\omega) = \sum_{\underline{k}} F_{\underline{k}}(\omega) e^{-i\underline{k}\cdot\underline{r}}}$, with wave vector $\underline{k}$ of length $|\underline{k}| = \frac{\omega}{c}$.

Calculating the velocity field that goes along with these pressure plane waves yields

$$\left.\begin{array}{l} -\nabla\hat{p}(\underline{r},\omega) = i\omega\rho_0\hat{\underline{v}}(\underline{r},\omega) \\ \hat{p}(\underline{r},\omega) = \sum_{\underline{k}} F_{\underline{k}}(\omega) e^{-i\underline{k}\cdot\underline{r}} \end{array}\right\} \Rightarrow \sum_{\underline{k}} i\underline{k}\, F_{\underline{k}}(\omega) e^{-i\underline{k}\cdot\underline{r}} = i\omega\rho\hat{\underline{v}}(\underline{r},\omega) \Rightarrow \hat{\underline{v}}(\underline{r},\omega) = \frac{1}{\rho c}\sum_{\underline{k}} \frac{\underline{k}}{|\underline{k}|} F_{\underline{k}}(\omega) e^{-i\underline{k}\cdot\underline{r}}$$

1-D : $\Rightarrow$ $\boxed{\hat{p}(x,\omega) = \rho c\,\hat{v}(x,\omega) = Z\,\hat{v}(x,\omega)}$, where Z is refered to as the acoustic impedance.

Boundary Conditions

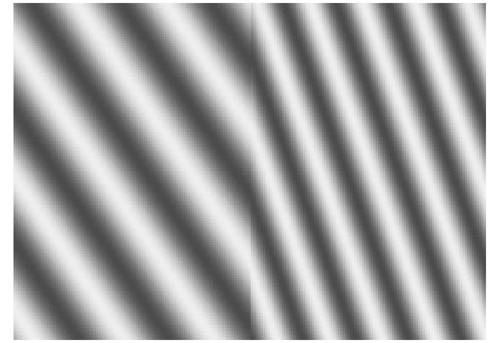

Consider a plane wave traveling in the (x, y)-plane in the direction $\underline{s}_1$, with velocity $c_1 : \hat{p}_1(\underline{r},\omega) = F(\omega)e^{-i\omega \underline{s}_1 \cdot \underline{r}}$

If the field meets a boundary between two media with different speed of sound,

part of the field will be reflected: $\hat{p}'_1(\underline{r},\omega) = F(\omega)e^{-i\omega \underline{s}'_1 \cdot \underline{r}}$,

and part of field will be refracted: $\hat{p}_2(\underline{r},\omega) = F(\omega)e^{-i\omega \underline{s}_2 \cdot \underline{r}}$.

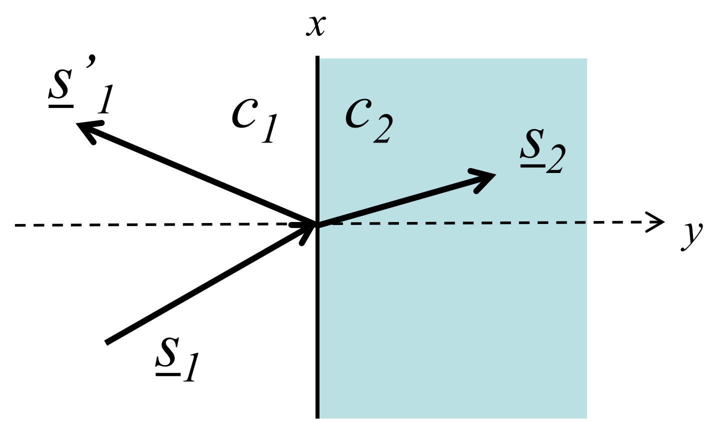

At $y = 0$, the following boundary conditions apply:

1) continuity of pressure: $\boxed{\hat{p}_1 + \hat{p}'_1 = \hat{p}_2}$; Why ?

2) continuity of normal component of the particle velocity: $\boxed{v_1^{\perp} + v'^{\perp}_1 = v_2^{\perp}}$

These boundary conditions may be used to show that

the reflection coefficient $R = \dfrac{Z_2 - Z_1}{Z_2 + Z_1}$, and the transmission coefficient $T = 1 - R = \dfrac{2Z_1}{Z_2 + Z_1}$.

Imaging

- An acoustic contrast gives rise to a reflected wave. By measuring the time between transmission and reception of the acoustic wave the distance to the object can be measured.

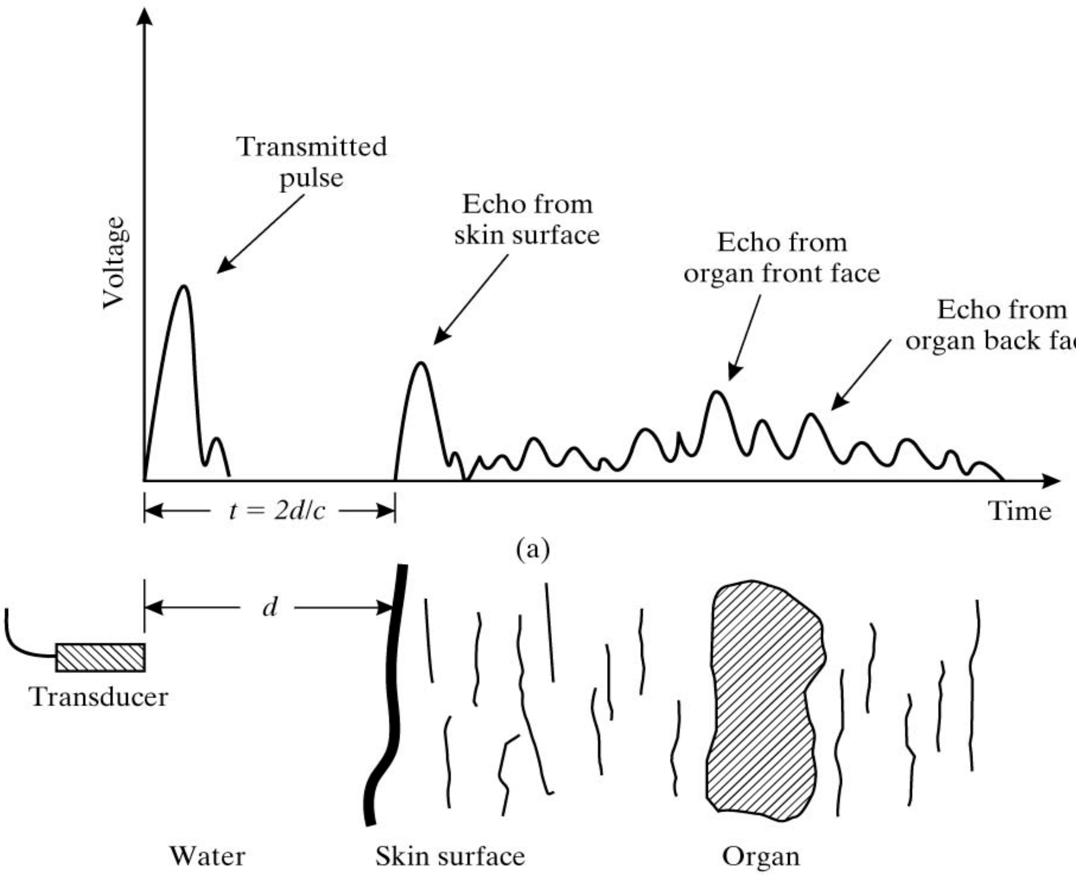

Image taken from J.L. Prince and J. Links, "Medical Imaging Signals and Systems", Prentice Hall (2005)

Beam forming

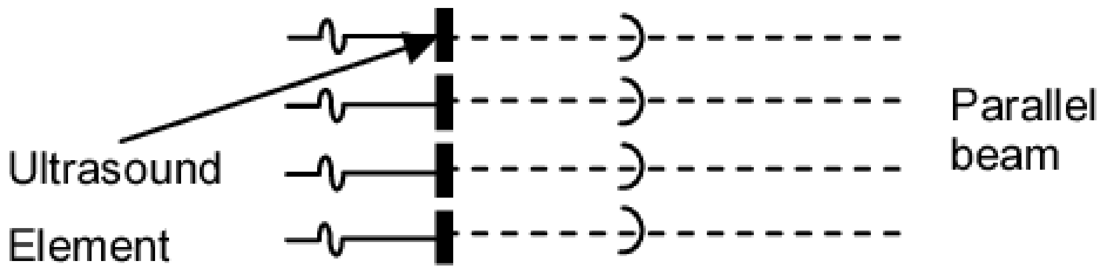

Image taken from Tan et al. "High intensity ultrasound phased array for surgical applications." *2006 International Conference on Biomedical and Pharmaceutical Engineering* (2006): 564-568.

Beam forming

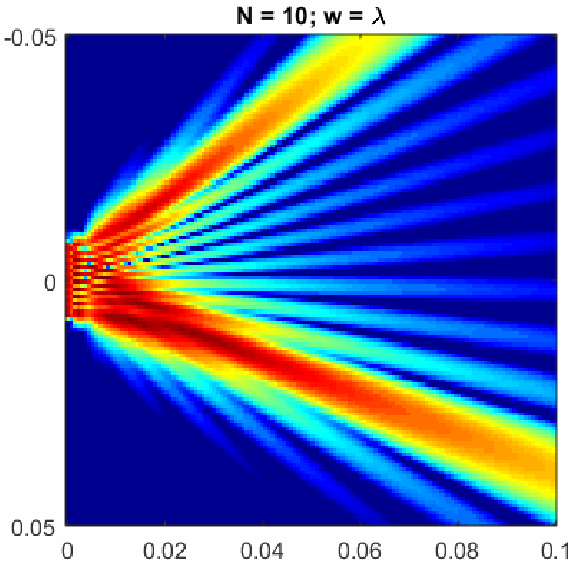

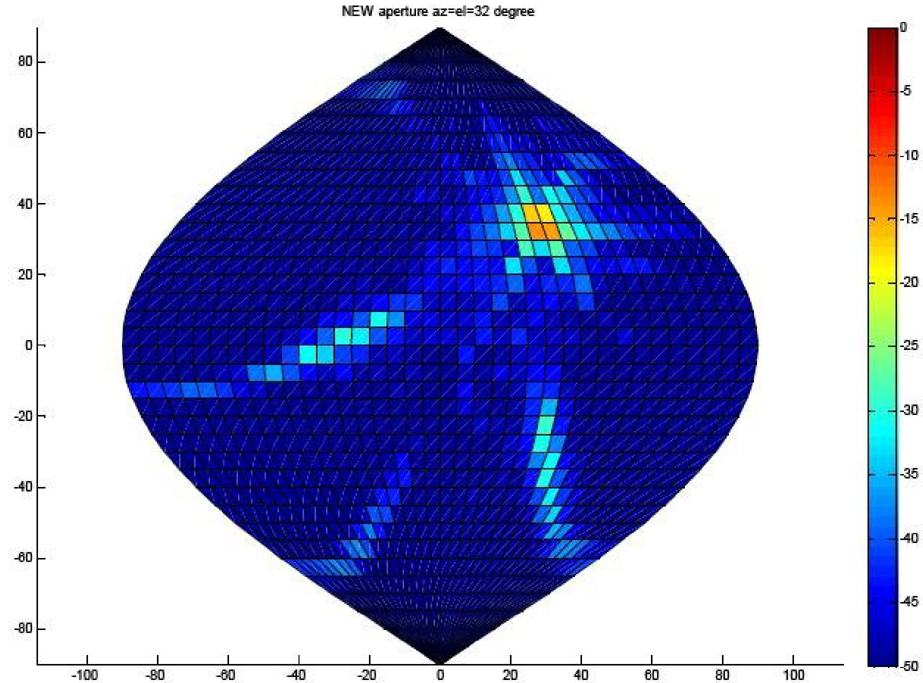

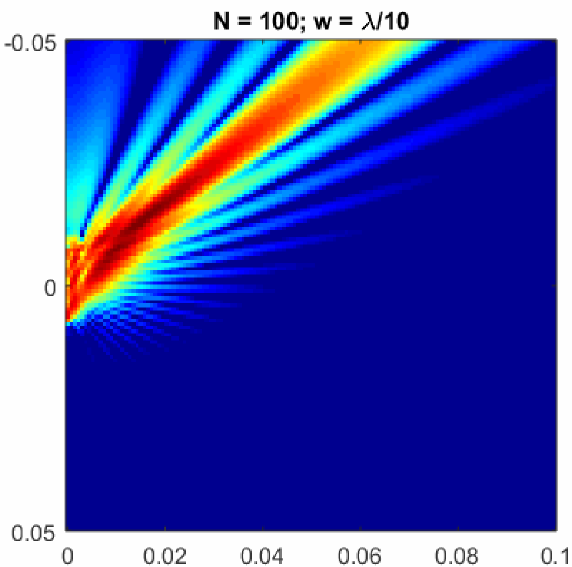

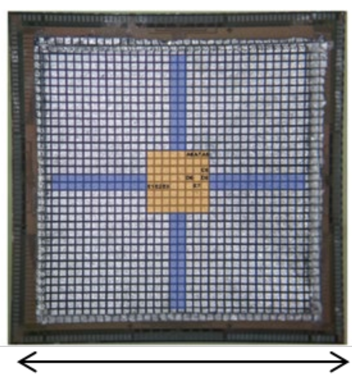

4.5 mm x 4.5 mm
(120μm X 120μm)

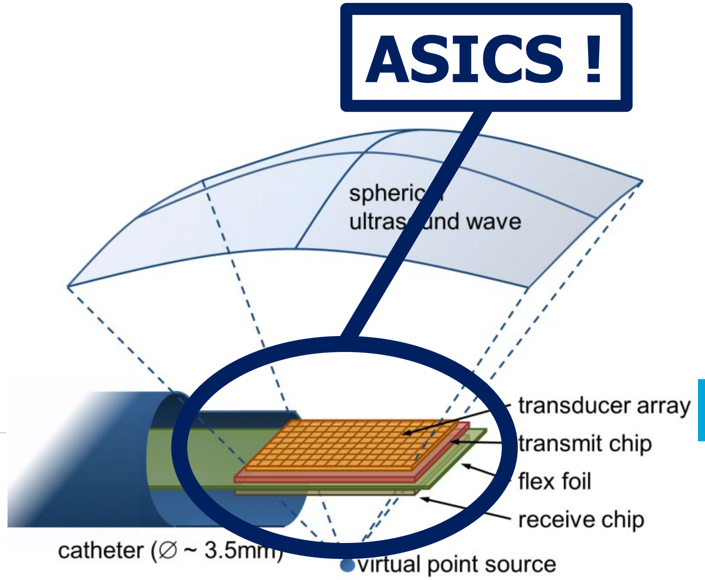

Non-linear Ultrasound

Arrays are used to steer the beam into a certain direction.
Due to the finite size of the elements and the spacing in between elements, side and grating lobes will occur, leading to a blurring of the image.

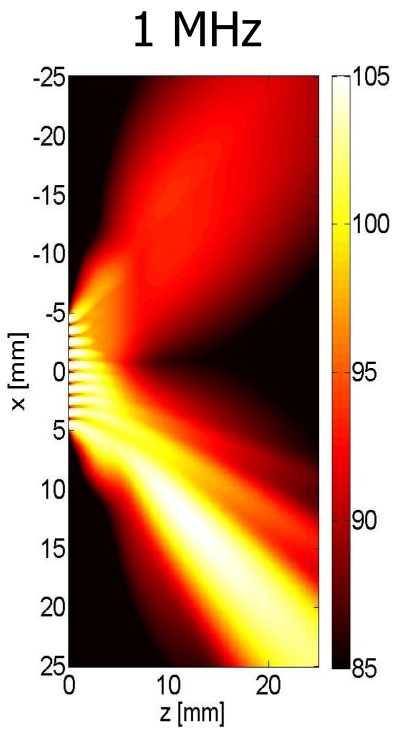

TU Delft

Non-Linear Ultrasound

To derive the linear wave equation, three approximations are made

- the volume density of mass was assumed to be constant, i.e. pressure independent:

$$\rho_0(p) = \rho_0(p_0) + \cancel{(p - p_0)\left(\frac{\partial \rho_0(p)}{\partial p}\right)\Bigg|_{p=p_0}},$$

- the compressibility was assumed to be constant, i.e. pressure independent:

$$\kappa_0(p) = \kappa_0(p_0) + \cancel{(p - p_0)\left(\frac{\partial \kappa_0(p)}{\partial p}\right)\Bigg|_{p=p_0}},$$

- the convection term of the material derivative was assumed to be zero:

$$\frac{dp(\underline{r},t)}{dt} \equiv \frac{\partial p(\underline{r},t)}{\partial t} + \cancel{\underline{v} \cdot \nabla p(\underline{r},t)}$$

Non-Linear Ultrasound

For small amplitude acoustics, experiments show that these assumptions are valid.

However, for high amplitude pressure fields, this approximation is no longer valid, moreover the volume density of mass $\rho(p)$ may be approximated by

$$\left.\begin{aligned}
&\rho(p) = \rho_0 + (p - p_0)\left.\frac{\partial \rho}{\partial p}\right|_{p-p_0} \\
&p_0\left(\Delta V\right)^{\gamma} = const \;\Rightarrow\; p_0\left(\rho_0\right)^{-\gamma} = p\left(\rho\right)^{-\gamma} \;\Rightarrow\; \frac{\partial \rho}{\partial p} = \rho\frac{1}{\gamma}p^{-1} \\
&\gamma p_0 = \frac{1}{\kappa_0}
\end{aligned}\right\} \Rightarrow \boxed{\rho(p) = \rho_0\left[1 + \kappa_0(p - p_0)\right]}$$

A similar expression may be obtained for the compressibilitiy $\kappa(p)$

$$\boxed{\kappa(p) = \kappa_0\left[1 + \kappa_0(1 - 2\beta)(p - p_0)\right]}$$

with β the coëfficient of non-linearity.

Non-Linear Ultrasound

Combination of the second order approximations

$$\frac{1}{c^2} = \kappa(p)\rho(p)$$

$$= \kappa_0\rho_0\left[1+\kappa_0 p\right]\left[1+\kappa_0(1-2\beta)p\right]$$

$$= \kappa_0\rho_0\left[1+2\kappa_0(1-\beta)p+\kappa_0^2(1-2\beta)p^2\right].$$

Typical values for β vary from 3.6 (water) to 10 (methane).

Hence, for

- increasing pressure we observe an increase in speed of sound c,
- decreasing pressure we observe an decrease in speed of sound c,

This will lead to a change of the shape of the waveform of the wavefield.

TU Delft

Non-Linear Ultrasound

Propagation (function of time) of intense acoustic wave that is sinusoidal at the source.

(a) $x = 0$ source waveform,
(b) distortion becoming noticeable,
(c) $x = \underline{x}$ shock formation,
(d) $x = (\pi/2)\underline{x}$ maximum shock amplitude,
(e) $x = 3\underline{x}$ full sawtooth shape,
(f) decaying sawtooth,
(g) shock beginning to disperse,
(h) old age.

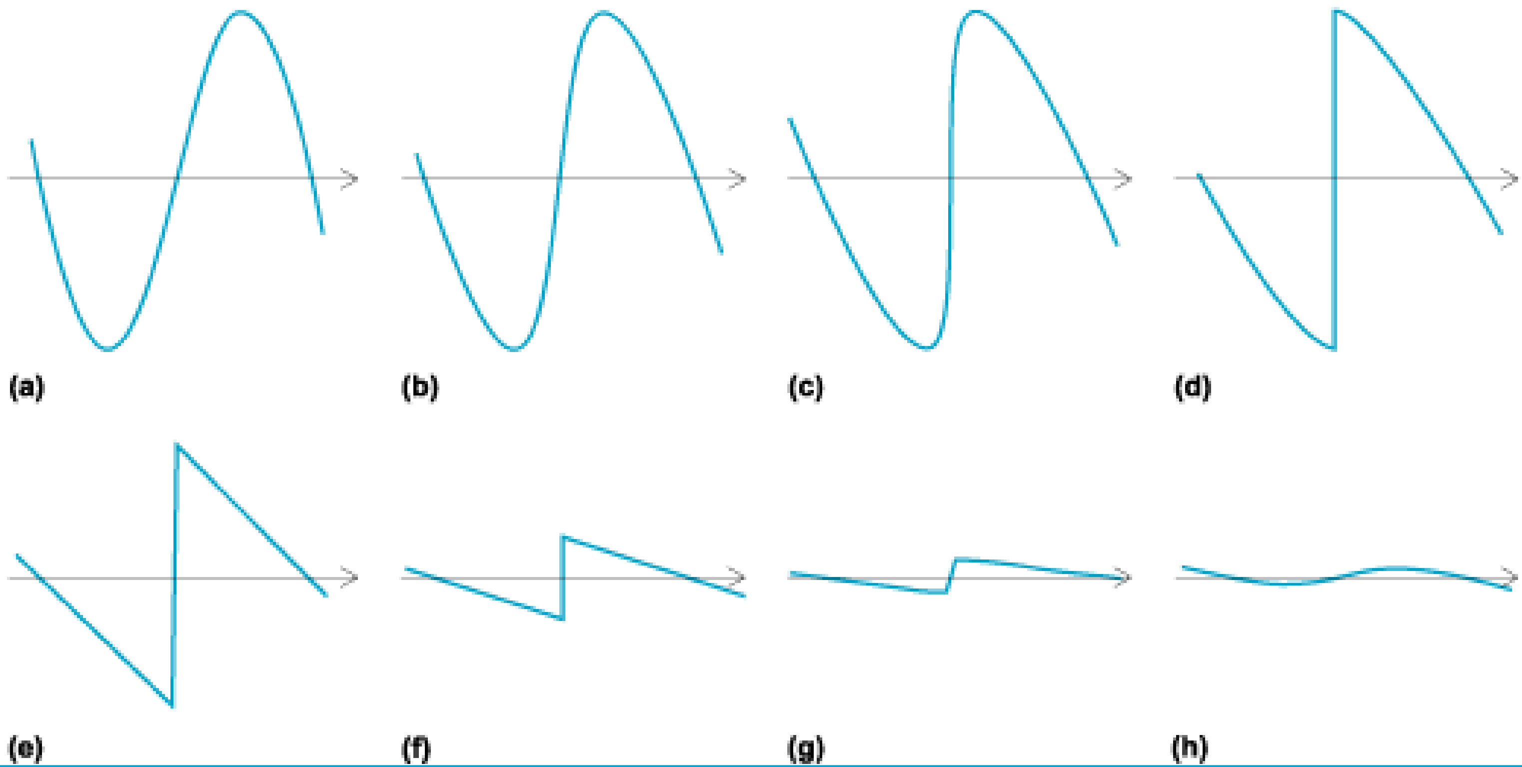

[1] J. A. Shooter et al., Acoustic saturation of spherical waves in water, J. Acous. Soc. Amer., 55:54–62, 1974

Non-Linear Ultrasound

The non-linear propagation leads to a steepening of the waveform.
In the frequency domain this corresponds to the formation of higher harmonic components.

Linear ultrasound

Non-linear ultrasound

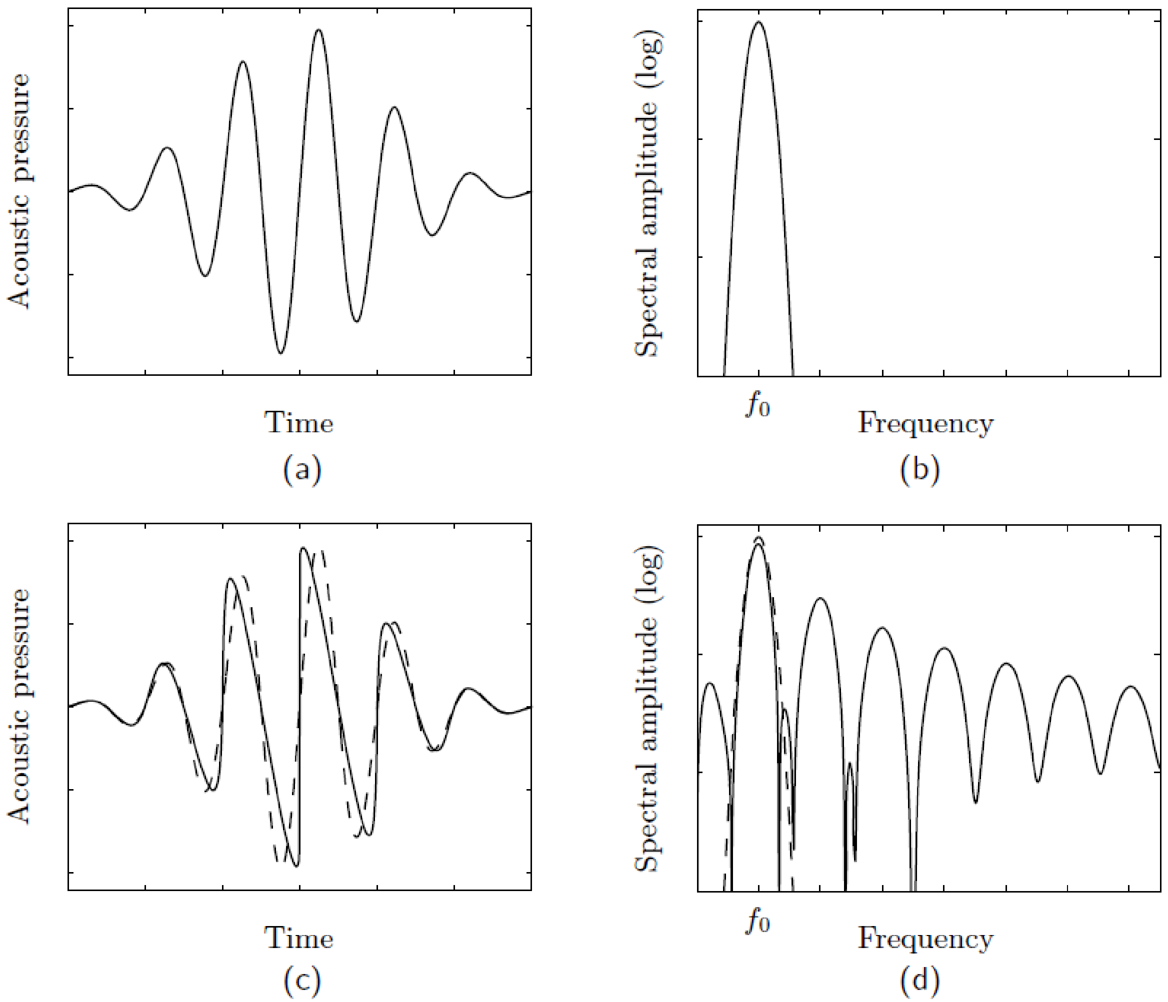

Non-Linear Ultrasound

The non-linear propagation leads to a steepening of the waveform.
In the frequency domain this corresponds to the formation of harmonic components.

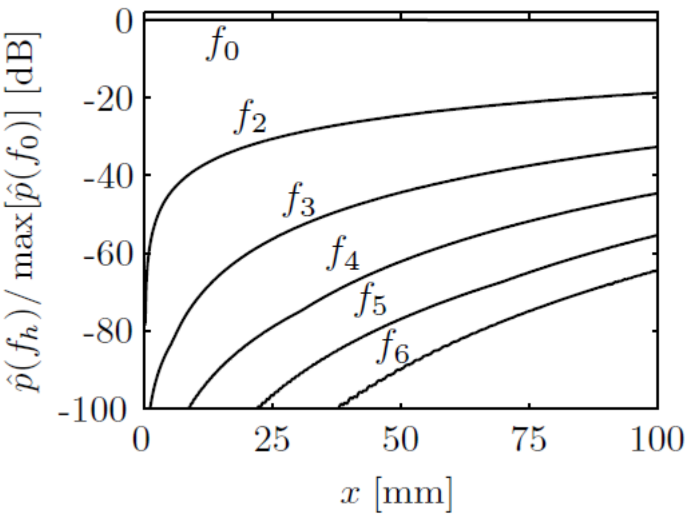

(a)

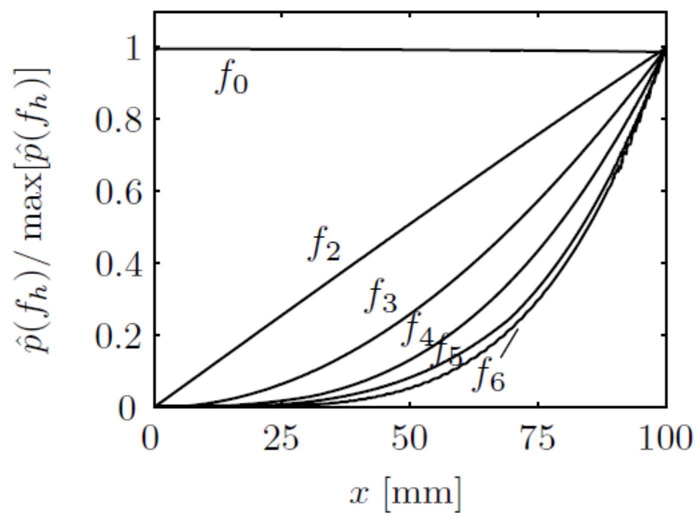

(b)

Non-Linear Ultrasound

Combination of the second order approximations

$$\rho(p) = \rho_0\left[1+\kappa_0(p-p_0)\right],$$
$$\kappa(p) = \kappa_0\left[1+\kappa_0(1-2\beta)(p-p_0)\right]$$

with Hooke's law $\nabla \underline{v} + \rho D_t p = 0,$ and Newtons law $\nabla p + \kappa D_t \underline{v} = 0,$

leads to the following set of equations

$$\nabla \underline{v} + \left(\rho_0\left[1+\kappa_0(p-p_0)\right]\right)\left(\partial_t + \underline{v}\cdot\nabla\right)p = 0$$
$$\nabla p + \left(\kappa_0\left[1+\kappa_0(1-2\beta)(p-p_0)\right]\right)\left(\partial_t + \underline{v}\cdot\nabla\right)\underline{v} = 0.$$

Combining the above set of equations and neglecting terms of third order and higher yields a *second-order non-linear wave equation* or *Westervelt equation*:

$$\boxed{\nabla^2 p - \frac{1}{c^2}\partial_t^2 p = -\frac{\beta}{\rho_0 c_0^4}\partial_t^2 p^2}$$

TU Delft

Non-Linear Ultrasound

Various methods exist to model non-linear ultrasound. If the nonlinearity is weak, the additional term may be considered as a contrast source. Next, a solution for the Westervelt equation, which equals

$$\nabla^2 p(\underline{r},t) - \frac{1}{c^2}\partial_t^2 p(\underline{r},t) = -S^{prime}(\underline{r},t) - \frac{\beta}{\rho_0 c_0^4}\partial_t^2 p^2(\underline{r},t),$$

may be obtained by recasting the differential equation into an integral equation, viz.

$$\hat{p}(\underline{r},\omega) = \hat{p}^{inc}(\underline{r},\omega) - \int_{\underline{r}\in D} G(\underline{r}-\underline{r}',\omega)\,\frac{\beta}{\rho_0 c_0^4}\,\omega^2\left\{\hat{p}(\underline{r},\omega) *_\omega \hat{p}(\underline{r},\omega)\right\} dV.$$

If the nonlinearity is weak, a Neumann scheme is sufficient to solve the integral equation. Note that with each iteration step, one additional harmonic is formed.

Non-Linear Ultrasound

Cardiac Imaging is a well known application for harmonic imaging, as the harmonic components are formed behind the ribs:

- no reflections from the ribs;
- a narrow beam profile.

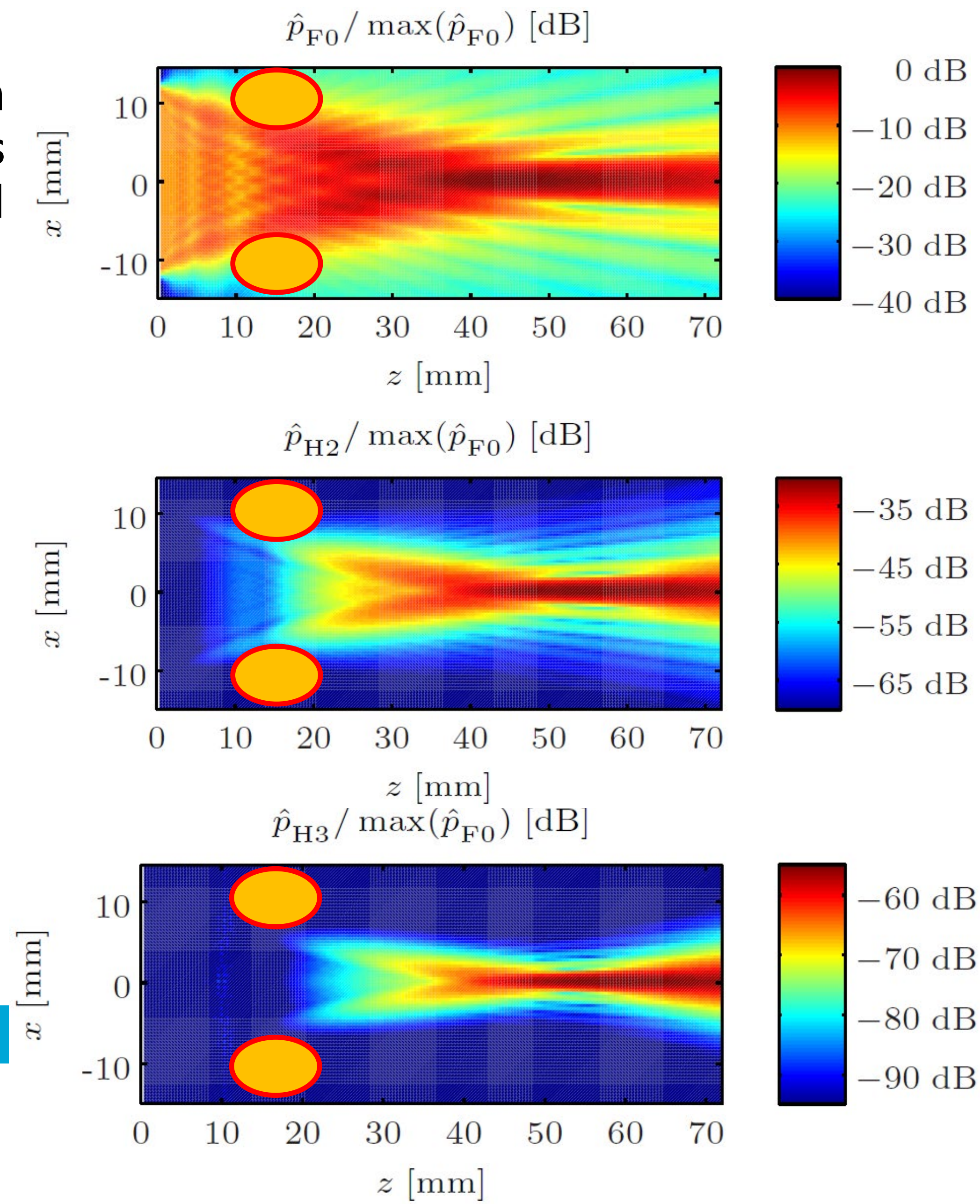

Non-linear Ultrasound

The non-linear propagation is also used to suppress side lobes which are mainly present within the fundamental component.

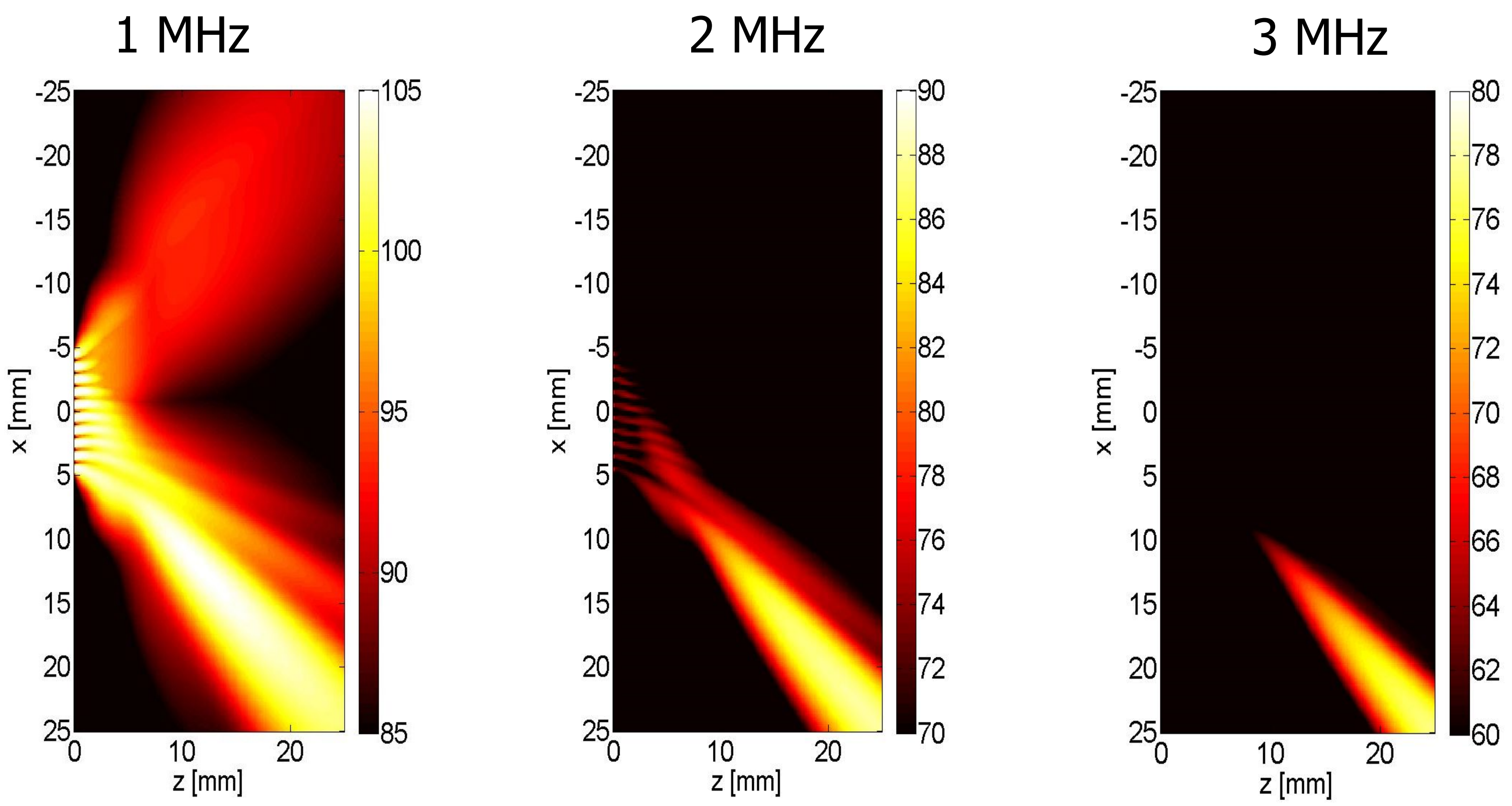

Beam Steering in 3-D

3 MHz 6 MHz

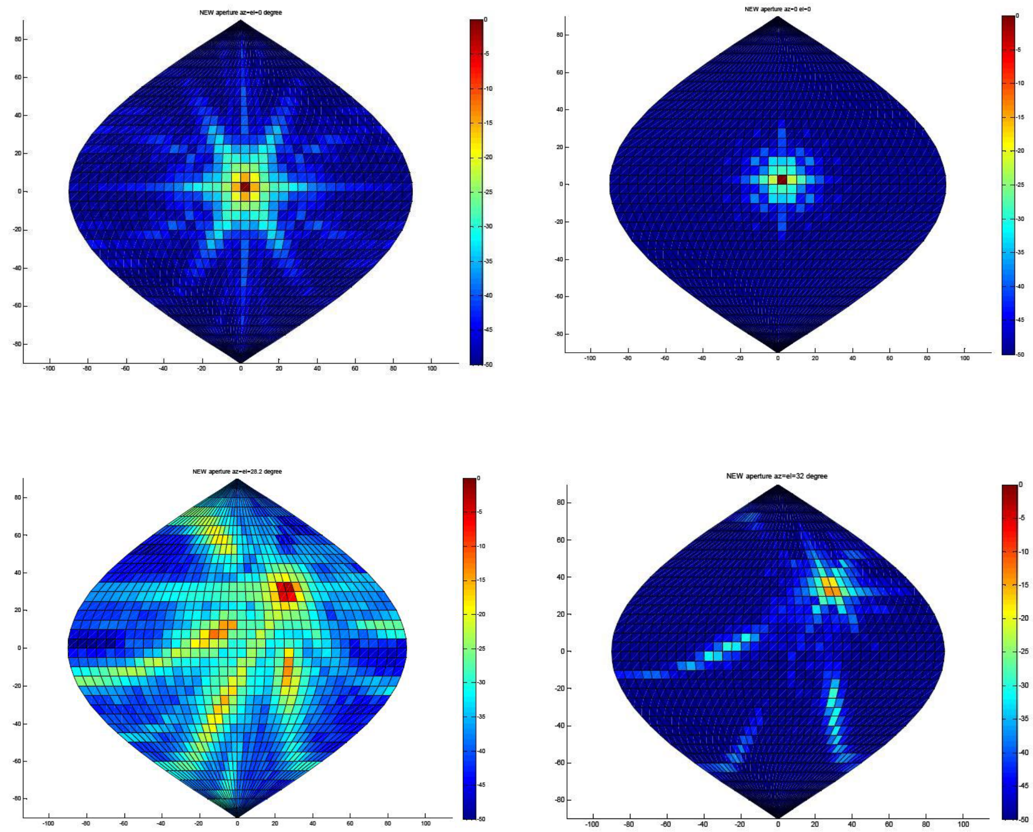

Non-linear Ultrasound

The non-linear propagation is also used to suppress side lobes which

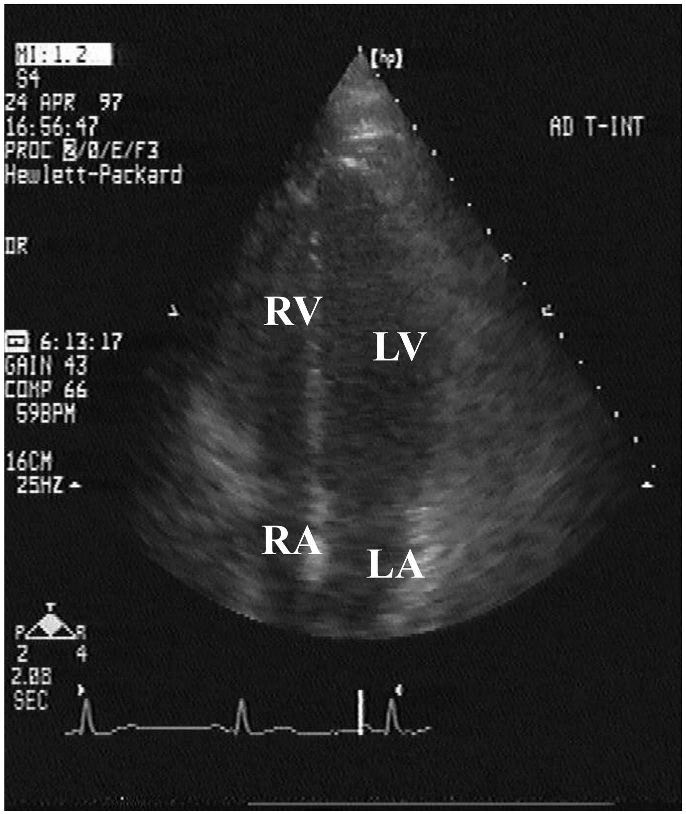

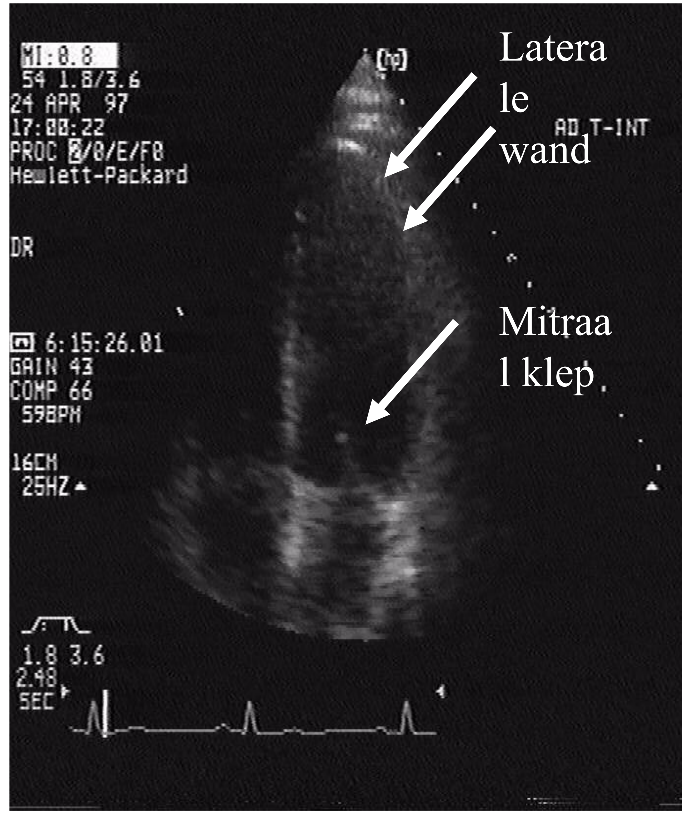

(Huygens – Fresnel) – Green – Kirchhoff – Rayleigh

- Wave-fields can be calculated as a function of space and time, from known values along a (closed) boundary.
- The oldest formulation of this process is Huygens' Principle. Later, Fresnel gave a more mathematical, but still somewhat heuristic description of wave-field extrapolation.
- Mathematically exact extrapolation of wave-fields is accomplished with the help of the Kirchhoff and Rayleigh integrals, which are based on Green's Theorem.
- The extrapolation algorithm is based on the wave equation and the causality of the wave propagation.
- Wave-fields can be extrapolated forward and backward in time and space.

Green's Theorem

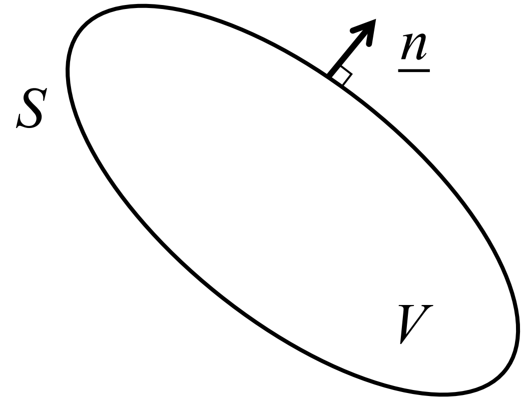

Consider Gauss' Theorem for any arbitrary vector field $\underline{a}(\underline{r})$ and arbitrary volume V, bounded by surface S :

$$\int_V \nabla \cdot \underline{a}(\underline{r})\, dV = \oint_S \underline{a}(\underline{r}) \cdot \underline{n}\, dS$$

For two functions f and g that are twice differentiable we can write:

$$\underline{a}(\underline{r}) = f(\underline{r}) \nabla g(\underline{r}) \qquad \Rightarrow \qquad \nabla \cdot \underline{a} = f \nabla^2 g + \nabla f \cdot \nabla g$$

and: $$\underline{a}'(\underline{r}) = g(\underline{r}) \nabla f(\underline{r}) \qquad \Rightarrow \qquad \nabla \cdot \underline{a}' = g \nabla^2 f + \nabla g \cdot \nabla f$$

$$\Rightarrow \qquad \nabla \cdot (\underline{a} - \underline{a}') = f \nabla^2 g - g \nabla^2 f$$

$$\Rightarrow \qquad \boxed{\int_V (f \nabla^2 g - g \nabla^2 f)\, dV = \oint_S (f \nabla g - g \nabla f) \cdot \underline{n}\, dS}$$

This is *Green's Second Identity.*

Kirchhoff Integral

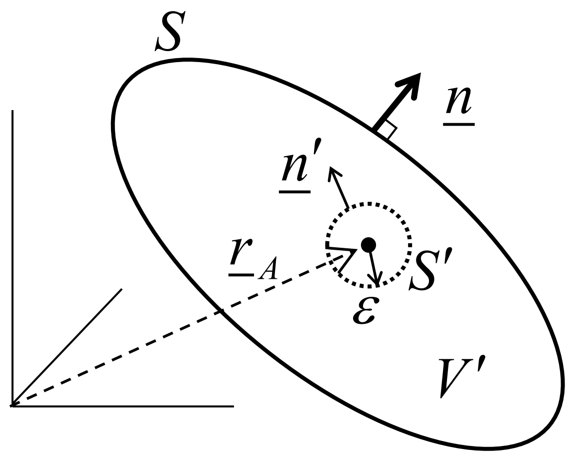

For f substitute $\hat{p}(\underline{r})$, which is a solution of the Helmholtz equation:

$$\nabla^2 \hat{p} + \frac{\omega^2}{c^2} \hat{p} = 0$$

everywhere in the volume V.

For g substitute $\hat{G}(\underline{r}) = \dfrac{e^{-i\omega|\underline{r}-\underline{r}_A|/c}}{4\pi|\underline{r}-\underline{r}_A|}$, which is a solution of:

$$\nabla^2 \hat{G}(\underline{r}) + \frac{\omega^2}{c^2} \hat{G}(\underline{r}) = -\delta(\underline{r}-\underline{r}_A)$$

in the volume V', which is inside S, *but outside* the surface S' around the point-source at $\underline{r}_A$ inside V.

$$\Rightarrow \qquad \int_{V'} \left(\hat{p} \nabla^2 \hat{G} - \hat{G} \nabla^2 \hat{p} \right) dV' = \int_{V'} \left(-\hat{p} \frac{\omega^2}{c^2} \hat{G} + \hat{G} \frac{\omega^2}{c^2} \hat{p} \right) dV' \equiv 0$$

$$\Rightarrow \qquad \oint_S \left(\hat{p} \nabla \hat{G} - \hat{G} \nabla \hat{p} \right) \cdot \underline{n} \, dS - \oint_{S'} \left(\hat{p} \nabla \hat{G} - \hat{G} \nabla \hat{p} \right) \cdot \underline{n}' \, dS' = 0$$

Kirchhoff Integral

For the integral over S' we can write:

$$\lim_{\varepsilon\to 0}\oint_{S'}\left(\hat{p}\,\nabla\hat{G}-\hat{G}\nabla\hat{p}\right)\cdot\underline{n}'\,dS'$$

$$=\lim_{\varepsilon\to 0}\int_0^{\pi}\int_0^{2\pi}\left[\hat{p}\left(\underline{r}_A+\cancel{\varepsilon\underline{n}'}\right)\frac{\partial}{\partial\varepsilon}\left(\frac{e^{-i\omega\varepsilon/c}}{4\pi\varepsilon}\right)-\cancel{\frac{e^{-i\omega\varepsilon/c}}{4\pi\varepsilon}\left(\nabla\hat{p}\cdot\underline{n}'\right)}\right]\varepsilon^2\sin\vartheta\,d\varphi\,d\vartheta$$

$$=\lim_{\varepsilon\to 0}\int_0^{\pi}\int_0^{2\pi}\left[\hat{p}\left(\underline{r}_A\right)\left(-\frac{1}{\varepsilon^2}-\cancel{\frac{i\omega}{c\varepsilon}}\right)e^{-i\omega\varepsilon/c}\,\frac{1}{4\pi}\right]\varepsilon^2\sin\vartheta\,d\varphi\,d\vartheta$$

$$=-\,\hat{p}\left(\underline{r}_A\right)$$

$$\Rightarrow\qquad\boxed{\hat{p}\left(\underline{r}_A\right)=-\oint_S\left(\hat{p}\,\nabla\hat{G}-\hat{G}\,\nabla\hat{p}\right)\cdot\underline{n}\,dS}$$

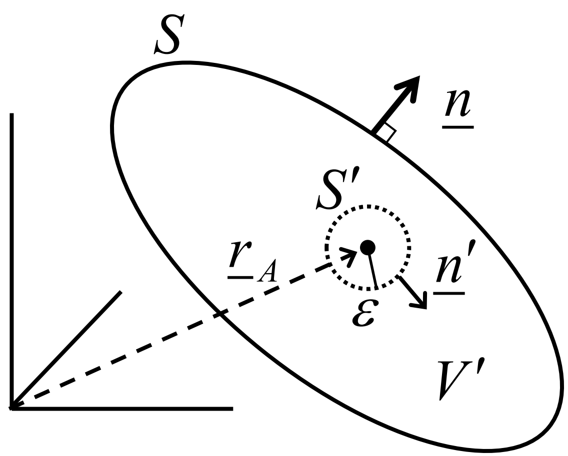

This is the *Kirchhoff integral.*

$$\hat{G}(\underline{r},\underline{r}_A,\omega)=\frac{e^{-i\omega\left|\underline{r}-\underline{r}_A\right|/c}}{4\pi\left|\underline{r}-\underline{r}_A\right|}$$

is called the *Green's function*.

Kirchhoff Integral

$$\hat{p}\left(\underline{r}_A\right) = -\oint_S \left(\hat{p}\nabla\hat{G} - \hat{G}\nabla\hat{p}\right)\cdot\underline{n}\, dS \qquad (\text{ point } A \text{ inside } S \text{ })$$

- The *Green's function* $\hat{G}(\underline{r},\omega)$ is the field of a point source located at $\underline{r}_A$ with delta-pulse wave-form.

- The field $\hat{G}$ does not co-exist with $\hat{p}$ in the same experiment. It is only introduced mathematically through Green's theorem.

- The Kirchhoff integral allows us to calculate the wave field $\hat{p}\left(\underline{r},\omega\right)$ at position $\underline{r}_A$, from recordings of $\hat{p}$ and $\left(\nabla\hat{p}\right)_n$ along any closed surface S around A.

- Application of the Kirchhoff integral can be cumbersome because:
  - We need recordings for both $\hat{p}$ and $\left(\nabla\hat{p}\right)_n$.
  - We need recordings along a closed surface.

- Under some limiting conditions there is a trick to be applied that circumvents both problems simultaneously.

Rayleigh Integral

In the Kirchhoff integral:

$$\hat{p}\left(\underline{r}_A,\omega\right) = -\oint_S \left(\hat{p}\,\nabla\hat{G} - \hat{G}\,\nabla\hat{p}\right)\cdot\underline{n}\;dS$$

there is a degree of freedom, since for any function $\hat{\Gamma}\left(\underline{r},\omega\right)$ that satisfies:

$$\nabla^2\hat{\Gamma} + \frac{\omega^2}{c^2}\hat{\Gamma} = 0$$

everywhere inside S, we can write:

$$\hat{p}\left(\underline{r}_A\right) = -\oint_S \left[\cancel{\hat{p}\,\nabla\left(\hat{G}+\hat{\Gamma}\right)} - \left(\hat{G}+\hat{\Gamma}\right)\nabla\hat{p}\right]\cdot\underline{n}\;dS$$

Obviously this is the case because:

$$\oint_S \left[\hat{p}\,\nabla\hat{\Gamma} - \hat{\Gamma}\,\nabla\hat{p}\right]\cdot\underline{n}\;dS = \int_V \left[\hat{p}\nabla^2\hat{\Gamma} - \hat{\Gamma}\nabla^2\hat{p}\right]dV = 0$$

Rayleigh Integral

We want to use the function Γ in the Kirchhoff integral:

$$\hat{p}\left(\underline{r}_A,\omega\right)=-\oint_S\left[\cancel{\hat{p}\nabla\left(\hat{G}+\hat{\Gamma}\right)}-\left(\hat{G}+\hat{\Gamma}\right)\nabla\hat{p}\right]\cdot\underline{n}\,dS$$

in such a way that either the term with $\hat{p}$ or the term with $\nabla\hat{p}$ vanishes over the relevant part of S.

What the relevant part of S is depends on where the sources are that generated the wave field $\hat{p}$ and whether we want to predict forward or backward in time.

If there are sources in all directions from the point A , the whole closed surface S is relevant and there exists no suitable choice for $\hat{\Gamma}$ that simplifies the Kirchhoff integral.

Rayleigh Integral

$$\hat{p}\left(\underline{r}_A,\omega\right) = -\oint_S \left[\hat{p}\nabla\left(\hat{G}+\hat{\Gamma}\right) - \left(\hat{G}+\hat{\Gamma}\right)\nabla\hat{p}\right]\cdot\underline{n}\, dS$$

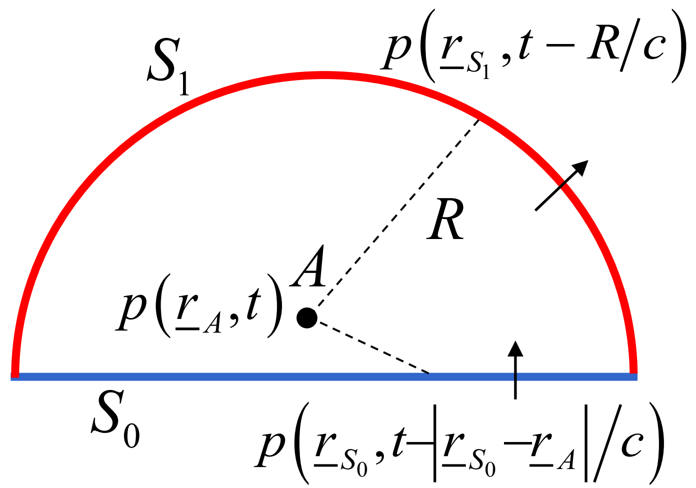

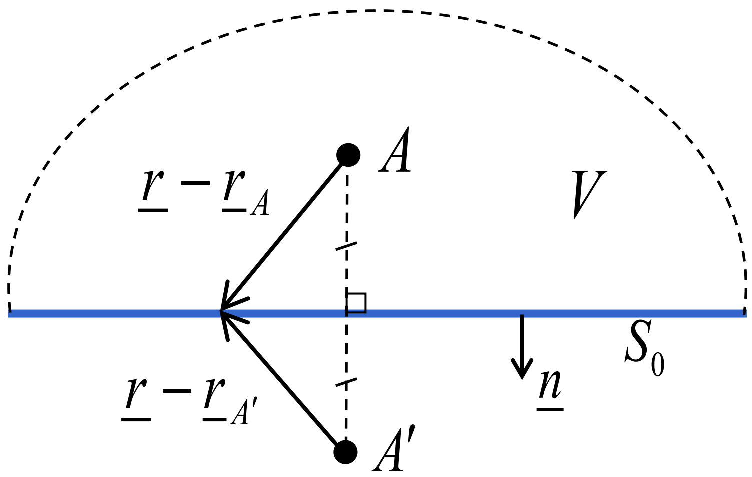

$$\hat{p}\left(\underline{r}_A,\omega\right) = \oint_S \left[\left(\hat{G}+\hat{\Gamma}\right)\nabla\hat{p}\right]\cdot\underline{n}\, dS \quad \leftarrow$$

$\nabla\left[\hat{G}(\underline{r}) + \hat{\Gamma}(\underline{r})\right] = 0$ for all $\underline{r} \in S_0$ (Rayleigh I)

$$\hat{p}\left(\underline{r}_A,\omega\right) = -\oint_S \hat{p}\nabla\left(\hat{G}+\hat{\Gamma}\right)\cdot\underline{n}\, dS \quad \leftarrow$$

$\hat{G}(\underline{r}) + \hat{\Gamma}(\underline{r}) = 0$ for all $\underline{r} \in S_0$ (Rayleigh II)

Rayleigh II Integral

We have established that in the case that all the sources of the field $\hat{p}$ are below the plane S_0 , we only need to integrate over S_0 .

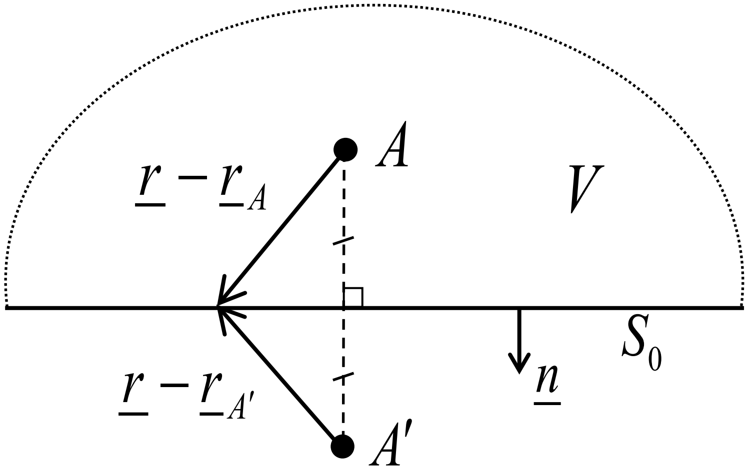

We now try to find a function $\hat{\Gamma}(\underline{r},\omega)$ that makes $\boxed{\hat{G}+\hat{\Gamma}=0 \text{ everywhere on } S_0}$.

Recalling that $\hat{G}$ is the wave field of a point source in point A , we can create a wave field $\hat{\Gamma}$ by putting a point-source with a negative source strength in the mirror point of A: A' .

This is legitimate because then the field $\hat{\Gamma}$ is not created by sources inside V and so satisfies the equation $\nabla^2\hat{\Gamma}+\left(\omega^2/c^2\right)\hat{\Gamma}=0$ everywhere inside V.

TU Delft

Rayleigh II Integral

If $\hat{G}+\hat{\Gamma}=0\big|_{\vec{r}\in S_0}$, the Kirchhoff integral reduces to:

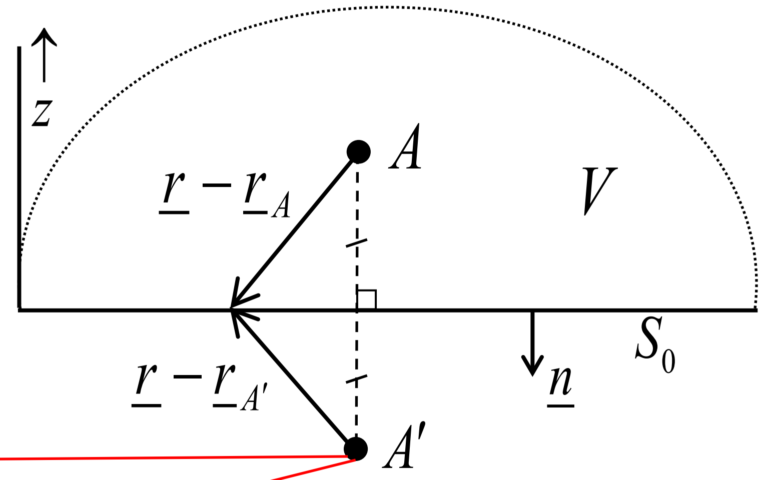

$$\hat{p}(\underline{r}_A) = -\int_{S_0} [\hat{p}\nabla(\hat{G}+\hat{\Gamma})]\cdot\underline{n}\; dS_0$$

with:

$$\hat{G}(\underline{r}) = \frac{e^{-i\omega|\underline{r}-\underline{r}_A|/c}}{4\pi|\underline{r}-\underline{r}_A|} \quad \text{and} \quad \hat{\Gamma}(\underline{r}) = -\frac{e^{-i\omega|\underline{r}-\underline{r}_{A'}|/c}}{4\pi|\underline{r}-\underline{r}_{A'}|}$$

where:

$$|\underline{r}-\underline{r}_A| = \sqrt{(x-x_A)^2+(y-y_A)^2+(z-z_A)^2}$$

$$|\underline{r}-\underline{r}_{A'}| = \sqrt{(x-x_A)^2+(y-y_A)^2+(z+z_A)^2}$$

On S_0 we have:

$$z=0 \quad , \quad |\underline{r}-\underline{r}_A| = |\underline{r}-\underline{r}_{A'}| \quad \text{and} \quad \nabla(\hat{G}+\hat{\Gamma})\cdot\underline{n} = -\left[\frac{\partial}{\partial z}(\hat{G}+\hat{\Gamma})\right]_{z=0}$$

Rayleigh II Integral

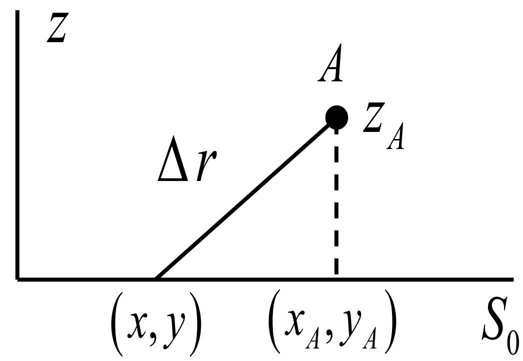

$$\frac{\partial}{\partial z}\left(\frac{e^{-i\omega|\underline{r}-\underline{r}_A|/c}}{4\pi|\underline{r}-\underline{r}_A|}\right) = -\frac{z-z_A}{|\underline{r}-\underline{r}_A|^3}\left(1+i\omega\frac{|\underline{r}-\underline{r}_A|}{c}\right)\frac{e^{-i\omega|\underline{r}-\underline{r}_A|/c}}{4\pi}$$

$$\frac{\partial}{\partial z}\left(-\frac{e^{-i\omega|\underline{r}-\underline{r}_{A'}|/c}}{4\pi|\underline{r}-\underline{r}_{A'}|}\right) = \frac{z+z_A}{|\underline{r}-\underline{r}_{A'}|^3}\left(1+i\omega\frac{|\underline{r}-\underline{r}_{A'}|}{c}\right)\frac{e^{-i\omega|\underline{r}-\underline{r}_{A'}|/c}}{4\pi}$$

$$\left[\frac{\partial}{\partial z}\left(\hat{G}+\hat{\Gamma}\right)\right]_{z=0} = \frac{z_A\left(1+i\omega\,\Delta r/c\right)}{2\pi\,\Delta r^3}e^{-i\omega\Delta r/c}$$

$$\Rightarrow \quad \boxed{\hat{p}(\underline{r}_A,\omega) = \frac{z_A}{2\pi}\int_{-\infty}^{\infty}\int_{-\infty}^{\infty}\hat{p}(x,y,0;\omega)\left(1+i\omega\frac{\Delta r}{c}\right)\frac{e^{-i\omega\Delta r/c}}{\Delta r^3}\,dxdy}$$

$$\Delta r = \sqrt{(x-x_A)^2+(y-y_A)^2+z_A^2}\ .$$

This is the *Rayleigh II integral*.

Rayleigh Integral

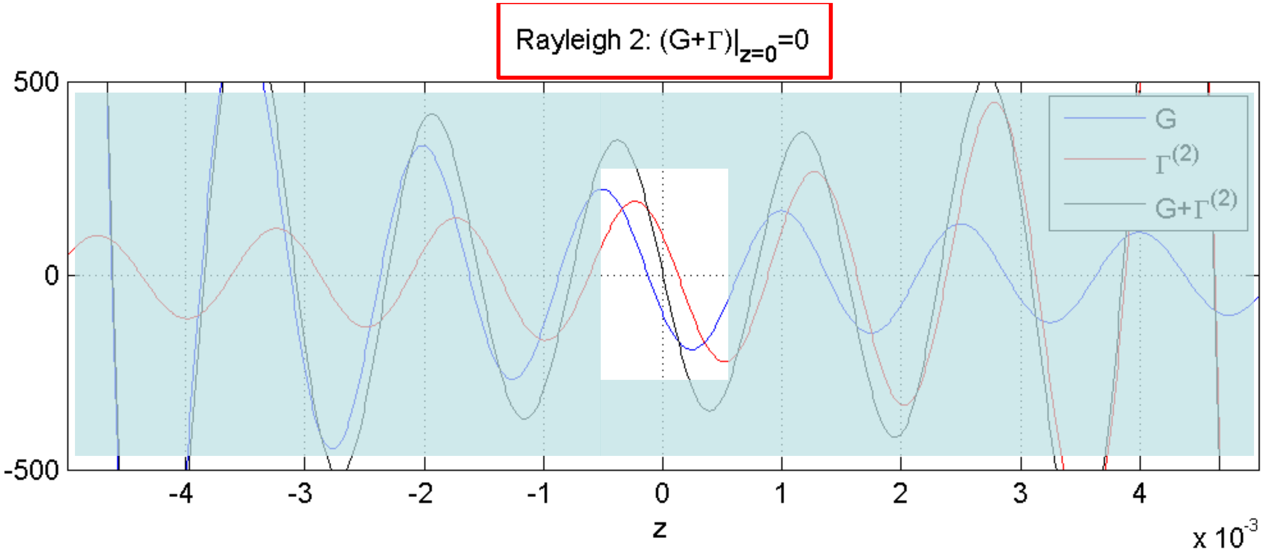

Rayleigh II example

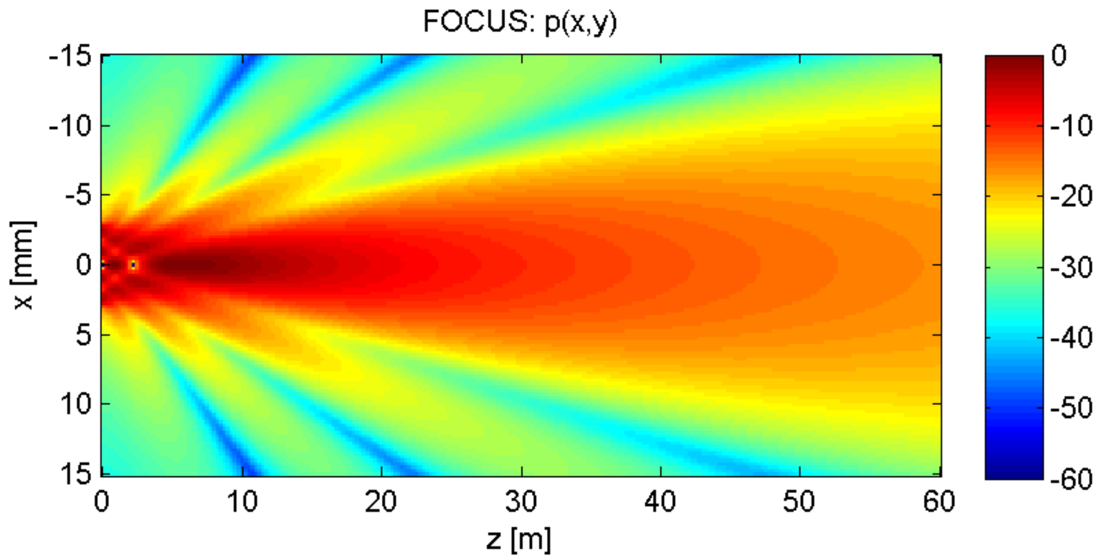

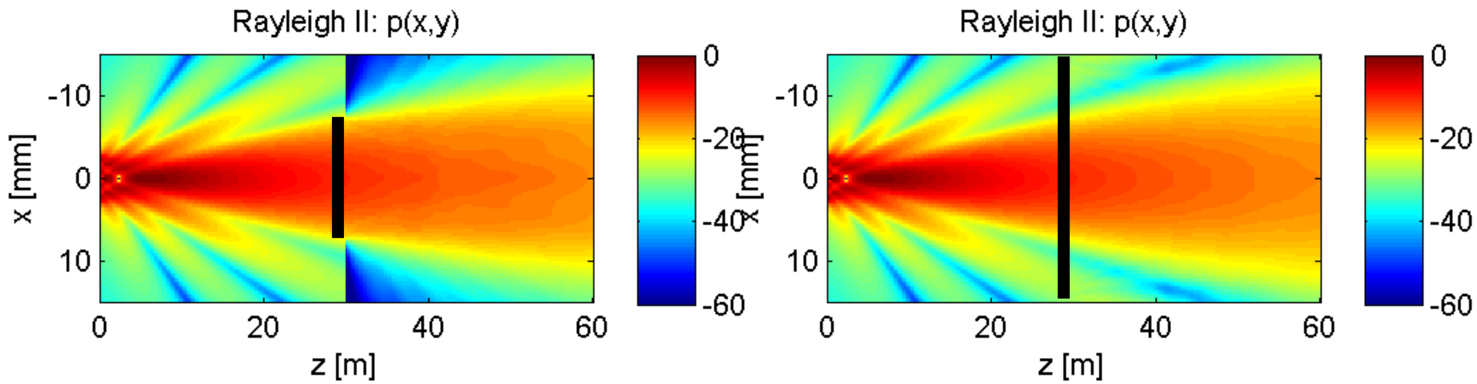

TU Delft

Rayleigh I Integral

An alternative choice for $\hat{\Gamma}$ in the Kirchhoff integral

$$\hat{p}\left(\underline{r}_A,\omega\right) = -\oint_S \left[\hat{p}\,\nabla\left(\hat{G}+\hat{\Gamma}\right) - \left(\hat{G}+\hat{\Gamma}\right)\nabla\hat{p}\right]\cdot\underline{n}\; dS$$

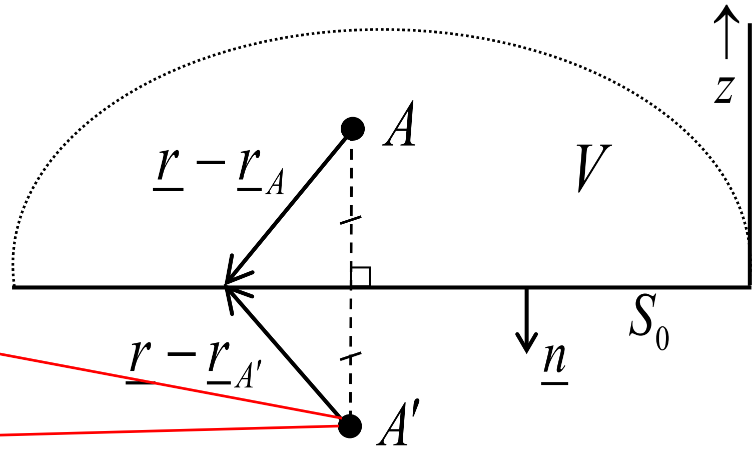

will cancel the term $\hat{p}\nabla\left(\hat{G}+\hat{\Gamma}\right)$.

By choosing:

$$\hat{G}(\underline{r}) = \frac{e^{-i\omega\left|\underline{r}-\underline{r}_A\right|/c}}{4\pi\left|\underline{r}-\underline{r}_A\right|} \quad \text{and} \quad \hat{\Gamma}\left(\underline{r}\right) = \frac{e^{-i\omega\left|\underline{r}-\underline{r}_{A'}\right|/c}}{4\pi\left|\underline{r}-\underline{r}_{A'}\right|}$$

we obtain the *Rayleigh I integral*:

$$\boxed{\hat{p}\left(\underline{r}_A,\omega\right) = -\frac{1}{2\pi}\int_{-\infty}^{\infty}\int_{-\infty}^{\infty} \frac{e^{-i\omega\Delta r/c}}{\Delta r}\left(\frac{\partial\hat{p}}{\partial z}\right)_{z=0} dxdy}$$

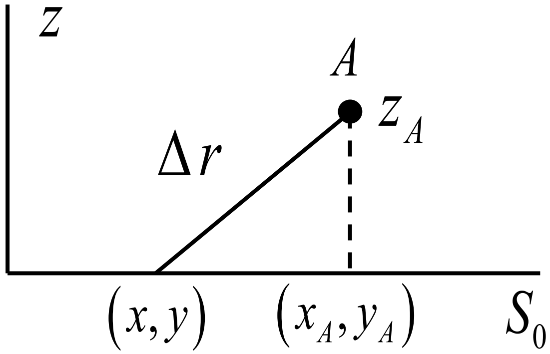

$$\Delta r = \sqrt{\left(x-x_A\right)^2 + \left(y-y_A\right)^2 + z_A^2}$$

Rayleigh Integral

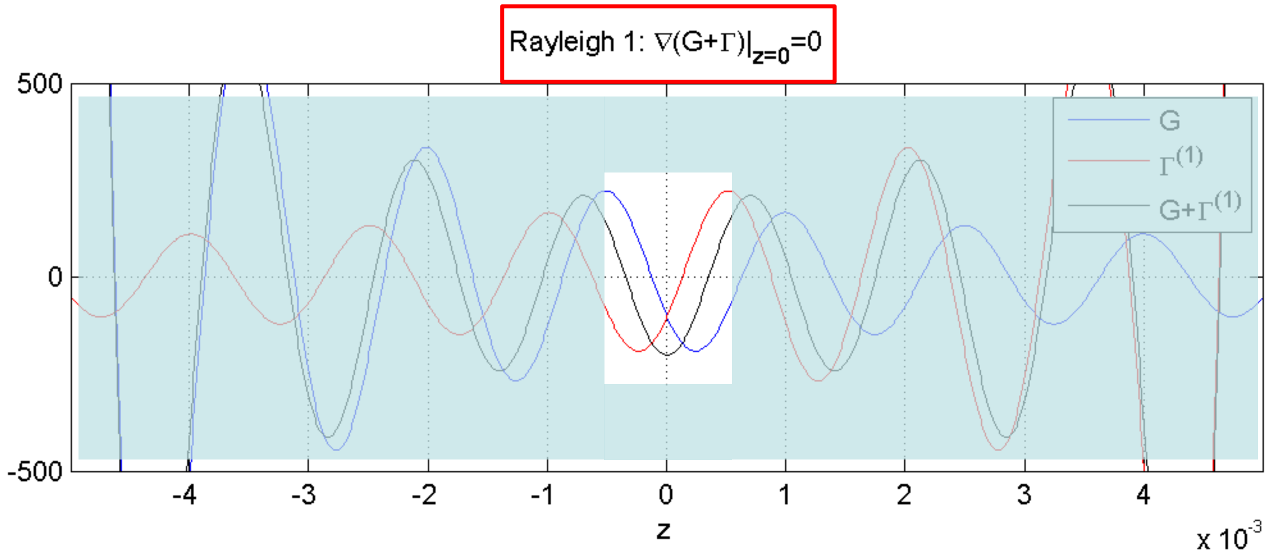

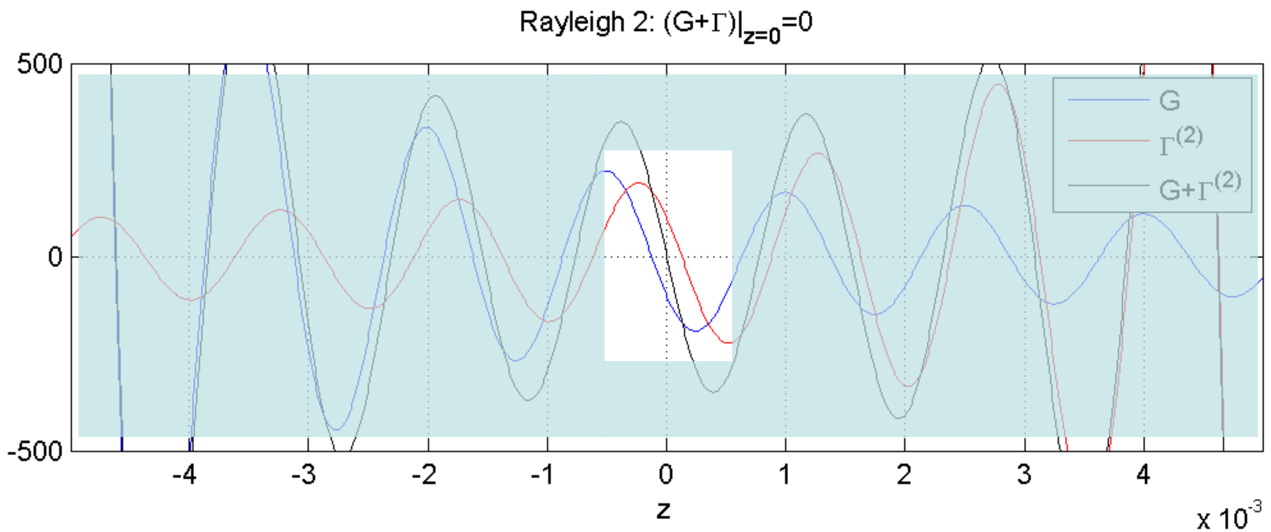

Helmholtz equation in the (k_x,k_y)-domain

We define the double spatial Fourier transform of $\hat{p}(x,y,z;\omega)$:

$$\tilde{\hat{p}}(k_x,k_y;z;\omega) \equiv \int_{-\infty}^{\infty}\int_{-\infty}^{\infty} e^{i(k_x x+k_y y)}\hat{p}(x,y,z;\omega)\,dxdy$$

So, double Fourier transformation of the Helmholtz equation to the (k_x,k_y)-domain:

$$\frac{\partial^2\hat{p}}{\partial x^2}+\frac{\partial^2\hat{p}}{\partial y^2}+\frac{\partial^2\hat{p}}{\partial z^2}+\frac{\omega^2}{c^2}\hat{p}=0 \quad\Rightarrow\quad \frac{\partial^2\tilde{\hat{p}}}{\partial z^2}+\left(\frac{\omega^2}{c^2}-k_x^2-k_y^2\right)\tilde{\hat{p}}=0$$

with $k_z \equiv \sqrt{(\omega/c)^2-k_x^2-k_y^2}$, we get: $\boxed{\dfrac{\partial^2\tilde{\hat{p}}}{\partial z^2}+k_z^2\tilde{\hat{p}}=0}$.

TUDelft

Helmholtz equation in the (k_x, k_y)-domain

Let us consider a wave field $\tilde{\tilde{p}}\left(k_x, k_y, z; \omega\right)$, generated by sources below the $z = z_0$ plane.

Then the source-free Helmholtz equation:

$$\frac{\partial^2 \tilde{\tilde{p}}}{\partial z^2} + k_z^2 \tilde{\tilde{p}} = 0 \qquad \text{with:} \qquad k_z = \sqrt{\frac{\omega^2}{c^2} - \left(k_x^2 + k_y^2\right)}$$

is valid for all $z \geq z_0$.

Since waves are travelling in the positive z direction only, the above differential equation in z is readily solved for $z \geq z_0$, by:

$$\boxed{\tilde{\tilde{p}}\left(k_x, k_y, z_0 + \Delta z; \omega\right) = \tilde{\tilde{p}}\left(k_x, k_y, z_0; \omega\right) e^{-ik_z \Delta z}} \quad , \qquad \Delta z > 0$$

where $\tilde{\tilde{p}}\left(k_x, k_y, z_0; \omega\right)$ represents the double spatial Fourier transform of the observations made in the $z = z_0$ plane.

The factor $e^{-ik_z \Delta z}$ is the multiplicative forward extrapolation operator in the $\left(k_x, k_y, z\right)$-domain.

TU Delft

Evanescent Field

For $k_x^2 + k_y^2 > \frac{\omega^2}{c^2}$, we have

$$k_z = \sqrt{\frac{\omega^2}{c^2} - \left(k_x^2 + k_y^2\right)} = \pm i\sqrt{\left|\frac{\omega^2}{c^2} - \left(k_x^2 + k_y^2\right)\right|}$$

and:

$$e^{-ik_z\Delta z} = e^{\pm\sqrt{\left|(\omega/c)^2 - \left(k_x^2 + k_y^2\right)\right|}\,\Delta z}$$

As the plus sign would be physically unacceptable in the half space $\Delta z \geq 0$, we get:

$$\tilde{\tilde{p}}\left(k_x, k_y, z\,;\omega\right) = \tilde{\tilde{p}}\left(k_x, k_y, z_0\,;\omega\right) e^{-\sqrt{\left|(\omega/c)^2 - \left(k_x^2 + k_y^2\right)\right|}\,\Delta z} \quad , \quad k_x^2 + k_y^2 > \frac{\omega^2}{c^2}$$

Any energy in $\tilde{\tilde{p}}\left(k_x, k_y, z_0\,;\omega\right)$ for which $k_x^2 + k_y^2 > \omega^2/c^2$, dies out very quickly with increasing Δz . This is called the *evanescent* field.

TU Delft

Evanescent Field

$$\left| e^{-iz\sqrt{(\omega/c)^2 - k_x^2 - k_y^2}} \right|$$

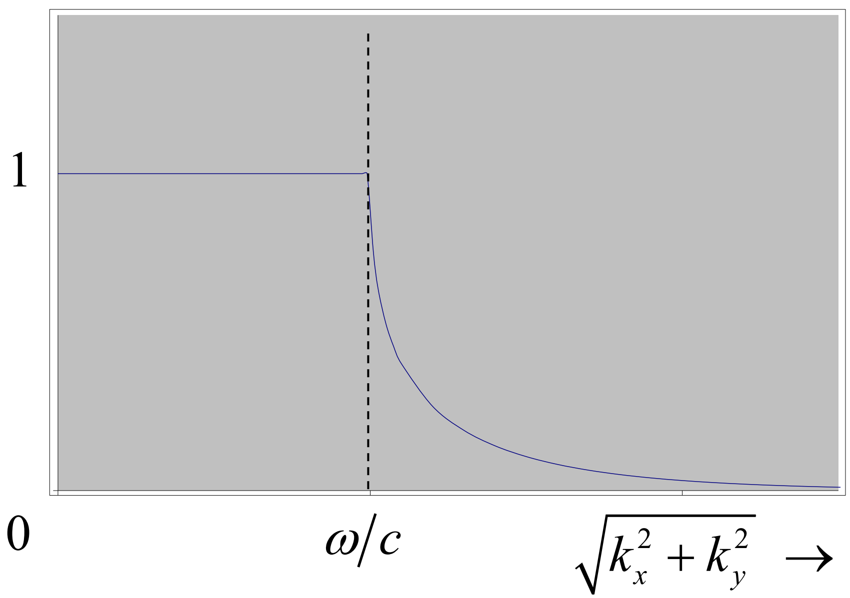

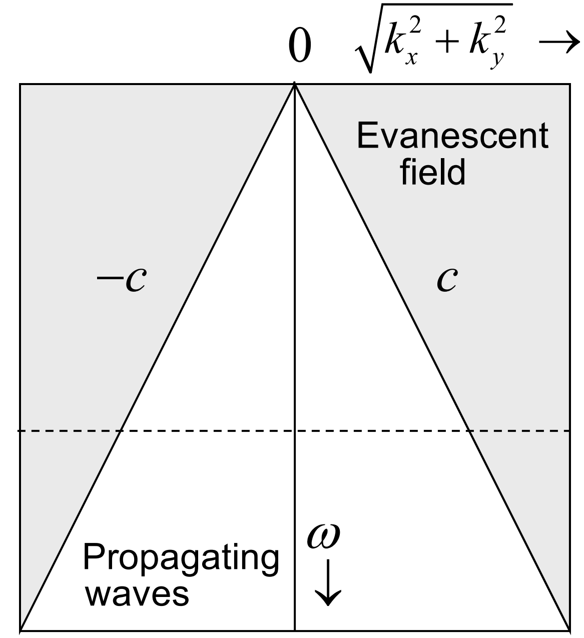

The evanescent field is observable only in 2-D plane-wave decompositions of wave-fields $\left(\text{remember } k_z \equiv \sqrt{(\omega/c)^2 - k_x^2 - k_y^2}\right)$.

Example

This technique can be used to reconstruct the velocity profile of an ultrasound transducer.

The pressure field at $z=a$ can be obtained from measurements at $z=0$ as follows:

$$\tilde{\tilde{p}}\left(k_x,k_y,z=a\,;\omega\right)=\tilde{\tilde{p}}\left(k_x,k_y,z=0\,;\omega\right)e^{-ik_z a} \quad ,$$

with $k_z=\sqrt{\dfrac{\omega^2}{c^2}-k_x^2-k_y^2}$, or $k_z=-i\sqrt{\left|\dfrac{\omega^2}{c^2}-k_x^2-k_y^2\right|}$ if $\dfrac{\omega^2}{c^2}<k_x^2+k_y^2$.

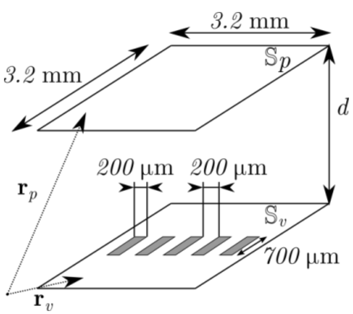

To obtain the field at $z=0$ from measurements at $z=a$,

means we devide by $e^{-ik_z a}$, i.e.

$$\tilde{\tilde{p}}\left(k_x,k_y,z=0\,;\omega\right)=\tilde{\tilde{p}}\left(k_x,k_y,z=a\,;\omega\right)e^{+ik_z a}.$$

However, problems arise for $k_z=-i\sqrt{\left|\dfrac{\omega^2}{c^2}-k_x^2-k_y^2\right|}$ if $\dfrac{\omega^2}{c^2}<k_x^2+k_y^2$.

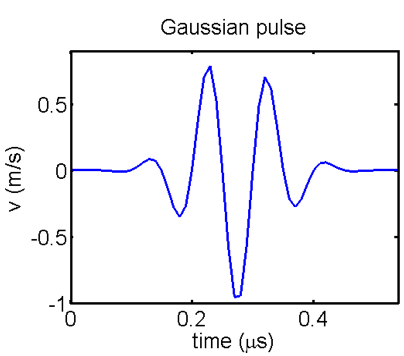

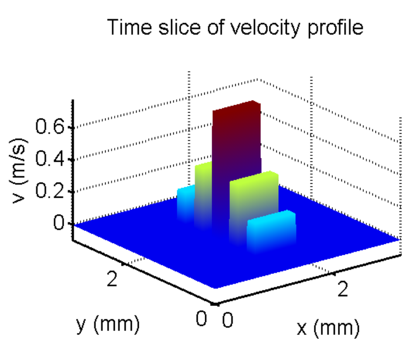

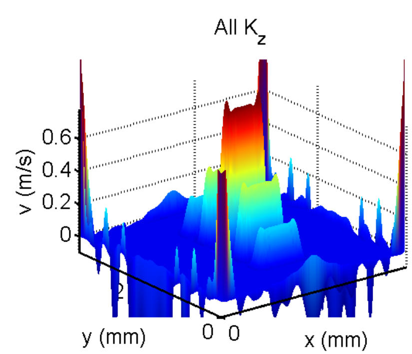

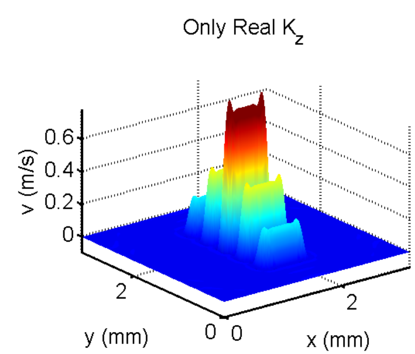

Example

- Reconstruction of the velocity profile of a damaged IVUS transducer.

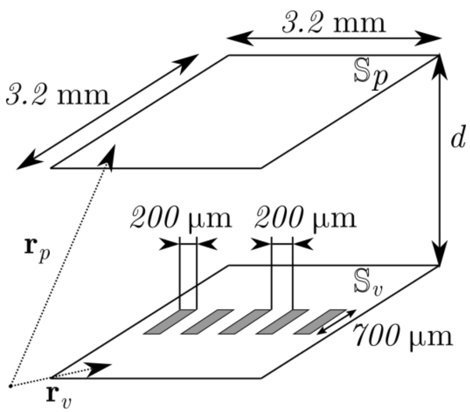

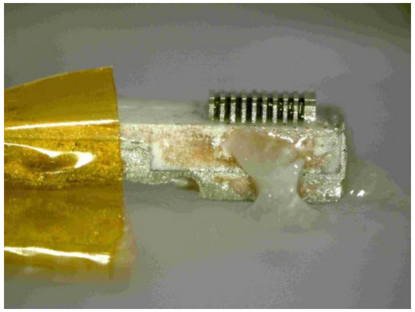

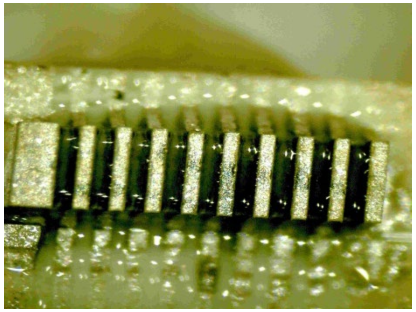

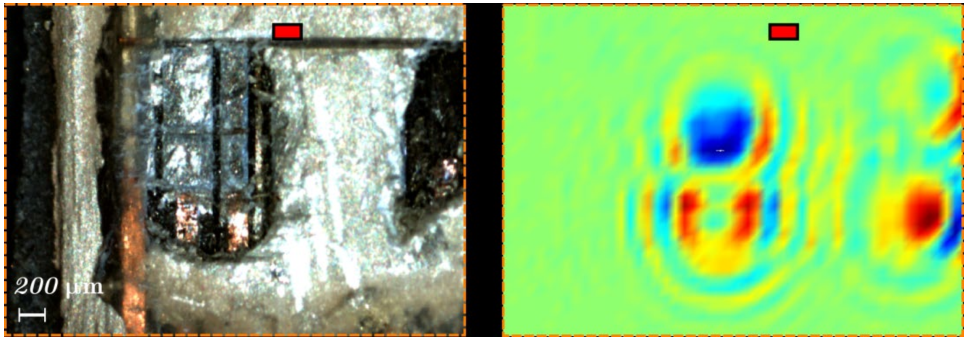

E.J. Alles and K.W.A. van Dongen, "Iterative reconstruction of the transducer surface velocity," IEEE Transactions on Ultrasonics, Ferroelectrics, and Frequency Control 60(5), pp. 954-962, May 2013.

Heterogeneous Media

- Incident, scattered and total field
- Forward and inverse problem

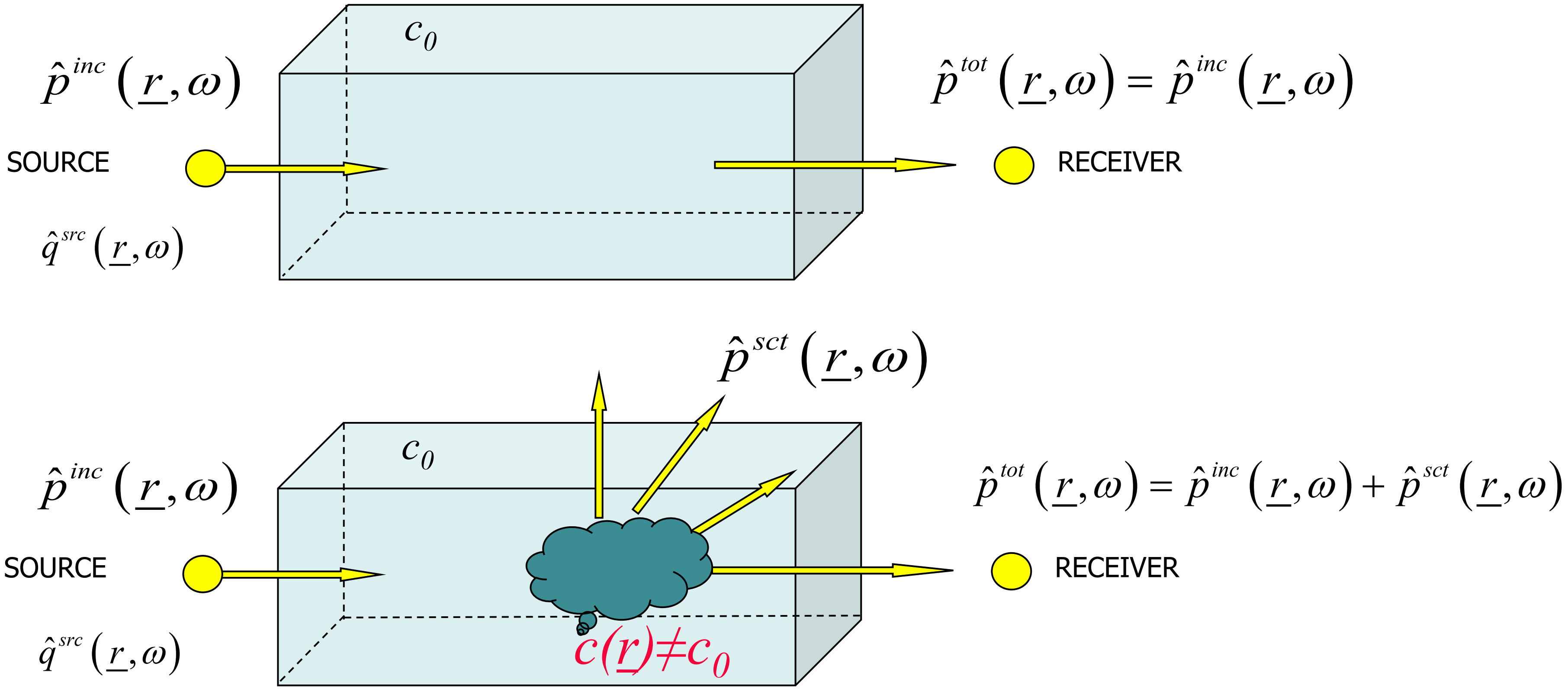

Heterogeneous Media – Field Equations

For heterogeneous media, the acoustic media parameters become spatially varying. Consequently, the resulting field equations will read

Hooke's law: $\nabla\cdot\underline{v}(\underline{r},t)+\kappa(\underline{r})\partial_t p(\underline{r},t)=q(\underline{r},t) \quad\Rightarrow\quad \begin{aligned}&\nabla\cdot\underline{v}(\underline{r},t)+\kappa_0\partial_t p(\underline{r},t)\\&\quad=q(\underline{r},t)+\{\kappa_0-\kappa(\underline{r})\}\partial_t p(\underline{r},t)\end{aligned}$

Newton's law: $\nabla p(\underline{r},t)+\rho(\underline{r})\partial_t\underline{v}(\underline{r},t)=\underline{f}(\underline{r},t) \quad\Rightarrow\quad \begin{aligned}&\nabla p(\underline{r},t)+\rho_0\partial_t\underline{v}(\underline{r},t)\\&\quad=\underline{f}(\underline{r},t)+\{\rho_0-\rho(\underline{r})\}\partial_t\underline{v}(\underline{r},t)\end{aligned}$

Combining the above field equations yield the following wave equation

$$\nabla^2 p(\underline{r},t)-\frac{1}{c_0^2}\partial_t^2 p(\underline{r},t)=-\underbrace{\{\rho_0\partial_t q(\underline{r},t)-\nabla\underline{f}(\underline{r},t)\}}_{S_{pr}(\underline{r},t)}-\underbrace{\{\rho_0\{\kappa_0-\kappa(\underline{r})\}\partial_t^2 p(\underline{r},t)-\nabla[\{\rho_0-\rho(\underline{r})\}\partial_t\underline{v}(\underline{r},t)]\}}_{S_{cs}(\underline{r},t)}$$

or

$$\nabla^2\hat{p}(\underline{r},\omega)+\frac{\omega^2}{c_0^2}\hat{p}(\underline{r},\omega)=-\{\rho_0 i\omega\hat{q}(\underline{r},\omega)-\nabla\hat{\underline{f}}(\underline{r},\omega)\}-\{-\rho_0\{\kappa_0-\kappa(\underline{r})\}\omega^2\hat{p}(\underline{r},\omega)-\nabla[\{\rho_0-\rho(\underline{r})\}i\omega\hat{\underline{v}}(\underline{r},\omega)]\}$$

TU Delft

Heterogeneous Media – Field Equations

Typically, spatial variations in the volume density of mass are neglected.

Consequently, the resulting field equations will read

Hooke's law:
$$\nabla\cdot\underline{v}(\underline{r},t)+\kappa(\underline{r})\partial_t p(\underline{r},t)=q(\underline{r},t) \quad\Rightarrow\quad \begin{aligned}&\nabla\cdot\underline{v}(\underline{r},t)+\kappa_0\partial_t p(\underline{r},t)\\ &\quad=q(\underline{r},t)+\{\kappa_0-\kappa(\underline{r})\}\partial_t p(\underline{r},t)\end{aligned}$$

Newton's law:
$$\nabla p(\underline{r},t)+\rho(\underline{r})\partial_t\underline{v}(\underline{r},t)=\underline{f}(\underline{r},t) \quad\Rightarrow\quad \begin{aligned}&\nabla p(\underline{r},t)+\rho_0\partial_t\underline{v}(\underline{r},t)\\ &\quad=\underline{f}(\underline{r},t)+\cancel{\{\rho_0-\rho(\underline{r})\}\partial_t\underline{v}(\underline{r},t)}\end{aligned}$$

Combining the above field equations yield the following wave equation

$$\nabla^2 p(\underline{r},t)-\frac{1}{c_0^2}\partial_t^2 p(\underline{r},t)=-\underbrace{\{\rho_0\partial_t q(\underline{r},t)-\nabla\cdot\underline{f}(\underline{r},t)\}}_{S_{pr}(\underline{r},t)}-\underbrace{\left\{\left(\frac{1}{c_0^2}-\frac{1}{c^2(\underline{r})}\right)\partial_t^2 p(\underline{r},t)-\cancel{\nabla\cdot\left[\{\rho_0-\rho(\underline{r})\}\partial_t\underline{v}(\underline{r},t)\right]}\right\}}_{S_{cs}(\underline{r},t)}$$

or

$$\nabla^2\hat{p}(\underline{r},\omega)+\frac{\omega^2}{c_0^2}\hat{p}(\underline{r},\omega)=-\{\rho_0 i\omega\hat{q}(\underline{r},\omega)-\nabla\cdot\hat{\underline{f}}(\underline{r},\omega)\}-\left\{-\left(\frac{1}{c_0^2}-\frac{1}{c^2(\underline{r})}\right)\omega^2\hat{p}(\underline{r},\omega)-\cancel{\nabla\cdot\left[\{\rho_0-\rho(\underline{r})\}i\omega\hat{\underline{v}}(\underline{r},\omega)\right]}\right\}$$

TU Delft

Heterogeneous Media – Integral Equation

Green's function $\hat{G}(\underline{r},\omega)=\dfrac{e^{-i\omega|\underline{r}|/c}}{4\pi|\underline{r}|}$ represents the field generated by a Dirac delta source.

Hence, the field generated by the primary sources $S_{pr}(\underline{r}',t)$ may be obtained by spatially convolving them with Green's function, hence

$$\hat{p}^{inc}(\underline{r},\omega)=\int_{\underline{r}'\in D}\hat{G}(\underline{r}-\underline{r}',\omega)\,S_{pr}(\underline{r}',t)\,dV(\underline{r}').$$

Based on the principle of superposition, one could argue that each contrast acts as a source generating an acoustic field. Adding all these fields together yields the following integral equation (Fredholm integral equation of the second kind)

$$\boxed{\hat{p}(r,\omega)=\hat{p}^{inc}(\underline{r},\omega)+\int_{\underline{r}'\in D}\hat{G}(\underline{r}-\underline{r}',\omega)\chi(\underline{r}')\omega^2\,\hat{p}(\underline{r}',\omega)\,dV(\underline{r}')}$$

with $\chi(\underline{r}')=\dfrac{1}{c^2(\underline{r}')}-\dfrac{1}{c_0^2}.$

TU Delft

Heterogeneous Media – Integral Equation

- Forward problem: sources and contrast are known,
  total/actual field is unknown
  => linear problem

- Inverse problem: sources are known,
  total/actual field is known at the boundary,
  contrast and field in ROI is unknown.
  => non-linear problem

- Green's function is defined for the background medium,
  however there is a freedom to choose it heterogeneous or homogeneous.
  Obvious choice is to choose a background for which we have an analytical expression of the Green's function (or the incident field).

WKBJ = Wentzel – Kramers – Brillouin – Jeffreys

Born Approximation

If the contrast $\chi(\underline{r})$, or ω , or V are small enough, the integral equation:

$$\hat{p}(\underline{r},\omega) = \hat{p}^{inc}(\underline{r},\omega) + \int_{\underline{r}'\in D} \hat{G}(\underline{r}-\underline{r}',\omega)\,\chi(\underline{r}')\,\omega^2\,\hat{p}(\underline{r}',\omega)\,dV(\underline{r}')$$

can be linearised in the contrast χ by replacing $\hat{p}$ with $\hat{p}^{inc}$ on the right-hand side of the equation. We then get:

$$\hat{p}(\underline{r},\omega) = \hat{p}^{inc}(\underline{r},\omega) + \int_{\underline{r}'\in D} \hat{G}(\underline{r}-\underline{r}',\omega)\,\chi(\underline{r}')\,\omega^2\,\hat{p}^{inc}(\underline{r}',\omega)\,dV(\underline{r}')$$

from which $\hat{p}$ can be evaluated directly. This is called the *Born approximation.*

Neumann Series

The Born approximation can be seen as the first step in an iterative solution method.

The total field resulting from the Born approximation, $\hat{p}^{(1)}$, can be substituted on the right-hand side of the integral equation, to obtain the next iteration result $\hat{p}^{(2)}$, towards a solution of the full integral equation:

$$\hat{p}^{(2)}(\underline{r},\omega) = \hat{p}^{inc}(\underline{r},\omega) + \int_{\underline{r}'\in D} \hat{G}(\underline{r}-\underline{r}',\omega)\, \chi\left(\underline{r}'\right) \omega^2\, \hat{p}^{(1)}(\underline{r}',\omega)\, dV(\underline{r}')$$

The resulting values $\hat{p}^{(1)}$, $\hat{p}^{(2)}$,..., $\hat{p}^{(n)}$, form a series, which is called the *Neumann series*.

For strong contrasts, the iterative scheme may diverge from the true solution resulting in a need for more advanced iterative solution methods such as conjugate gradient methods.

Conjugate Gradient Method

The integral equation:

$$\hat{p}(\underline{r},\omega) = \hat{p}^{inc}(\underline{r},\omega) + \int_{\underline{r}'\in D} \hat{G}(\underline{r}-\underline{r}',\omega)\, \chi\left(\underline{r}'\right) \omega^2\ \hat{p}(\underline{r}',\omega)\, dV(\underline{r}')$$

can also be recast in an operator equation

$$\mathrm{p}^{inc} = \mathrm{p} - \mathrm{G}[\mathrm{p}] = \mathrm{L}[\mathrm{p}]$$

which can be solved iteratively

$$\mathrm{p}_n = \mathrm{p}_{n-1} + \alpha \mathrm{d}_n$$

by minimizing the L_2-norm of the error

$$\mathrm{Err} = \|\mathrm{r}_n\| = \left\|\mathrm{p}^{inc} - \mathrm{L}[\mathrm{p}_n]\right\| \quad .$$

Minimizing this error functional using e.g. a CG is known to be very efficient.

TU Delft

Exact Solutions – Spherical Contrast

A plane wave scattering at an acoustically penetrable sphere in a homogeneous background medium maybe modelled using an integral equation formulation.

There also exists an exact solution for this problem.

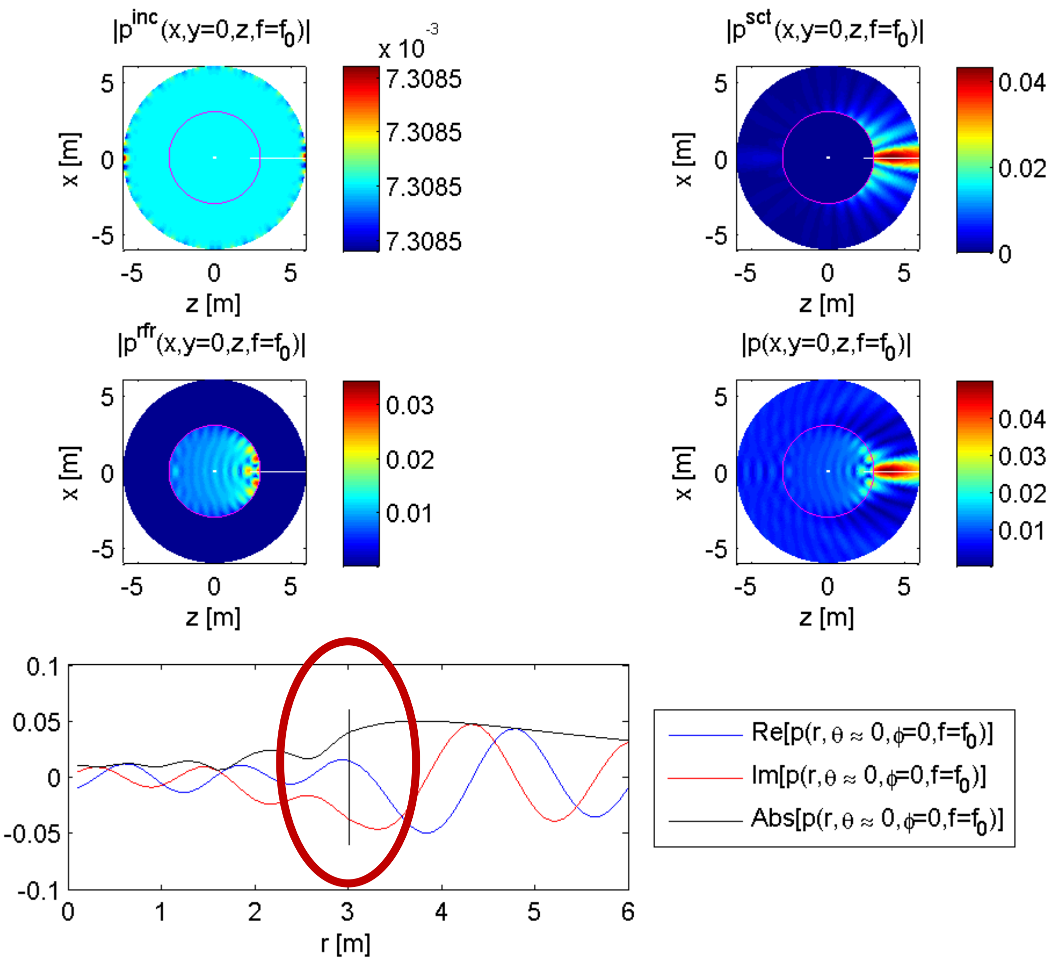

TU Delft

Exact Solutions – Spherical Contrast

By applying a Fourier transformation, time domain results are obtained.

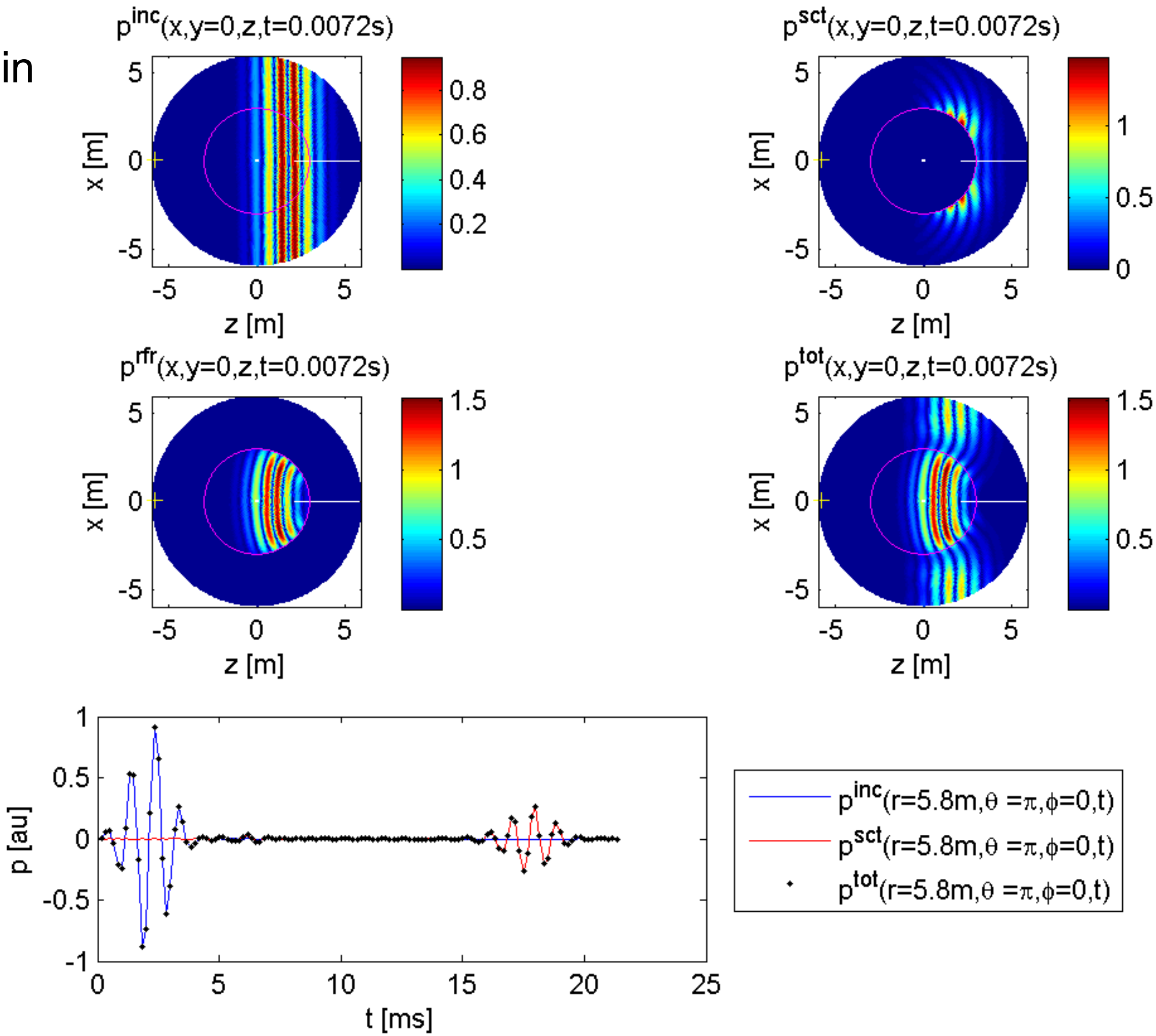

Exact Solutions – Spherical Contrast

Comparison of the obtained results using the exact and the iterative solution method shows that the iterative method is rather accurate.

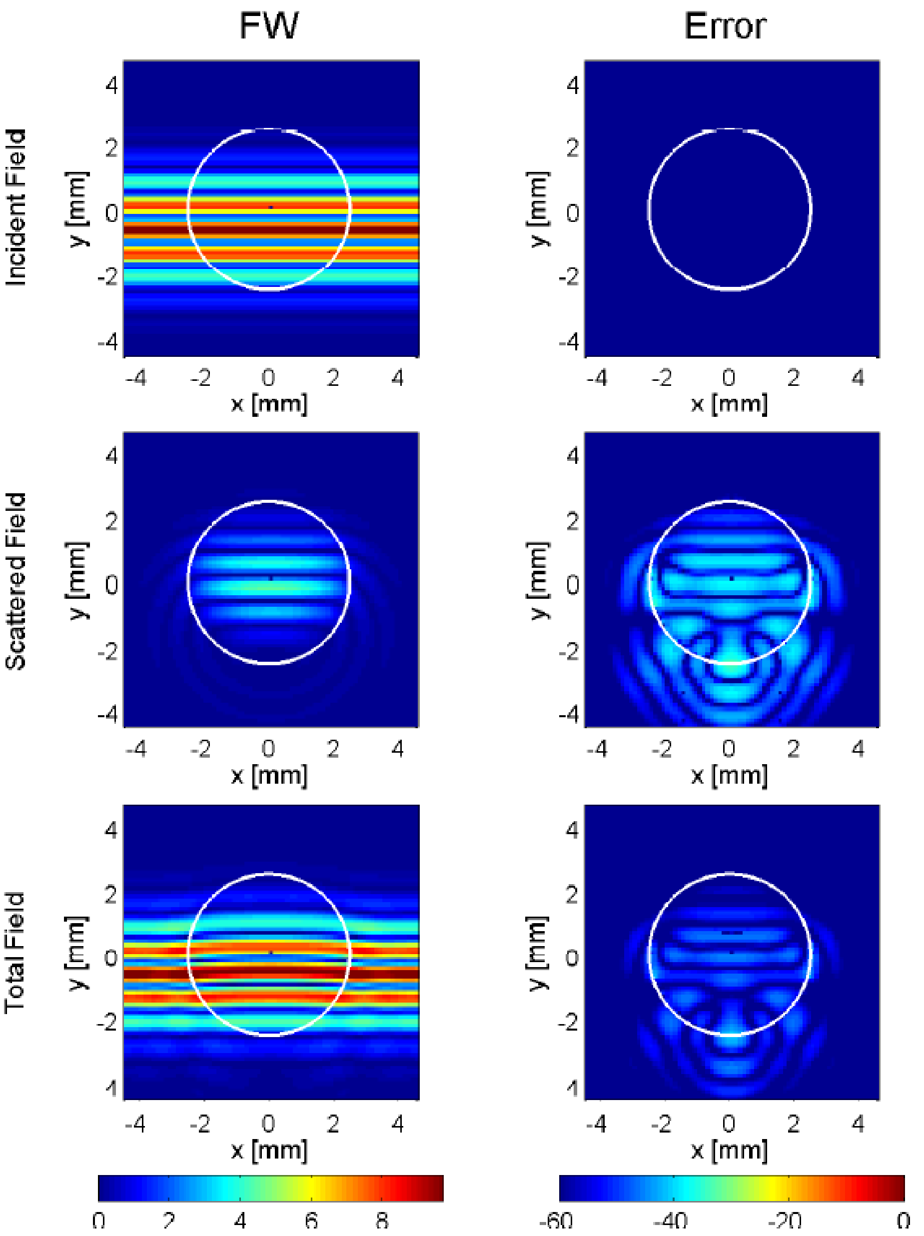

Transcranial ultrasound

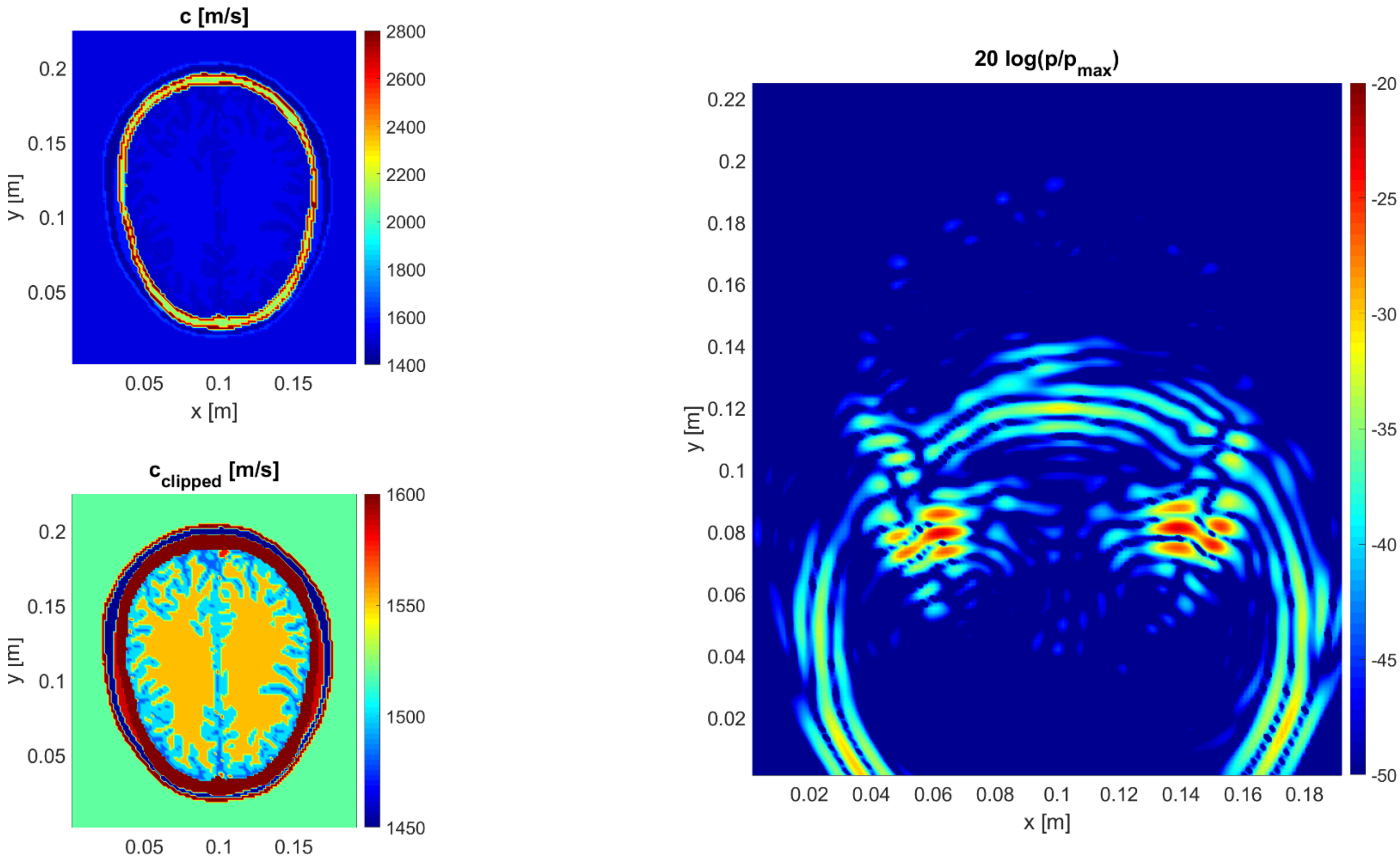

Imaging and Inversion

Acoustic and elastic wave fields may by used to image the interior of an object. Applications vary from:

- medical imaging (e.g. breast cancer detection)
- seismic surveys for the oil and gas industry
- Non-Destructive Testing (NDT)

Although no real definition exist,

- imaging is typically a direct method aiming at localizing contrasts,
- inversion is often an iterative method used for reconstructing acoustic medium parameters.

Imaging and Inversion

Imaging and Inversion starts with probing the volume of interest with an acoustic wave field.

To test different imaging and inversion methods we start with a simple example; a cancerous breast probed with an 0.1 MHz pulse.

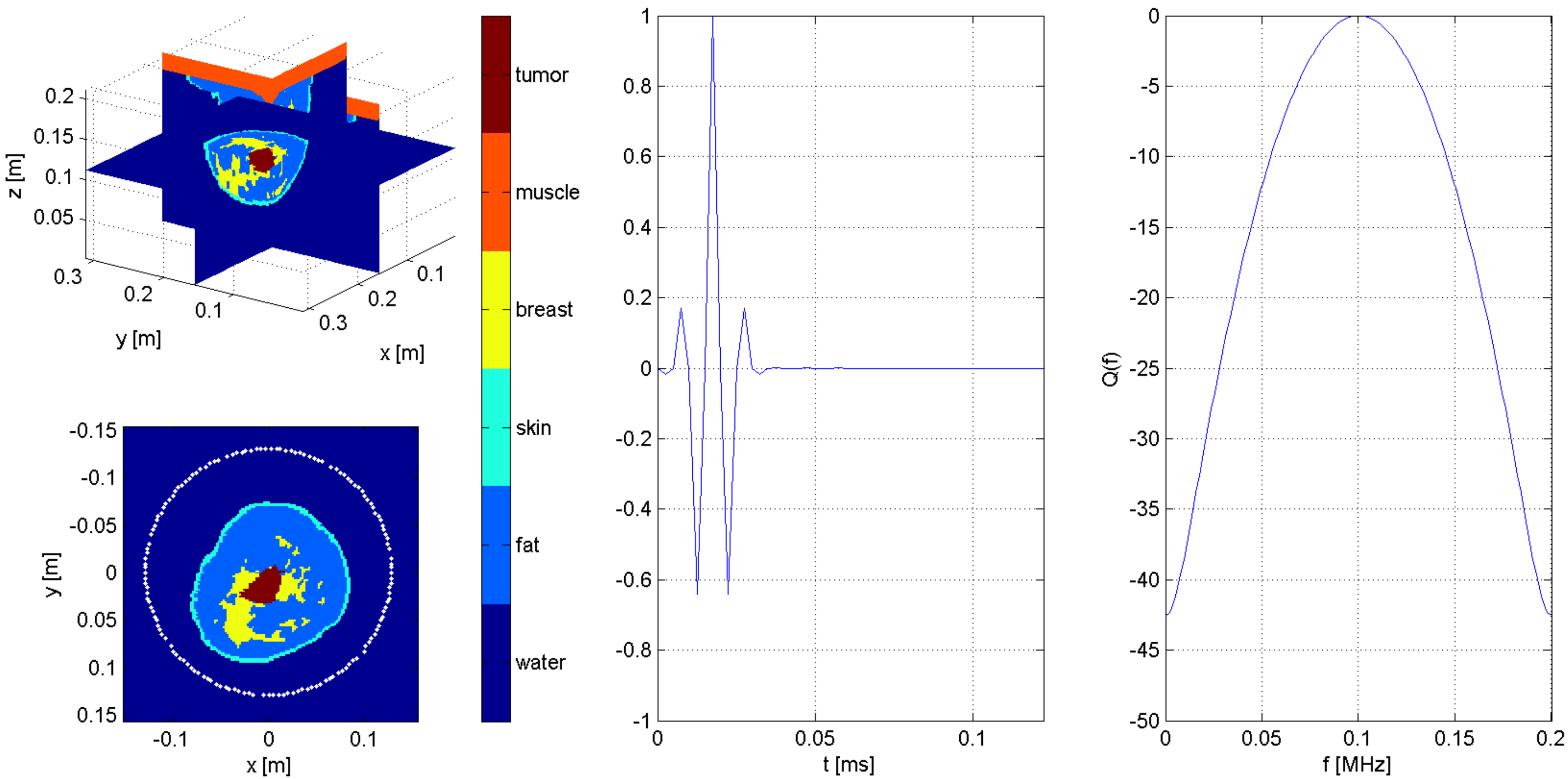

Forward Problem

Synthetic measurements are obtained by solving the forward problem.

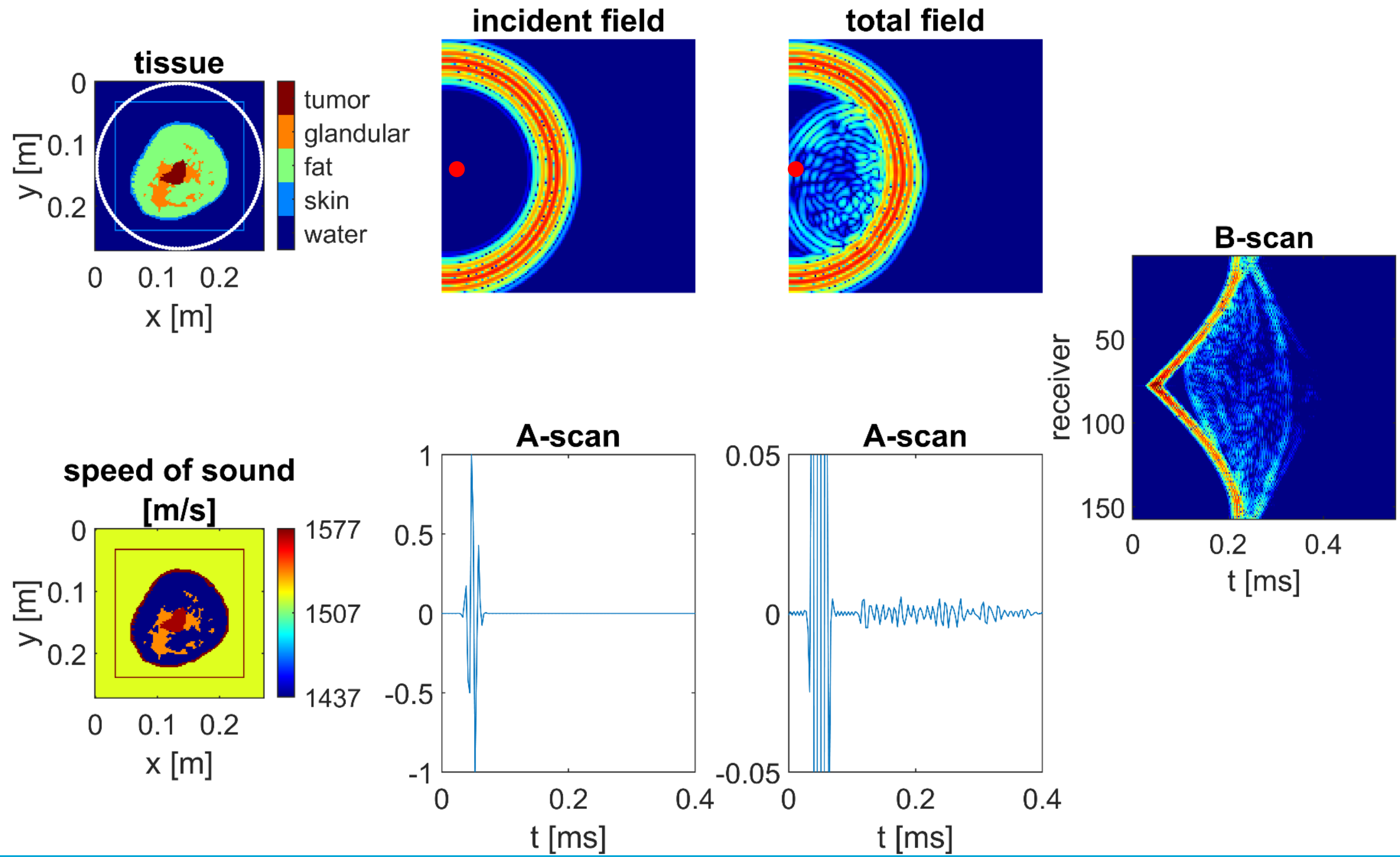

Time of Flight Reconstruction

Due to its success with CT-scans, tomographic reconstructions methods are applied where it is assumed that the wave field travels approximately along a straight path from source to receiver.

The variation in arrival times is then fully explained by a locally spatially varying speed of sound. Computing these variations in arrival time is referred to as the Radon transform.

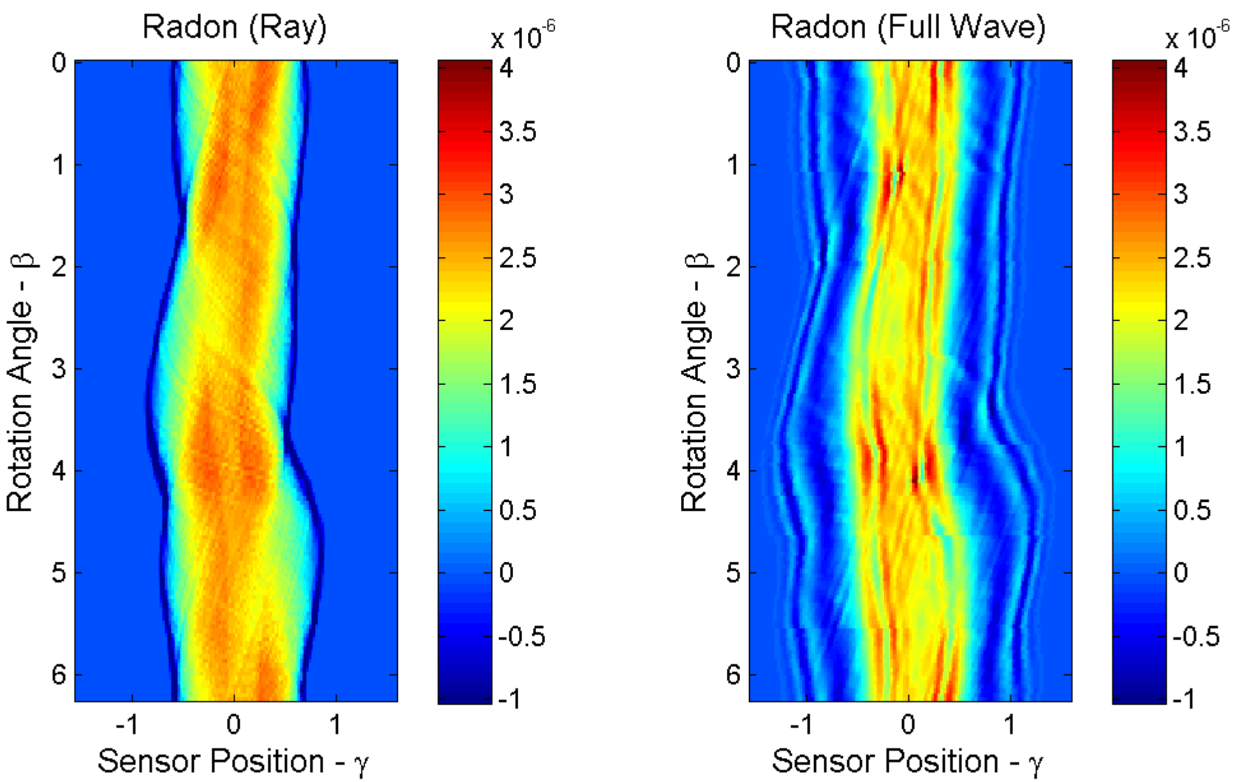

Time of Flight Reconstruction

A speed of sound profile may be obtained via the Inverse Radon transform; alternatives are algebraic reconstruction, or inverse Eikonal methods.

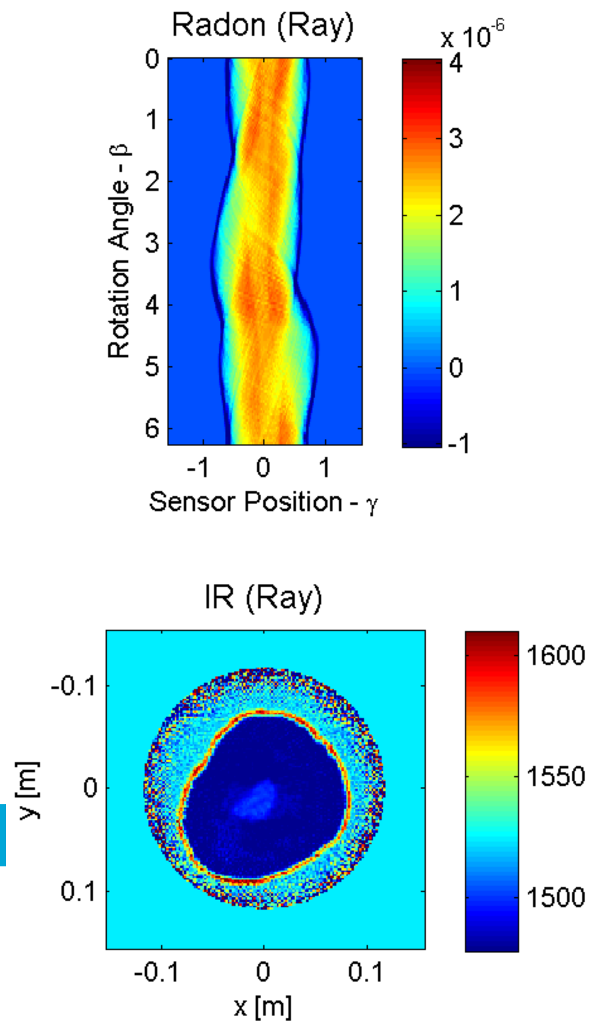

TUDelft

Synthetic Aperture Focussing Technique

- SAFT is a fast method with the disadvantage that it does not correct for geometrical spreading and radiation patterns.
- Imaging reflections only.

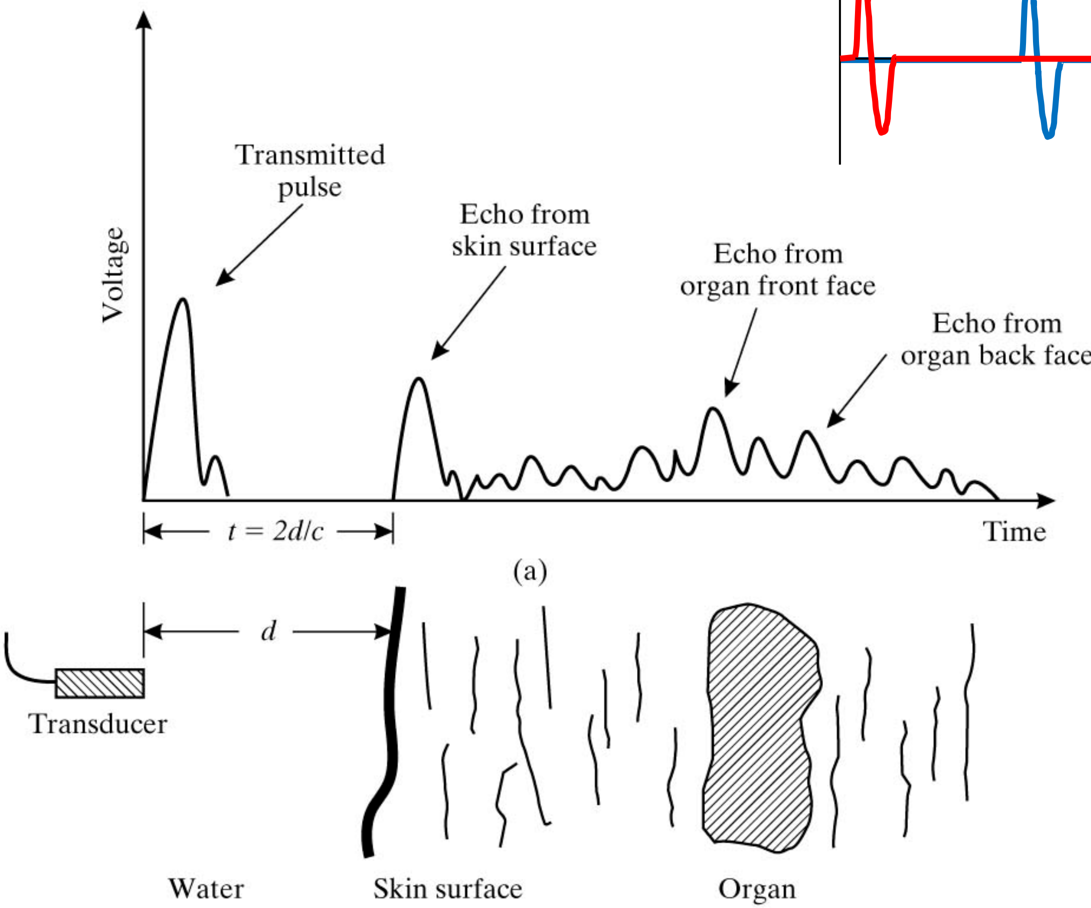

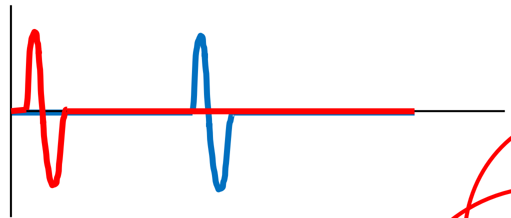

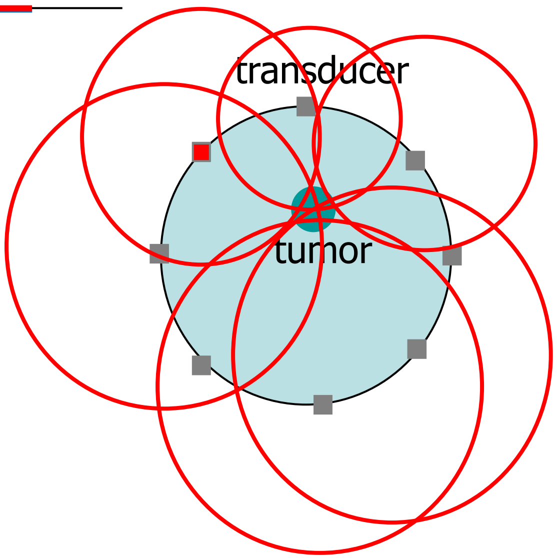

Image taken from J.L. Prince and J. Links, "Medical Imaging Signals and Systems", Prentice Hall (2005)

Imaging: SAFT / SAR / DAS

Synthetic Aperture Focusing Technique
Synthetic Aperture Radar
Delay and Sum

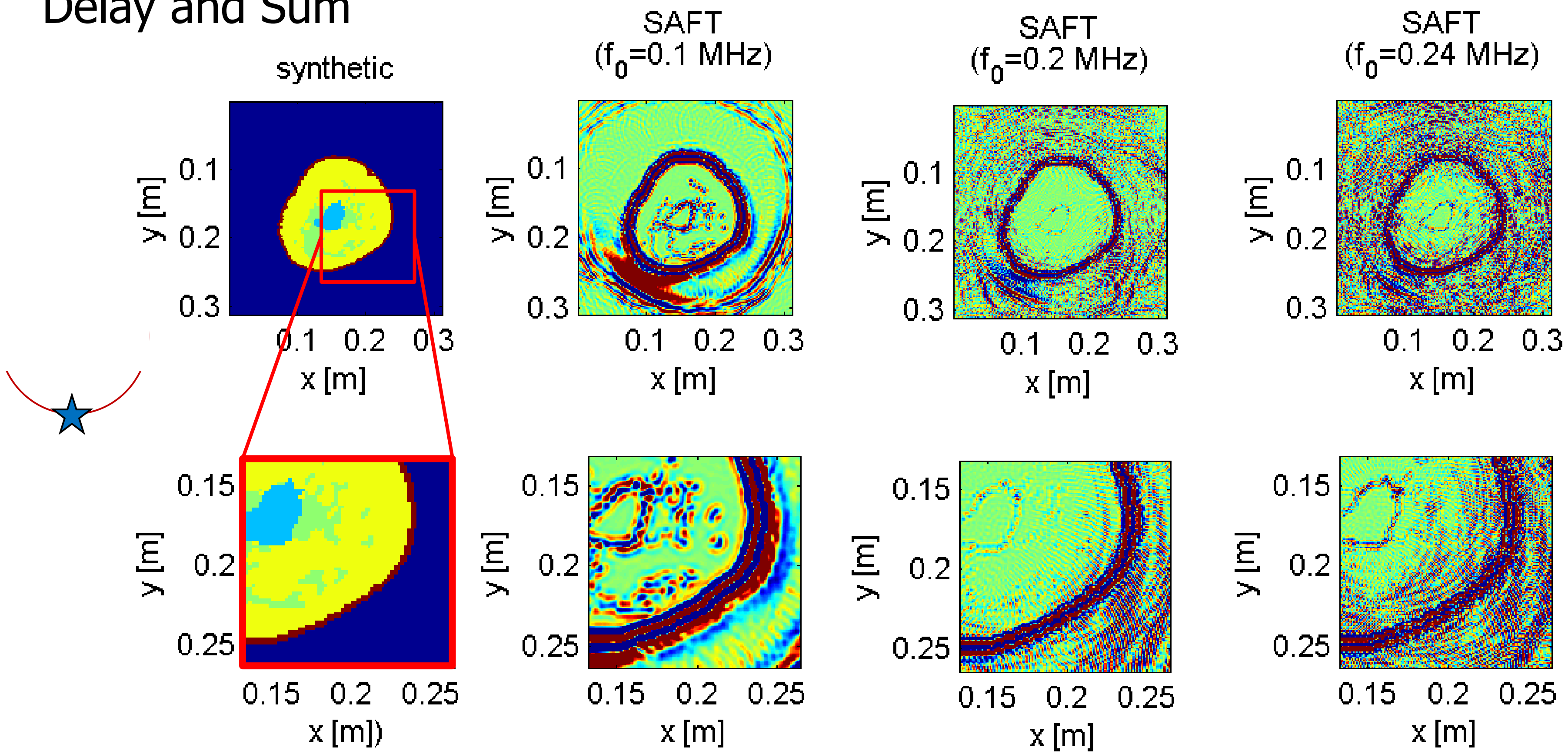

N_{src} = 157
N_{rec} = 38

TU Delft

Exersice

- Write your own SAFT script and test it on experimental data.

Imaging by Inversion

Imaging of acoustic data is an inverse problem.

For imaging heterogeneous acoustic media we want to invert the scatter integral equation:

$$\underbrace{\hat{p}^{tot}(\underline{r},\omega)}_{known} = \underbrace{\hat{p}^{inc}(\underline{r},\omega)}_{known} + \int_V \underbrace{\hat{G}(\underline{r}'-\underline{r},\omega)\,\omega^2}_{known}\, \underbrace{\chi(\underline{r}')}_{unknown}\, \underbrace{\hat{p}^{tot}(\underline{r}',\omega)}_{unknown}\, dV(\underline{r}')$$

where $\hat{p}^{tot}$ is only known along a data acquisition plane and
we need to find the unknown contrast $\chi(\underline{r})$ in the object space.

We are free to choose the background medium against which the contrasts are defined, as long as we are able to calculate $\hat{p}^{inc}$ and $\hat{G}$. For the calculation of $\hat{p}^{inc}$ we need to know, the distribution of the sources and the source signature wavelets.

Regularisation

- Inversion for the contrasts of the scattering integral equation is usually an **ill-posed problem**, by which we mean that the inversion is numerically unstable. Small variations in the measured response may give large variations in the contrasts.

- This is even the case under the **Born approximation**.

- The problem is alleviated by **regularisation** (and stabilisation).

- By regularisation is meant **introduction of a priori knowledge** on the distribution of the parameters in the solution space. We can impose sparseness, smoothness, flatness, or any other characteristic of the solution space that we have reason to believe to apply.

Linear or Born Inversion

$$\hat{p}^{tot}(\underline{r},\omega) = \hat{p}^{inc}(\underline{r},\omega) - \int \hat{G}(\underline{r}-\underline{r}',\omega)\,\omega^2 \chi(\underline{r}')\,\hat{p}^{tot}(\underline{r}',\omega)\,\mathrm{d}V$$

Born Approximation:

$$\hat{p}^{tot}(\underline{r}) = \hat{p}^{inc}(\underline{r}) - \int \hat{G}(\underline{r}-\underline{r}')\,\omega^2 \chi(\underline{r}')\,\hat{p}^{inc}(\underline{r}')\,\mathrm{d}V$$

$$p^{sct} = p^{inc} - p^{tot} = G*[\chi p^{inc}]$$ (b=Ax)

$$\chi_n = \chi_{n-1} + \alpha d_n$$

$$r_n = p^{sct} - G*[\chi_n p^{inc}]$$

n=1 Back-Propagation (BP)

n>1 Conjuge gradient scheme

Linear or Born Inversion

- Linear Inversion is an unstable process due to the Born-approximation.

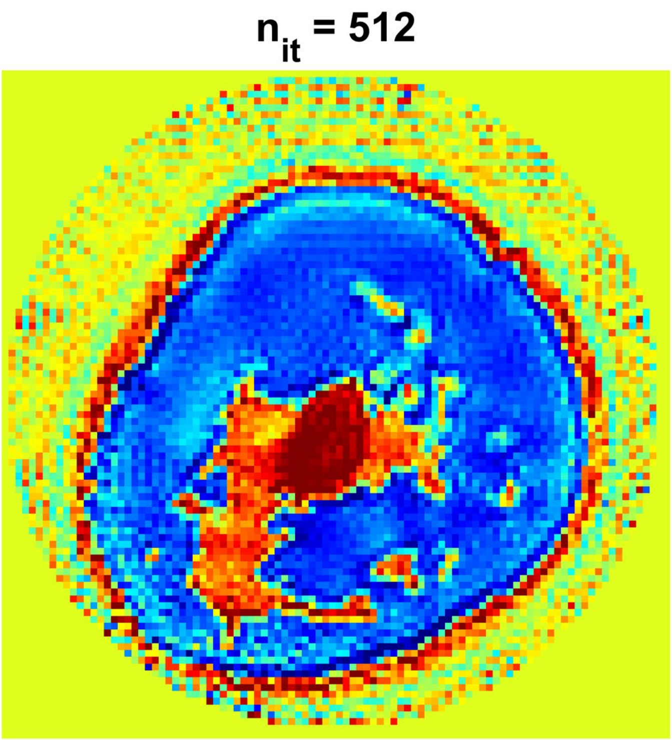

Linear or Born Inversion

synthetic

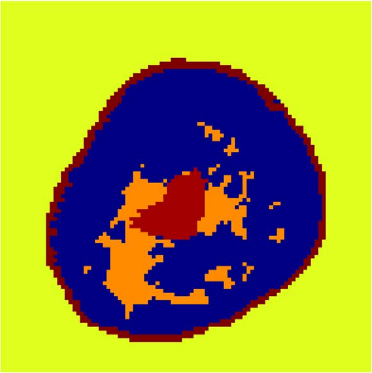

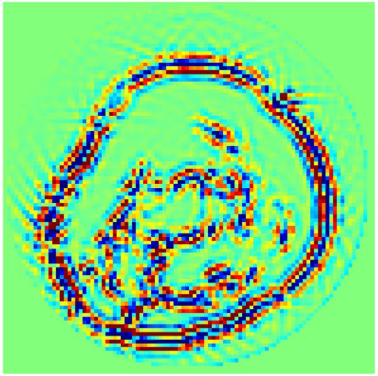

SAFT

Born Inversion

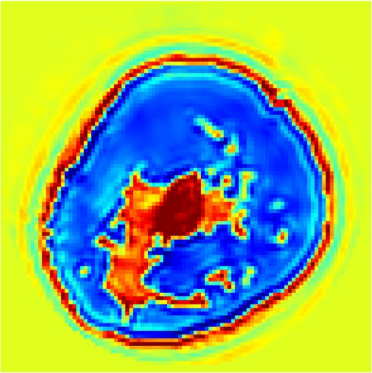

Linear or Born Inversion

synthetic

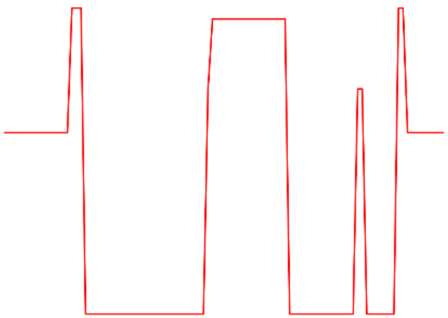

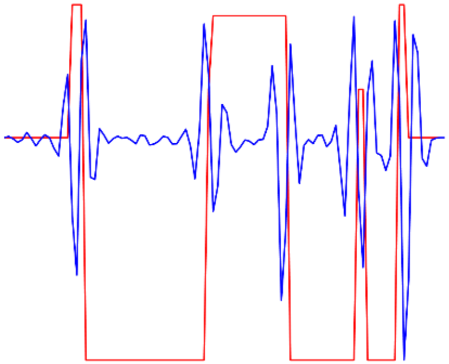

SAFT

Born Inversion

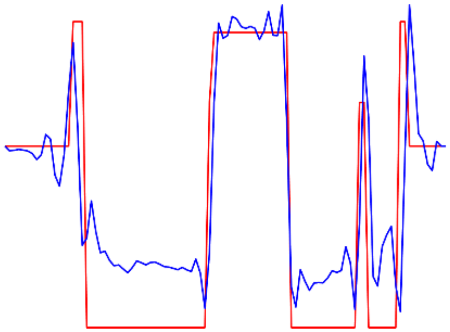

Linear or Born Inversion

- Two distinct cylinders of $\frac{3}{4}\lambda$ at $\frac{3}{4}\lambda$ apart
- Test domain D of $3\lambda \times 3\lambda$; mesh of 29×29 sub-squares
- Real contrast of $\chi = 0$.
- Measurements on circle of radius 3λ: 29 sources $\times$ 29 receivers
- Exact data with 10 % noise

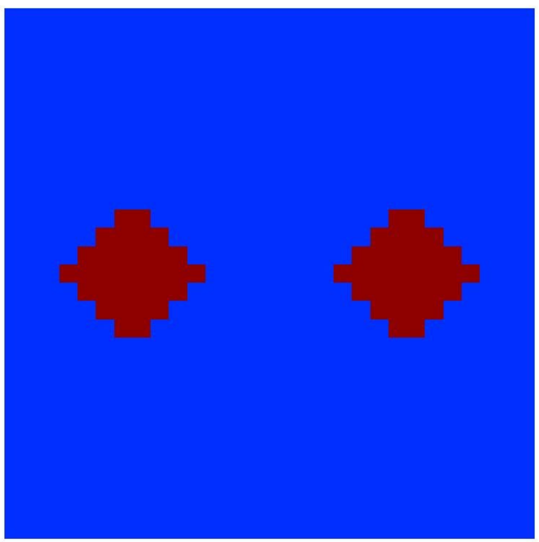

Original profile

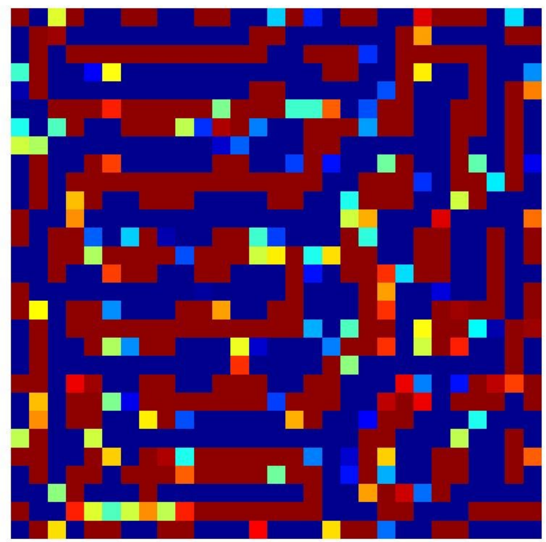

Reconstruction

$n = 1024$

TU Delft

Linear or Born Inversion

Born inversion is unstable. Consequently, it is very sensitive for noise in the data.

To stabilise the inversion process, regularization is required. A succesfull aproach for regulizing is by taking the total variation (TV) of the reconstructed profile into account.

Consequently, the error functional for regularized Born inversion reads

$$Err = \sum_{\omega, src, rec} \left| p^{sct} - G * [\chi_n p^{inc}] \right|^2 \times \frac{\sum_{\underline{r} \in D} \left| \nabla^2 \chi_n + \delta \right|^2}{\sum_{\underline{r} \in D} \left| \nabla^2 \chi_{n-1} + \delta \right|^2}$$

Born and Regularized Born Inversion

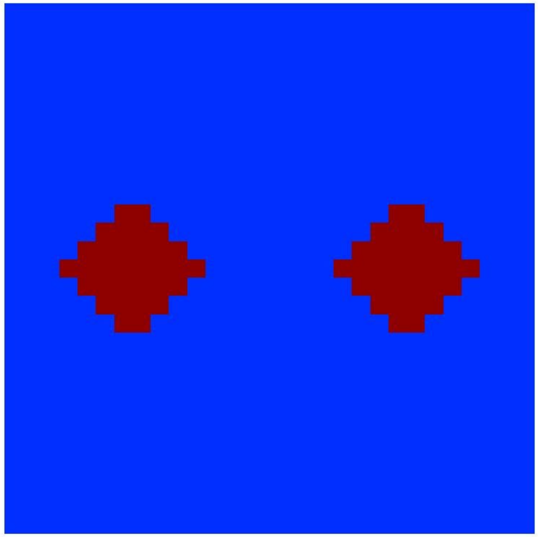

Original profile

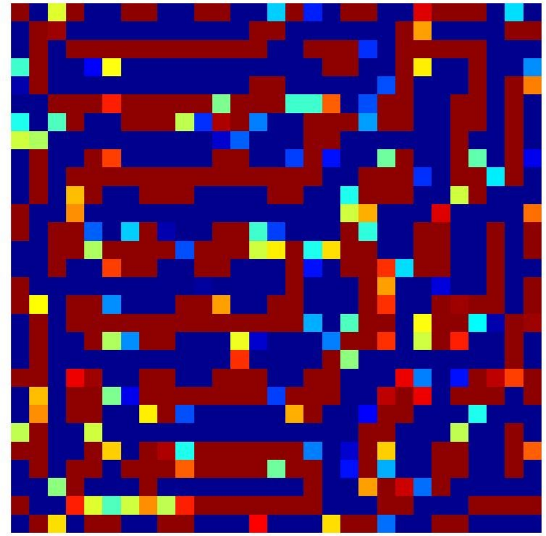

Born Inversion

Regularised Born Inversion

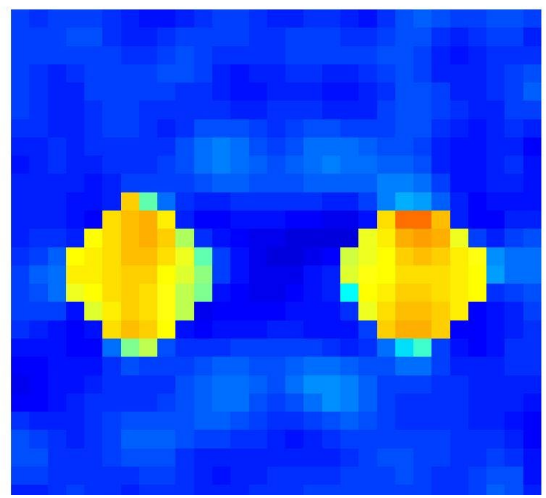

$n = 1024$

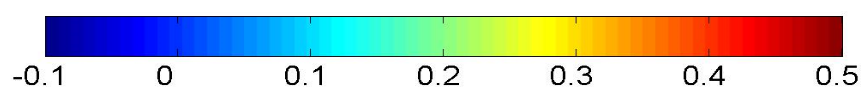

Non-Linear Inversion

With full-waveform non-linear inversion the original / complete integral equation (or wave equation) is solved:

$$\hat{p}^{tot}(\underline{r},\omega) = \hat{p}^{inc}(\underline{r},\omega) - \int \hat{G}(\underline{r}-\underline{r}',\omega)\,\omega^2 \chi(\underline{r}')\,\hat{p}^{tot}(\underline{r}',\omega)\,\mathrm{d}V$$

However, as there are multiple unknowns the problem is highly non-linear.

Various approaches have been tested in the past such as Modified Gradient and Contrast Source Inversion (CSI).

Non-Linear Inversion

$$p^{tot}(\underline{r}) = p^{inc}(\underline{r}) - \int G(\underline{r}-\underline{r}')\,\omega^2 \chi(\underline{r}')\, p^{tot}(\underline{r}')\,\mathrm{d}V$$

Born Approximation:

$$\hat{p}^{tot}(\underline{r}) = \hat{p}^{inc}(\underline{r}) - \omega^2 \int \hat{G}(\underline{r}-\underline{r}')\,\chi(\underline{r}')\,\hat{p}^{inc}(\underline{r}')\,\mathrm{d}V$$

Fullwave non-linear CSI inversion:

$$\hat{p}^{tot}(\underline{r}) = \hat{p}^{inc}(\underline{r}) - \omega^2 \int \hat{G}(\underline{r}-\underline{r}')\,\hat{w}(\underline{r}')\,\mathrm{d}V \qquad p^{tot} = p^{inc} - G * w$$

$$\hat{w}(\underline{r}') = \chi(\underline{r}')\,\hat{p}^{tot}(\underline{r}') \qquad w = \chi p^{tot}$$

$$Err_n = \frac{\left\| p^{tot} - p^{inc} + G * w_n \right\|}{\left\| p^{inc} \right\|} + \frac{\left\| w_n - \chi_{n-1}\left(p^{inc} - G * w_n\right) \right\|}{\left\| \chi_{n-1} p^{inc} \right\|}$$

Non-Linear Inversion

- Non-linear Inversion is a stable process as it uses the full wave equation.

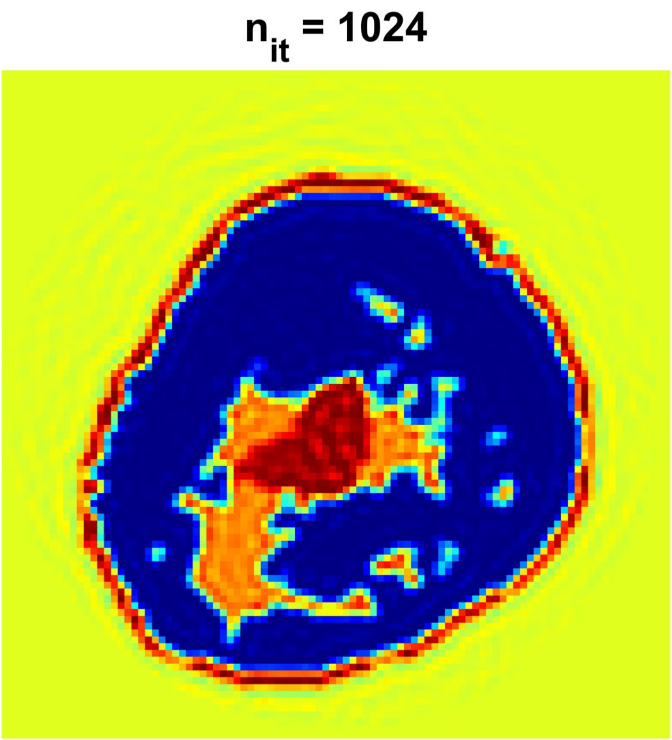

Non-Linear Inversion

synthetic

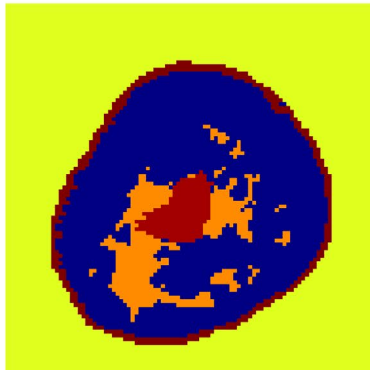

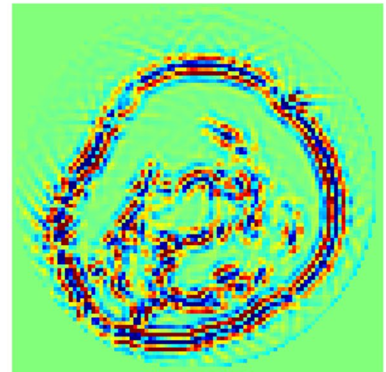

SAFT

Born
Inversion

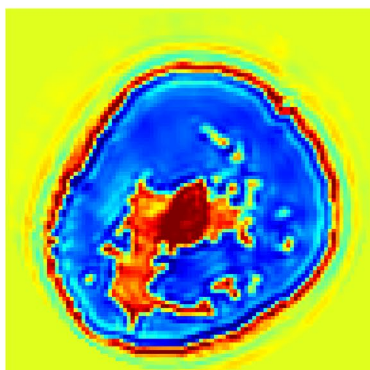

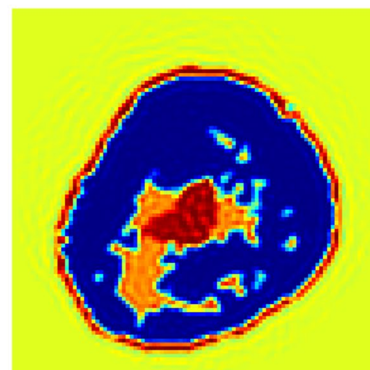

Full waveform
Inversion

Non-Linear Inversion

synthetic

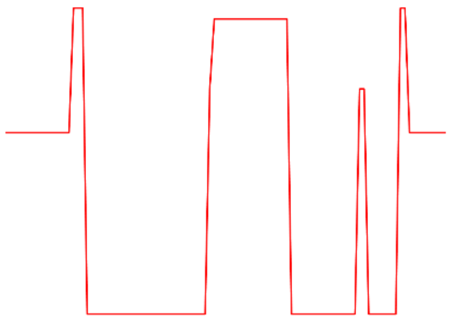

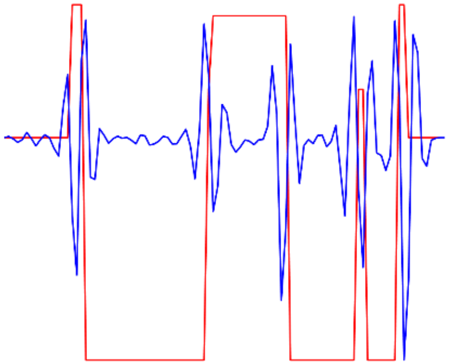

SAFT

Born Inversion

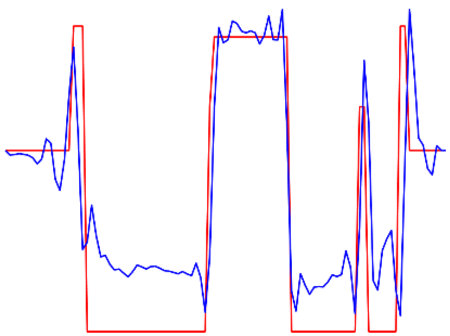

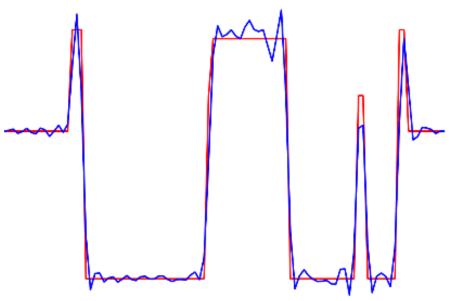

Full waveform Inversion

Regularized Non-linear inversion

$$p^{tot}(\underline{r}) = p^{inc}(\underline{r}) - \int G(\underline{r}-\underline{r}')\,\omega^2 \chi(\underline{r}')\, p^{tot}(\underline{r}')\,\mathrm{d}V$$

Born Approximation:

$$\hat{p}^{tot}(\underline{r}) = \hat{p}^{inc}(\underline{r}) - \omega^2 \int \hat{G}(\underline{r}-\underline{r}')\, \chi(\underline{r}')\, \hat{p}^{inc}(\underline{r}')\,\mathrm{d}V$$

Fullwave non-linear CSI inversion:

$$\hat{p}^{tot}(\underline{r}) = \hat{p}^{inc}(\underline{r}) - \omega^2 \int \hat{G}(\underline{r}-\underline{r}')\, \hat{w}(\underline{r}')\,\mathrm{d}V \qquad p^{tot} = p^{inc} - G * w$$

$$\hat{w}(\underline{r}') = \chi(\underline{r}')\hat{p}^{tot}(\underline{r}') \qquad w = \chi p^{tot}$$

$$Err^{(n)} = \left[\frac{\left\| p^{tot} - p^{inc} + G * w^{(n)} \right\|}{\left\| p^{inc} \right\|} + \frac{\left\| w^{(n)} - \chi^{(n-1)}\left(p^{inc} - G * w^{(n)}\right) \right\|}{\left\| \chi^{(n-1)} p^{inc} \right\|} \right] + (\ldots)$$

Regularization

- Total Variation
- sparsity
  - w
  - χ

5% noise

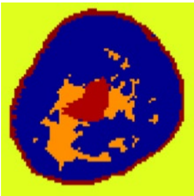

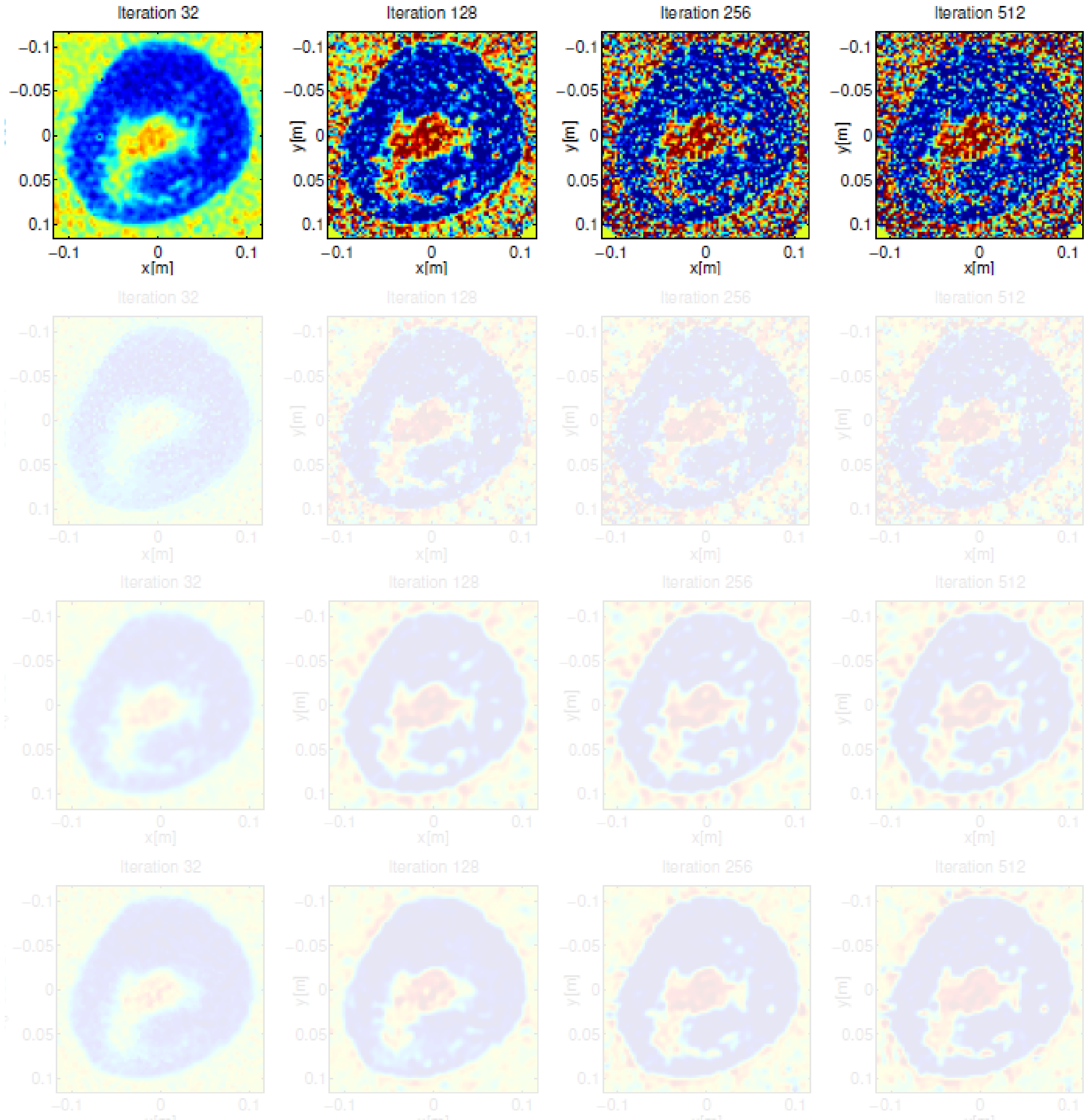

$$E_{TV} = \eta_{TV} \int_{\vec{x} \in D} \sqrt{\left|\nabla \chi_n(\vec{x})\right|^2}\, dA$$

$$\eta_S E_S + \eta_D E_D$$

$$s.t. \begin{cases} \left\| F\left[\hat{w}_j\right] \right\|_0 < s_1 \\ \left\| \Phi\left[\chi\right] \right\|_0 < s_2 \end{cases}$$

All tools

Multi-parameter Inversion

In reality, there are contrasts in both compressibility and density, besides attenuation. By taking the velocity field into account it is feasible to reconstruct for both medium parameters.

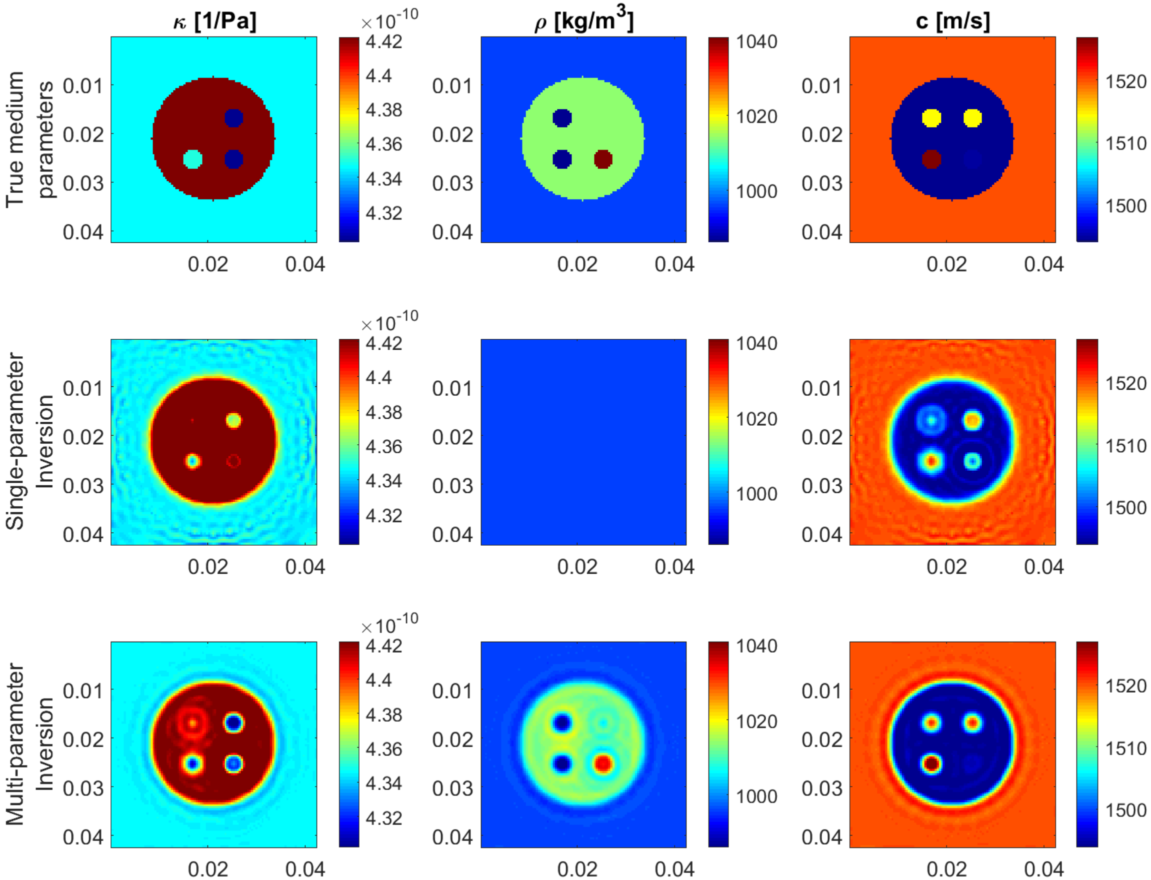

If needed, the velocity profile can be reconstructed from the pressure field!

U. Taskin et al, "Redatuming of 2-D Breast Ultrasound," IEEE Trans Ultrason Ferroelectr Freq Control 67(1)

U. Taskin et al, "Multi-parameter inversion with the aid of particle velocity field reconstruction," JASA 47(6)

Machine learning for tissue classification

- QT Ultrasound
  - Based on 13 breasts
  - Tissue parameters only (?)

- Problems will occur to apply method to different systems

- Delphinus:
  Tissue parameters and Texture.

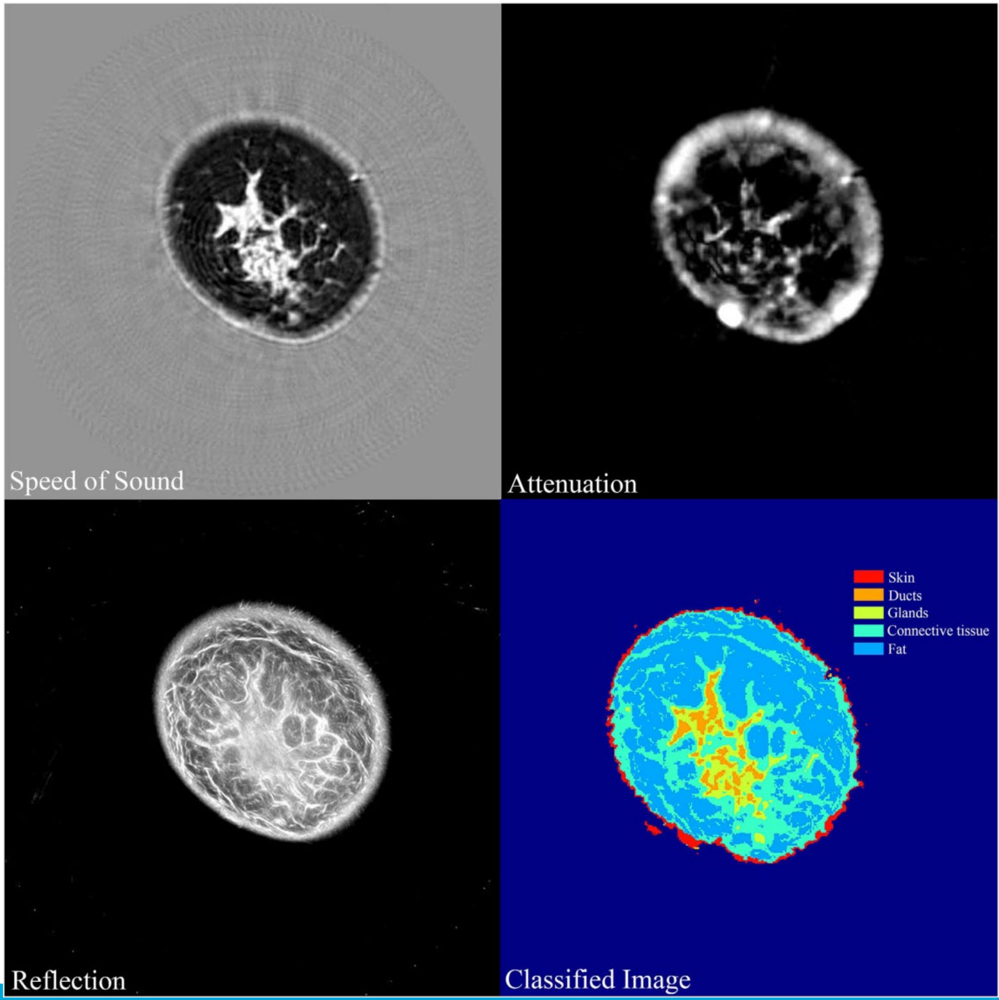

B. Malik, et al. "Objective breast tissue image classification using Quantitative Transmission ultrasound tomography," Scientific Reports, 2016

TUDelft

Machine learning for inversion

On synthetic data

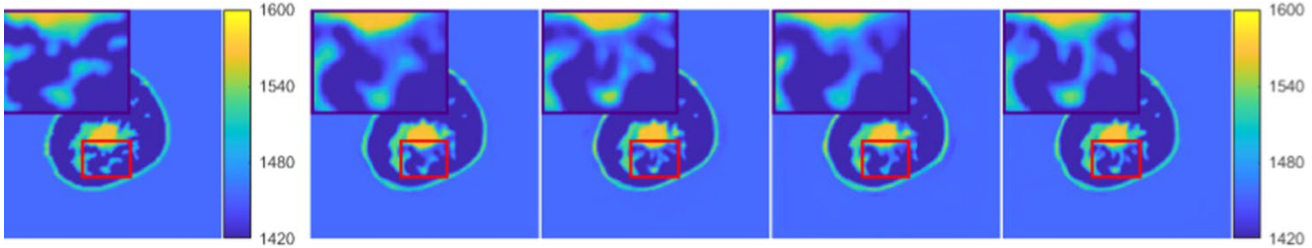

On real data

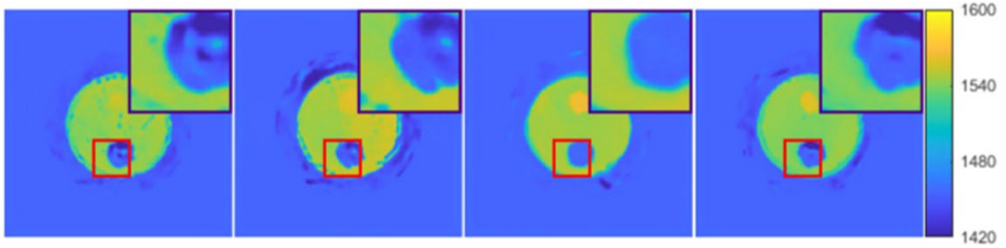

Zhao *et al* 2023, "Simulation-to-real generalization for deep-learning-based refraction-corrected ultrasound tomography image reconstruction," *Phys. Med. Biol.* **68** (2023)

SAFT – Full-Wave Form Inversion

Original

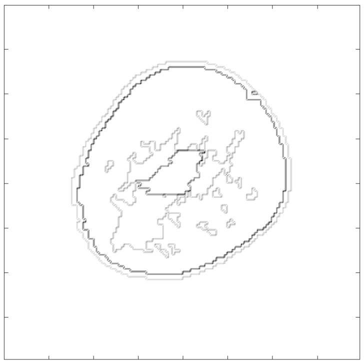

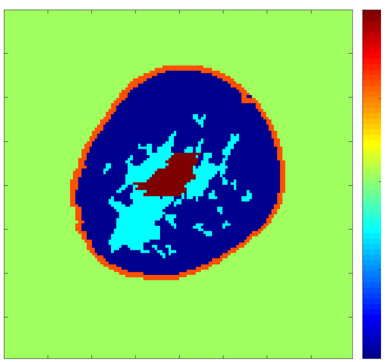

Reconstruction

$F_0 = 0.125$ MHz
$N_{src} = 10$
$N_{rec} = 100$

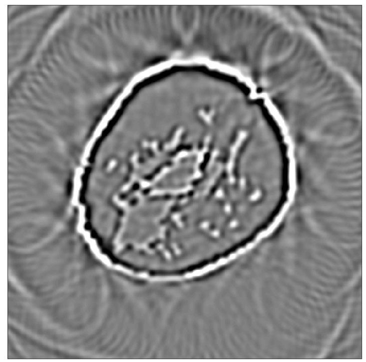

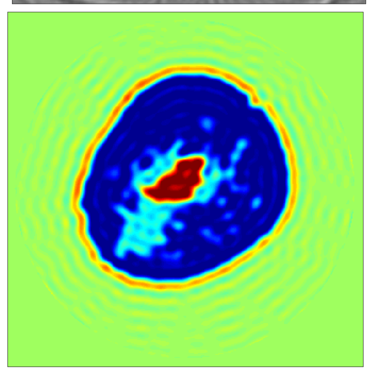

$F_0 = 0.5$ MHz
$N_{src} = 10$
$N_{rec} = 320$

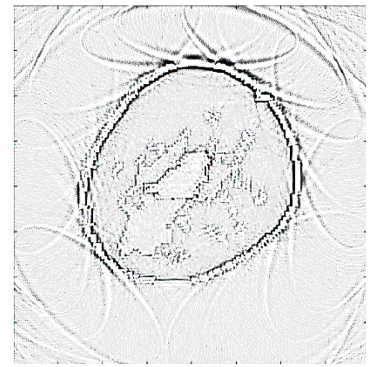

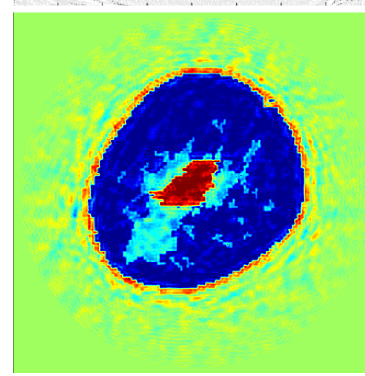

Discussion and Conclusion

SAFT

- Echogenicity
- Data volume: $N = N_{src} \times N_{rec} \times N_t$

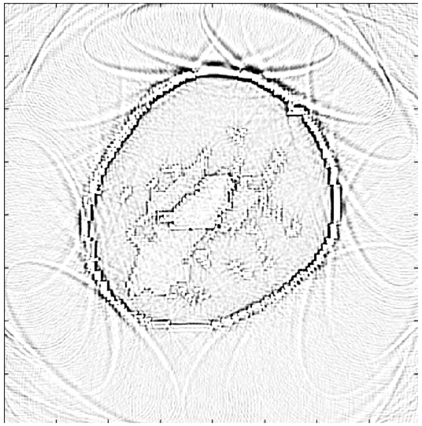

Born Inversion

- Neglects multiple scattering and phase shifts
- "Speed of sound"
- Convergence
- Data volume: $N = N_{src} \times N_{rec} \times N_f$

Full-Wave Form Inversion

- Inversion of *nonlinear* integral equation
- Taking advantage of multiple scattering and phase shifts
- Speed of sound
- Computational heavy
- Data volume: $N = N_{src} \times N_{rec} \times N_f$

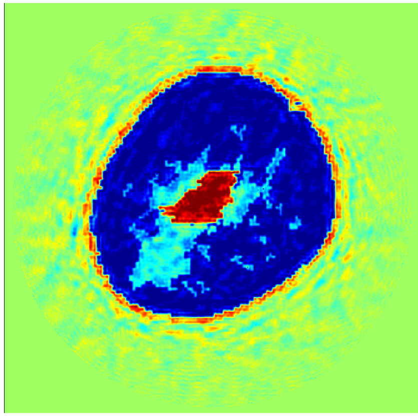

Multi-parameter

Machine learning

TU Delft

Recommended Reading

- Ozmen *et al*, "Comparing different ultrasound imaging methods for breast cancer detection", IEEE T Ultrason Ferr 62(4), pp. 637-646, 2015.

- Dries Gisolf and Eric Verschuur (2010). The Principles Of Quantitative Acoustical Imaging.
- Jacob T. Fokkema and Peter M. van den Berg (1993). Seismic applications of acoustic reciprocity.
- Adrianus T. de Hoop (1995 / 2008). Handbook of Radiation and Scattering of Waves.

- Mark F. Hamilton, David T. Blackstock (2008). Nonlinear Acoustics.

- Richard S.C. Cobbold (2006). Foundations of Biomedical Ultrasound.
- Thomas L. Szabo (2013). Diagnostic Ultrasound Imaging: Inside Out.

Acknowledgements

Some of the slides / results presented have been made by:

E. Alles, J. Bakker, P. van den Berg, R. Dapp, L. Demi, G. van Dijk, D. Gisolf, K. Huijssen, N. Ozmen, A. Ramirez, U. Taskin, E. Verschuur, M. Verweij

References

A majority of the images are based on the following publications:

- U. Taskin and K.W.A. van Dongen, "Multi-parameter inversion with the aid of particle velocity field reconstruction," Journal of the Acoustical Society of America 47(6), pp. 4032-4040, May 2020.
- U. Taskin, J. van der Neut, G. Hartmut and K.W.A. van Dongen, "Redatuming of 2-D Breast Ultrasound," IEEE Transactions on Ultrasonics, Ferroelectrics, and Frequency Control 67(1), pp. 173-179, January 2020.
- U. Taskin, N. Ozmen, H. Gemmeke, and K.W.A. van Dongen, “Modeling breast ultrasound; on the applicability of commonly made approximations,” Archives of Acoustics 43(3), pp. 425-435, April 2018.
- A.B. Ramirez and K.W.A. van Dongen, “Sparsity Constrained Contrast Source Inversion,” Journal of Acoustical Society of America 140(3), 1749-1757, August 2016.
- N. Ozmen, R. Dapp, M. Zapf, H. Gemmeke, N.V. Ruiter and K.W.A. van Dongen, “Comparing different ultrasound imaging methods for breast cancer detection,” IEEE Transactions on Ultrasonics, Ferroelectrics, and Frequency Control 62(4), pp. 637-646, April 2015.
- E.J. Alles and K.W.A. van Dongen, “Iterative reconstruction of the transducer surface velocity,” IEEE Transactions on Ultrasonics, Ferroelectrics, and Frequency Control 60(5), pp. 954-962, May 2013.

Thank you for your attention …

and

enjoy our conference.